University of Szeged

Faculty of Pharmacy

Department of Pharmacognosy

Isolation and structure determination of bioactive metabolites from *Clitocybe nebularis* and *Pholiota populnea*

Ph.D. Thesis

Morteza Yazdani

Supervisors:

Prof. Dr. Judit Hohmann DSc

Dr. Attila Ványolós PhD

Szeged, Hungary

2023

LIST OF PUBLICATIONS RELEATED TO THE THESIS

Yazdani, M., Béni, Z., Dékány, M., Szemerédi, N., Spengler, G., Hohmann, J., Ványolós, A.

Triterpenes from *Pholiota populnea* as cytotoxic agents and chemosensitizers to overcome multidrug resistance of cancer cells.

Journal of Natural Products **2022**; 85, 910-916

DOI: 10.1021/acs.jnatprod.1c01024

IF: 4.803 (D1)

Yazdani, M., Barta, A., Berkecz, R., Agbadua, O.G., Ványolós, A., Hohmann, J.

Pholiols E–K, lanostane-type triterpenes from *Pholiota populnea* with anti-inflammatory properties.

Phytochemistry **2023**, *205*, 113480

DOI: 10.1016/j.phytochem.2022.113480

IF: 4.004 (Q1)

Yazdani, M., Barta, A., Hetényi, A., Berkecz, R., Spengler, G., Ványolós, A., Hohmann, J.

Isolation of the lanostane triterpenes pholiols L–S from *Pholiota populnea* and evaluation of their antiproliferative and cytotoxic activities.

Pharmaceuticals **2023**, *16*, 104.

DOI: 10.3390/ph16010104

IF: 5.215 (Q1)

Yazdani, M., Béni, Z., Dékány, M., Papp, V., Lázár, A., Burián, K., Hohmann, J., Ványolós, A.

Isolation and characterization of chemical constituents from the mushroom *Clitocybe nebularis*.

Journal of Research in Pharmacy **2020**, *24*, 908-913.

DOI: 10.35333/jrp.2020.250

IF: - (Q3)

TABLE OF CONTENTS

1. INTRODUCTION ---------- 1
2. AIMS OF THE STUDY ---------- 3
3. LITERATURE OVERVIEW ---------- 4
3.1 Morphology, chemistry, and pharmacology of *Pholiota populnea* ---------- 4
3.2 Morphology, chemistry, and pharmacology of *Clitocybe nebularis* ---------- 4
4. MATERIALS and METHODS ---------- 5
4.1 Mushroom materials ---------- 5
4.1.1 *Pholiota populnea* ---------- 5
4.1.2 *Clitocybe nebularis* ---------- 6
4.2 Extraction ---------- 6
4.2.1 *Pholiota populnea* ---------- 6
4.2.2 *Clitocybe nebularis* ---------- 6
4.3 Isolation of compounds ---------- 7
4.3.1 Thin layer chromatography (TLC) ---------- 7
4.3.2 Gel filtration chromatography (GFC) ---------- 7
4.3.3 Flash chromatography (FC) ---------- 7
4.3.4 High-performance liquid chromatography (HPLC) ---------- 8
4.3.5 Structure determination of the isolated compounds ---------- 9
4.4 Pharmacological tests ---------- 9
4.4.1 Cell line cultures ---------- 10
4.4.2 Antiproliferative assay ---------- 10
4.4.3 Cytotoxicity assay ---------- 11
4.4.4 Rhodamine 123 accumulation assay ---------- 11
4.4.5 Checkerboard combination assay ---------- 12
4.4.6 Testing for antimicrobial activity ---------- 12
4.4.7 Testing for anti-inflammatory activity ---------- 14
5. RESULTS ---------- 16
5.1 Isolation of compounds from the investigated species ---------- 16
5.1.1 Isolation of compounds from *Pholiota populnea* ---------- 16
5.1.2 Isolation of compounds of *Clitocybe nebularis* ---------- 19
5.2 Characterization and structure determination of the isolated compounds ---------- 20

5.2.1 Compounds from *Pholiota populnea*---------- 20
5.2.2 Compounds from *Clitocybe nebularis* ---------- 32
5.3 Pharmacological activities of the isolated compounds---------- 32
5.3.1 Antiproliferative assay of the compounds from *Pholiota populnea* ---------- 32
5.3.2 Cytotoxic effect of the compounds from *Pholiota populnea* ---------- 33
5.3.3 Rhodamine 123 accumulation assay of the compounds from *Pholiota populnea* ---- 35
5.3.4 Checkerboard combination assay of the compounds from *Pholiota populnea*-------- 36
5.3.5 Antimicrobial assay of the compounds from *Pholiota populnea*---------- 36
5.3.6 Antimicrobial assay of the compounds from *Clitocybe nebularis* ---------- 36
5.3.7 Anti-inflammatory assay of the compounds from *Pholiota populnea*---------- 37
6. DISCUSSION ---------- 38
6.1 Investigation of *Pholiota populnea* and *Clitocybe nebularis* ---------- 38
6.2 Isolation of the bioactive compounds---------- 38
6.3 Structure elucidation ---------- 39
6.3.1 Triterpenes and nucleosides from *Pholiota populnea*---------- 39
6.3.2 Triterpenes and an organic acid from *Clitocybe nebularis*---------- 40
6.4 Biological activities of the compounds of investigated species---------- 41
6.4.1 *Pholiota populnea*---------- 41
6.4.2 *Clitocybe nebularis* ---------- 42
7. SUMMARY ---------- 43
8. REFERENCES ---------- 1

ABBREVIATIONS AND SYMBOLS

1D, 2D	One-dimensional, two-dimensional
A549	Human non-small cell lung cancer
CID	Collision-induced dissociation
CLSI	Clinical and Laboratory Standards Institute
Colo205	Human colon adenocarcinoma cells (sensitive)
Colo320	Human colon adenocarcinoma cells (resistant)
COSY	Correlation spectroscopy
COX	Cyclooxygenase
DMSO	Dimethyl sulfoxide
ELS	Evaporative light scattering
EMEM	Eagle's Minimal Essential Medium
ESI	Electrospray ionization
EtOAc	Ethyl acetate
FAR	Fluorescence activity ratio
FC	Flash chromatography
GFC	Gel filtration chromatography
HeLa	Human cervix adenocarcinoma
HMBC	Heteronuclear multiple-bond correlation
HPLC	High-performance liquid chromatography
HRMS	High-resolution mass spectrometry
HSQC	Heteronuclear single quantum correlation
IC_{50}	Half maximal inhibitory concentration
iNOS	Inducible nitric oxide synthase
JMOD	J-modulated spin-echo
LOX	Lipoxygenase
MCF-7	Human breast adenocarcinoma cells
MIC	Minimal inhibitory concentration
MRC-5	Human embryonic lung fibroblast cell line
MS	Mass spectrometry
MTT	3-(4,5-dimethylthiazol-2-yl)-2,5-diphenyltetrazolium bromide
NMR	Nuclear magnetic resonance
NOESY	Nuclear Overhauser effect spectroscopy
NP	Normal phase
OCC	Open column chromatography
OD	Optical density
PBS	Phosphate-buffered saline
P-gp	P-glycoprotein
PTLC	Preparative thin-layer chromatography
RNA	Ribonucleic acid
ROESY	Rotating-frame nuclear Overhauser effect spectroscopy
RP	Reverse phase
RS	RediSep Rf Gold
SDS	Sodium dodecyl sulphate
TLC	Thin-layer chromatography
UV-VIS	Ultraviolet-visible

INTRODUCTION

Mushrooms are fungi visible to the naked eye and found worldwide, growing as fleshy fruiting bodies on soil, dead wood, or other sources. They are classified into either Ascomycota or Basidiomycota[1]. More than 5000 species of mushrooms are found worldwide, with over 1000 of these species having been scientifically identified. Out of the known species, around 50-100 types are known to be poisonous, while approximately 200-300 are considered safe for consumption[2–4]. The nutritional, medicinal, and bioremediation importance of mushrooms has recently grown due to their high concentration of nutrients and bioactive substances, including polysaccharides, proteins, fats, phenolics, alkaloids, terpenoids, nucleosides, lectins, minerals, and vitamins[5–10]. Triterpenoids are common fungal metabolites that can be classified into nine primary groups based on their carbon skeletons, which include squalene, lanostane, ergostane, fernane, friedelane, lupane, malabaricane, eburicane, and cucurbitane[11]. The most frequently occurring triterpenes in mushrooms are based on lanostane and ergostane skeletons. Other triterpenoids are relatively uncommon as fungal metabolites. Generally, these compounds are substituted with hydroxy, keto, aldehyde, and carboxyl groups or have ether and acetonide functionalities. Esterification is also characteristic of some fungal triterpenes, with esterifying acids being simple organic or fatty acids. Additionally, some compounds have special structures, including lactones, seco-ring-A, or nor-triterpenoids. Numerous studies have reported that mushrooms produce various primary and secondary bioactive metabolites that contribute to their medicinal properties, including anti-inflammatory[12], antitumor[13], antioxidant[14], antibacterial[15], cytotoxic[16], antimalarial[17], and immunomodulatory[18] activities.

Cancer is one of the primary reasons for morbidity and mortality worldwide. The Global Cancer Statistics report indicates that approximately 19.3 million new cancer diagnoses were reported worldwide in 2020, including 1.148 million cases of colon cancer (which represents 6.0% of all cancer cases)[19]. One of the primary challenges in clinical cancer treatment is the development of multidrug resistance (MDR) to cytotoxic drugs. MDR occurs when cancer cells become resistant to multiple drugs, making it difficult to effectively treat cancer. MDR is associated with alterations in cellular pharmacokinetics, such as reduced drug accumulation, increased ability to remove drugs from the cell, and increased

ability to detoxify drugs. Additionally, the drugs may be redistributed within the cell, making them less effective at killing cancer cells. One of the most widespread mechanisms of resistance involves the efflux of drug molecules out of the cells. In particular, ATP-binding cassette (ABC) transporters have received great interest; one such transporter that has been investigated in detail is P-glycoprotein (P-gp)[20]. Some triterpenoids have been shown to reverse cell resistance to chemotherapy by inhibiting P-gp function. One such compound, ginsenoside Rh2, obtained from red ginseng, has been found to exhibit this effect in human breast cancer MCF-7 cells that are resistant to doxorubicin[21].

Anti-tumor activity refers to the ability of a substance or treatment to prevent or reduce the growth of tumors or cancer cells. This can be achieved through various mechanisms, such as inhibiting cell division, inducing apoptosis (programmed cell death), reducing inflammation, or enhancing the body's immune response to cancer cells.

In the literature numerous examples can be found that demonstrate the efficacy of fungal triterpenes in anti-inflammatory test models. For instance, lepiotaprocerins, which are lanostane triterpenes obtained from *Macrolepiota procera*, were found to inhibit the production of nitric oxide (NO)[22]. *Wolfiporia cocos*, which is a cultivated edible mushroom, is also a rich source of lanostane triterpenes. One of its components, poricoic acid GM, was found to be effective in inhibiting NO production with an IC_{50} value of 9.73 μM, inducible nitric oxide synthase (iNOS) and cyclooxygenase-2 (COX-2) proteins in LPS-induced RAW264.7 murine macrophages[23]. Moreover, triterpenes of *Hypholoma lateritium* were found to have a notable inhibitory effect on COX-2 and were able to activate the Nrf2 pathway[24].

The genus *Pholiota* is composed of saprotrophic mushrooms in the family Strophariaceae. *Pholiota* species are small to medium-sized, fleshy mushrooms, which are typically live on woods. The genus contains about 150 species, and has a widespread distribution, especially in temperate regions[25]. According to the literature, the number of studies on the genus *Pholiota* has recently increased. This can be exemplified by *Pholiota nameko*[26–32] and *Pholiota adiposa*[33], from which polysaccharides with antioxidant properties have been identified. From *Pholiota adiposa* ergosta-4,6,8(14),22-tetraen-3-one with antidiabetic effects, methyl gallate with antioxidant and anti-HIV activities were isolated

besides of stigmasterol, and a novel spiroaxane sesquiterpene[34–37]. Moreover, novel polyketides from *Pholiota sp*[38,39], and a highly potent antimicrobial styrene, bisnoryangonin were obtained from *Pholiota aurivella*[40]. Despite previous investigations, several members of the genus *Pholiota* have not yet been investigated and their mycochemical, pharmacological potential remains unexplored.

The genus *Clitocybe* predominantly consists of saprotrophic species, decaying forest ground litter. There are estimated to be around 300 species in the widespread genus. Only a few representatives of the genus are thought to be edible; the majority are poisonous, many of which contain the toxin muscarine. Seldom are *Clitocybe* mushrooms harvested for food[41]. *C. nebularis* waspreviously studied for macromolecules and polar compounds, therefore our study aimed at the characterization of the lipophilic metabolites[42].

The current thesis summarizes the chemical and pharmacological experiments conducted on *Pholiota populnea* and *Clitocybe nebularis*. It provides a detailed pharmacological evaluation of their metabolites to identify undescribed natural products with promising antiproliferative, cytotoxic, and anti-inflammatory activities.

AIMS OF THE STUDY

Recently, the research team of Department of Pharmacognosy at the University of Szeged started a screening program to investigate the pharmacological activities of Hungarian fungi and identify the bioactive compounds found in specific mushrooms. As part of the ongoing project, the primary goal of this study was to identify the biologically active components of *Pholiota populnea* and *Clitocybe nebularis* mushrooms, as well as to analyze their chemical and pharmacological properties. To accomplish the objectives, the following activities were undertaken:

Review the literature and previous screening results related to the selected species, placing particular emphasis on its chemical composition and pharmacological properties.

Grind the mushroom materials that have been collected and carrying out extraction with methanol.

Perform solvent-solvent partition and various chromatographic methods to separate and isolate the pure components.

Structure elucidation of the isolated compounds using NMR and MS methods (collaborating with the Institute of Pharmaceutical Analysis, University of Szeged, Szeged, Hungary, and Richter Gedeon Plc., Hungary). Provide characteristic NMR spectroscopic data for the undescribed constituents.

Evaluate the isolated compounds for their pharmacological potential (at the Department of Pharmacognosy in collaboration with the Department of Medical Microbiology and Immunobiology, Szeged, Hungary).

LITERATURE OVERVIEW

Morphology, chemistry, and pharmacology of *Pholiota populnea*

Pholiota populnea (Pers.) Kuyper & Tjall.-Beuk. (syn. *Pholiota destruens* (Brond.) Quel., *Hemipholiota populnea*) is member of the Strophariaceae family, distributed worldwide wherever cottonwood occurs. This mushroom species is usually saprophytic, but sometimes parasitic, and grows on broad-leaved woods, mainly on various poplars, but also on willow and birch, playing an important role in decomposing the deadwood of cottonwoods[43]. The chemistry and pharmacology of *P. populnea* were poorly studied previously, with only pholiotic acid, 3,5-dichloro-4-methoxybenzaldehyde, and 3,5-dichloro-4-methoxybenzyl alcohol with weak antifungal and cytostatic activities[44]. In a recent paper by Mleczek et al. the mineral element composition of *P. populnea* was determined[45].

Morphology, chemistry, and pharmacology of *Clitocybe nebularis*

Clitocybe nebularis (Batsch) P. Kumm. [syn.: *Lepista nebularis* (Fr.) Harmaja] known as clouded agaric or cloud funnel, member of the family Tricholomataceae is a common species of both conifer and broad-leaved forests in temperate and hemiboreal zones across Europe and North America[46]. *C. nebularis* is generally considered edible, but the strong, aromatic odor dissuades some people and can cause upset after consuming[47]. Several bioactive compounds have been identified and documented from the fruiting bodies of *C. nebularis*. Nebularine, a purine riboside with bacteriostatic properties, was the first biologically active substance to be discovered and identified from this mushroom[48]. In 1994, four fatty acids, (12*Z*)-9,10-dihydroxy-12-octadecenoic acid, (8*E*)-10-hydroxy-8-decenoic acid, (8*E*)-10-oxo-8-decenoic acid, (*E*)-2-decenedioic acid, together with two linear 1,3-diarylpropanoids,

2,4-diphenyl-2-butenal, and 4-hydroxy-2,4-diphenyl-2-butenal were reported from *C. nebularis* by Pang et al.[49]. Based on a study of Figedal et al. a cerebroside, *N*-2′-hydroxyhexadecanoyl-1-*O*-*β*-D-glucopyranosyl-9-methyl-4,8-D-erythro-sphingadienine, was isolated from this species[50]. Brzin et al. reported that clitocypin, a new type of cysteine proteinase inhibitor was obtained from the fruit bodies of *C. nebularis*[51]. Mycochemical analysis of Kim et al. led to the isolation of nebularine, phenylacetic acid, purine, uridine, adenine, uracil, benzoic acid, and mannitol from the fruiting body of *C. nebularis*. Nebularine and phenylacetic acid revealed mild and significant antifungal activity, respectively[52]. The extensive study of the fermentation broth of *C. nebularis* by Schrey et al. resulted in the identification of seven sesquiterpenoids, named nebucanes A–G. Nebucane G exhibited significant cytotoxicity against MCF-7 and A431 cell lines, while nebucane D displayed antifungal effects against *Rhodotorula glutinis*[53]. In another investigation, novel drimane sesquiterpenoids, named nebularic acids A and B, and nebularilactones A and B, were obtained from the fungus *C. nebularis*. Nebularic acid A and especially nebularic acid B, which contains an *α*,*β*-epoxy carboxylate group, showed antifungal and antibacterial properties[54]. Important phenolic compounds with strong antioxidant activity, such as catechin, myricetin, quercetin, rutin, gallic acid, and vanillic acid, have also been found in the ethanolic extract[55]. Recently, the findings of Onar et al. showed that the ethanolic extract of *C. nebularis* has a synergistic effect with 5-FU by inhibiting cell proliferation of colon cancer cells and inducing cell cycle arrest in the S phase[56]. Dimitrijevic et al. determined the levels of biologically essential elements (such as Ca, P, Co, Fe, Sr, and Mn) and toxic elements (such as Al, Ba, Cd, Hg, and As) in the extract of *C. nebularis*. Additionally, high amounts of fatty acids such as linoleic acid and oleic acid were reported[57].

MATERIALS AND METHODS

Mushroom materials

Pholiota populnea

Samples of *Pholiota populnea* (Pers.) Kuyper & Tjall.-Beuk. (Strophariaceae) were collected in the autumn of 2017 near Szeged, Hungary (GPS coordinates are 46°24′ 02.0"N, 20°11'26.0"E), and identified by Attila Sándor (Mushroom Society of Szeged, Hungary). Fruiting bodies of *P. populnea* (4.2 kg) were stored at −20 °C until processing. A voucher

specimen (No. H019) was deposited at the Department of Pharmacognosy, University of Szeged, Hungary.

Clitocybe nebularis

Samples of *Clitocybe nebularis* (Batsch) P. Kumm. were collected in 2017 from the environs of Sándorfalva and Csákányospuszta, Hungary and identified by A. Sándor (Hungarian Mycological Society) and V. Papp. Voucher specimens have been deposited in the mycological collection of the Hungarian Natural History Museum (VPapp-1110171).

Extraction

Pholiota populnea

The fruiting bodies (4.2 kg) of *P. populnea* were ground with a grinder (Retsch Grindomix GM 200) and then percolated with MeOH (20 L) for 72 hours at room temperature. After evaporation of the solvent using a Büchi Rotavapor R-300 combined with a V-300 Vacuum Pump and a B-300 Heating Bath and a Julabo F1000 cooler, the dry extract (151 g) was dissolved in 50% aqueous MeOH and subjected to liquid–liquid partition using *n*-hexane (5 × 500 mL), chloroform (5 × 500 mL), and then EtOAc (5 × 500 mL). The organic phases were dried using the same method leading to 24.0 g, 63.2 g, and 16.7 g dry samples, respectively.

Clitocybe nebularis

The fresh mushroom materials (5.6 kg) were crushed in a Waring industrial blender and extracted with MeOH (20 L) for 72 hours at room temperature. This extract was concentrated using a Büchi Rotavapor R-210 combined with a V-100 Vacuum Pump, a B491 Heating Bath, and a Julabo F250 cooler, resulting 54 g of dry material. This extract was dissolved in 50% aqueous MeOH for solvent-solvent partition. For this process *n*-hexane (5 × 500 mL), $CHCl_3$ (5 × 500 mL), and EtOAc (5 × 500 mL) were employed; evaporation of the solvents afforded 15.71 g, 2.12 g and 4.15 g samples, respectively.

Isolation of compounds

Thin layer chromatography (TLC)

Thin layer chromatography (TLC) was carried out on RP (Merck, TLC Silica Gel 60 RP-18 F_{254S}, Darmstadt, Germany) and NP (Merck, TLC Silica gel 60 F_{254}, Darmstadt, Germany) silica gel-covered aluminum sheets. For preparative thin-layer chromatography (PTLC) the following solvent systems were used:

PTLC1: Mixture of *n*-hexane–acetone (45:55 v/v)
PTLC2: Mixture of $CHCl_3$–MeOH (95:5 v/v)
PTLC3: Mixture of *n*-hexane–EtOAc–MeOH (5:4:1 v/v)
PTLC4: Mixture of *n*-hexane–acetone (1:1 v/v)
PTLC5: Mixture of $CHCl_3$–MeOH (97:3 v/v)

Gel filtration chromatography (GFC)

Sephadex LH-20 (25–100 μm, Sigma-Aldrich, MO, USA) was employed for gel filtration chromatography (GFC).

GFC1: CH_2Cl_2–MeOH (1:1)
GFC2: CH_2Cl_2– MeOH (1:1)

Flash chromatography (FC)

Flash chromatography was performed using a CombiFlash Rf+ Lumen instrument with integrated UV, UV-vis, and ELS detection. As stationary phases 4 g (FC15), 20 g (FC4), 40 g (FC6, FC8, FC10, and FC13), and 80 g (FC1, FC7, FC9, and FC14) normal-phase flash columns filled with silica 60 (Molar Chemicals, Halásztelek, Hungary) with a particle size range of 0.045-0.063 mm were used, as well as 4 g (FC3), 12 g (FC2), and 20 g (FC1) reversed-phase flash columns (RediSep C_{18} Bulk 950, Teledyne Isco, Lincoln, NE, USA). Additionally, 12 g (FC2, FC5, FC11, and FC12) normal phase silica flash columns (RediSep Rf Gold, Teledyne Isco) were used. Mobile phases and separation times were as follows:

NP-FC1: Increasing polarity of *n*-hexane–acetone (0% to 100% acetone), t = 55 min
NP-FC2: Increasing polarity of *n*-hexane–acetone (0% to 30% acetone), t = 50 min
NP-FC3: Increasing polarity of *n*-hexane–acetone (0% to 35% acetone), t = 40 min

NP-FC4: Increasing polarity of *n*-hexane–acetone (0% to 80% acetone), t = 50 min
NP-FC5: Increasing polarity of *n*-hexane–acetone (0% to 50% acetone), t = 55 min
NP-FC6: Increasing polarity of *n*-hexane–acetone (0% to 25% acetone), t = 45 min
NP-FC7: Increasing polarity of *n*-hexane–acetone (0% to 100% acetone), t = 55 min
NP-FC8: Increasing polarity of *n*-hexane–acetone (0% to 100% acetone), t = 60 min
NP-FC9: Increasing polarity of *n*-hexane–EtOAc (40% to 100% acetone), t = 70 min
NP-FC10: Increasing polarity of *n*-hexane–EtOAc (45% to 100% acetone), t = 60 min
NP-FC11: Increasing polarity of cyclohexane–EtOAc (0% to 100% acetone), t = 50 min
NP-FC12: Increasing polarity of *n*-hexane–acetone (0% to 100% acetone), t = 65 min
NP-FC13: Increasing polarity of *n*-hexane–acetone (0% to 100% acetone), t = 60 min
NP-FC14: Increasing polarity of *n*-hexane–acetone (0% to 35% acetone), t = 60 min
NP-FC15: Increasing polarity of *n*-hexane–acetone (25% to 70% acetone), t = 50 min
RP-FC1: Decreasing polarity of H_2O–MeOH (60% to 90% methanol), t = 50 min
RP-FC2: Decreasing polarity of H_2O–MeOH (40% to 90% methanol), t = 45 min
RP-FC3: Decreasing polarity of H_2O–MeOH (50% to 95% methanol), t = 45 min

High-performance liquid chromatography (HPLC)

We used both normal and reverse phase separations on different HPLC instruments to purify the compounds. Shimadzu LC-10 AS HPLC instrument equipped with a UV–Vis detector (Shimadzu, Co., Ltd., KYOTO, Japan) was employed for separations using normal-phase HPLC (NP-HPLC, LiChrospher Si60, 5 μm, 250 × 4 mm) (SL60) and reverse-phase HPLC (RP-HPLC, LiChrospher RP-18, 5 μm, 250 × 4 mm) (SL18) columns. Moreover, NP-HPLC was carried out using a Zorbax-Sil column (250 × 9.4 mm, 5 μm; Agilent Technologies, Santa Clara, CA, USA) (ZSil) on a Waters HPLC instrument equipped with a PDA detector (Waters, Co., Ltd., Milford, USA).

NP-HPLC1: Isocratic mixture of *n*-hexane–EtOAc–MeOH (10:9:1, SL60 column)
NP-HPLC2: Isocratic mixture of cyclohexane–EtOAc (1:4, ZSil column)
NP-HPLC3: Isocratic mixture of *n*-hexane–EtOAc–MeOH (10:9:1, ZSil column)
NP-HPLC4: Isocratic mixture of cyclohexane–EtOAc (1:3, SL60 column)
NP-HPLC5: Isocratic mixture of cyclohexane–EtOAc (1:1, SL60 column)
RP-HPLC1: Isocratic mixture of H_2O–MeOH (1:4, SL18 column)

RP-HPLC2: Isocratic mixture of H_2O–MeCN (2:3, SL18 column)

RP-HPLC3: Isocratic mixture of H_2O–MeCN (1:3, SL18 column)

RP-HPLC4: Isocratic mixture of H_2O–MeOH (28:72, SL18 column)

RP-HPLC5: Isocratic mixture of H_2O–MeOH (1:3, SL18 column)

RP-HPLC6: Isocratic mixture of H_2O–MeOH (2:8, SL18 column)

RP-HPLC7: Decreasing polarity of H_2O–MeOH (1:3 to 1:19, SL18 column)

RP-HPLC8: Isocratic mixture of H_2O–MeOH (1:9, SL18 column)

RP-HPLC9: Isocratic mixture of H_2O–MeOH (1:19, SL18 column)

Structure determination of the isolated compounds

The JASCO p-2000 polarimeter (JASCO International Co., Ltd. in Hachioji, Tokyo, Japan) was used to measure the optical rotations. High-resolution mass spectrometry (HRMS) was conducted on a Thermo Velos Pro Orbitrap Elite (Thermo Fisher Scientific, Bremen, Germany) device using the electron spray ionization (ESI) method. The instrument was operated in either the positive or negative ion mode. The (de)protonated molecular ion peaks were fragmented by the collision-induced dissociation method (CID) at a normalized collision energy of 35%. During the CID experiments, helium was used as the collision gas. The data obtained from the experiments were collected and analyzed using MassLynx software. The Bruker Avance DRX 500 spectrometer (Bruker, Billerica, MA, USA) was used to record NMR spectra at 500 MHz for proton (^{1}H) and 125 MHz for carbon (^{13}C) in $CDCl_3$ or CD_3OD. The signals of the deuterated solvents were considered as references. The standard Bruker software was used for conducting two-dimensional (2D) NMR measurements. In the HMBC, HSQC, and COSY experiments, gradient-enhanced versions were used.

Pharmacological tests

Pharmacological studies were conducted in collaboration with the Department of Medical Microbiology (Albert Szent-Györgyi Health Center and Albert Szent-Györgyi Medical School, University of Szeged, Szeged, Hungary).

Cell line cultures

The human colon adenocarcinoma cell lines, Colo205 (ATCC-CCL-222) doxorubicin-sensitive parent, and Colo320/MDR-LRP (ATCC CCL-220.1) doxorubicin-resistant expressing ABCB1, were purchased from LGC Promochem (Teddington, UK). The human colon adenocarcinoma cells were cultured in RPMI-1640 medium, which was enhanced with 10% heat-inactivated fetal bovine serum (FBS), 2 mM L-glutamine, 1 mM Na-pyruvate, 100 mM HEPES. The MCF-7 (ATCC HTB-22) hormone-responsive breast cancer cell line and the human embryonic lung fibroblast cell line MRC-5 (ATCC CCL-171) were purchased from Sigma-Aldrich (Merck KGaA, Darmstadt, Germany). The MRC-5 and MCF-7 cells were cultured in EMEM, which contained 4.5 g/L of glucose and supplemented with a selection of vitamins, a non-essential amino acid mixture, and 10% FBS. The cell lines were kept in a 37 °C environment with a 5% CO_2 and 95% air atmosphere during incubation. The cells were detached with Trypsin-Versene (EDTA) solution for 5 min at 37 °C. Brigitte Marian (Institute of Cancer Research, Department of Medicine I, Medical University of Vienna, Austria) kindly provided the A549 cell line. The A549 cells were cultured in EMEM supplemented with 10% heat-inactivated fetal bovine serum.

Antiproliferative assay

The antiproliferative effect of the compounds was tested in decreasing serial dilutions of compounds (starting with 100 μM, then two-fold serial dilution) on human cell lines (Colo205, Colo320, MCF-7, A549, and MRC-5) in 96-well flat-bottomed microtiter plates. Firstly, the compounds were diluted in 100 μL of the medium, and then, 6×10^3 cells (Colo205, Colo320) in 100 μL of RPMI medium were added to each well, excluding the medium control wells. The adherent MCF-7, A549, and MRC-5 cells (6×10^3 cells/well) were seeded in EMEM medium for at least 4 h before the assay. The two-fold serial dilutions of the compounds were made in a separate plate (100–0.19 μM) and then transferred to the plates containing the adherent-corresponding cell line. Culture plates were incubated at 37 °C for 72 h, and at the end of the incubation period, 20 μL of MTT (thiazolyl blue tetrazolium bromide) solution (from a 5 mg/mL stock solution) was added to each well and incubated for an additional 4 h. Then, 100 μL of sodium dodecyl sulfate (SDS) solution (10% SDS in 0.01 M HCl) was added to each well, and the plates were further incubated at 37 °C overnight

in a CO_2 incubator. Cell growth was determined by measuring the optical density (OD) at 540/630 nm with a Multiscan EX ELISA reader (Thermo Labsystems, Cheshire, WA, USA). The percentage of inhibition of cell growth was determined according to equation (1), and expressed as IC_{50} values, defined as the concentration that induces 50% growth inhibition. IC_{50} values and the standard deviation (SD) of triplicate experiments were calculated using GraphPad Prism 5 software for Windows. Doxorubicin (2 mg/mL, Teva Pharmaceuticals, Budapest, Hungary) was used as a positive control and the vehicle DMSO as the negative control.

$$IC_{50} = \left[\frac{OD_{sample} - OD_{medium\ control}}{OD_{cell\ control} - OD_{medium\ control}}\right] X\ 100$$

Cytotoxicity assay

The effects of increasing concentrations of the compounds on cell growth were tested in 96-well flat-bottomed microtiter plates, as described for the antiproliferative assay, using 1×10^4 cells/well. The culture plates were incubated at 37 °C for 24 h; at the end of the incubation period, 20 µL of MTT solution (from a 5 mg/mL stock solution) was added to each well. After incubation at 37 °C for 4 h, 100 µL of sodium dodecyl sulfate (SDS) solution (10% SDS in 0.01 M HCl) was added to each well, and the plates were further incubated at 37 °C overnight. Cell growth was determined by measuring the OD at 540 nm (ref 630 nm) with a Multiscan EX ELISA reader (Thermo Labsystems, Cheshire, WA, USA). Inhibition of cell growth was expressed as IC_{50}.

Sample preparation: The compounds were dissolved in DMSO to achieve the final concentration of 5 mM. The starting concentration of the compounds was 100 µM and 2-fold serial dilutions were prepared for the antiproliferative and cytotoxic assays. The following concentrations were used: 100-50-25-12.5-6.25-3.125-1.56-0.78-0.39-0.195 µM.

Rhodamine 123 accumulation assay

The cell numbers of the human colon adenocarcinoma cell lines were adjusted to 2×10^6 cells/mL, resuspended in serum-free RPMI 1640 medium, and distributed in 0.5 mL aliquots into Eppendorf centrifuge tubes. The tested compounds were added at 2 or 20 µM concentrations, and the samples were incubated for 10 min at room temperature. Tariquidar was applied as positive control at 0.2 µM. DMSO at 2% v/v was used as solvent control.

Next, 10 μL (5.2 μM final concentration) of the fluorochrome and ABCB1 substrate rhodamine 123 (Sigma) were added to the samples, and the cells were incubated for a further 20 min at 37 °C, washed twice, and resuspended in 1 mL of PBS for analysis. The fluorescence of the cell population was measured with a PartecCyFlow flow cytometer (Partec, Münster, Germany). The FAR was calculated as the quotient between FL-1 of the treated/untreated resistant Colo320 cell line over the treated/untreated sensitive Colo205 cell line according to the following equation:

$$\mathrm{FAR} = \frac{\mathrm{Colo320_{treated}} \,/\, \mathrm{Colo320\ _{control}}}{\mathrm{Colo205_{treated}} \,/\, \mathrm{Colo205\ _{control}}}$$

Checkerboard combination assay

A checkerboard microplate method was applied to study the effect of drug interactions between the compounds (**2**, **4**, **21**, and **22**) and the chemotherapeutic drug doxorubicin. The assay was carried out on the Colo320 colon adenocarcinoma cell line. The final concentration of the compounds and doxorubicin used in the combination experiment was chosen in accordance with their cytotoxicity toward this cell line. The dilutions of doxorubicin were made in a horizontal direction in 100 μL, and the dilutions of the compounds vertically in the microtiter plate in a 50 μL volume. Then, 6×10^3 of Colo320 cells in 50 μL of the medium were added to each well, except for the medium control wells. The plates were incubated for 72 h at 37 °C in a 5% CO_2 atmosphere. The cell growth rate was determined after MTT staining. At the end of the incubation period, 20 μL of MTT solution (from a stock solution of 5 mg/mL) was added to each well. After incubation at 37 °C for 4 h, 100 μL of SDS solution (10% in 0.01 M HCI) was added to each well, and the plates were further incubated at 37 °C overnight. OD was measured at 540 nm (ref 630 nm) with a Multiscan EX ELISA reader. CI values at 50% of the growth inhibition dose were determined using CompuSyn software (ComboSyn, Inc., Paramus, NJ, USA) to plot four to five data points at each ratio. CI values were calculated by means of the median-effect equation, according to the Chou–Talalay method, where CI < 1, CI = 1, and CI > 1 represent synergism, additive effect (or no interaction), and antagonism, respectively[58,59].

Testing for antimicrobial activity

Bacterial strains and culture conditions

The test microorganisms used in the study were 4 standard and 1 clinical isolates with different antibiotic resistance profile. The standard Gram-positive strains were *Streptococcus agalactiae* (ATCC 13813), and *Staphylococcus epidermidis* (ATCC 12228). The standard Gram-negative strains were *Moraxella catarrhalis* (ATCC 25238), and *Haemophilus influenzae* (ATCC 49766). Moreover, *Proteus mirabilis* (HNCMB 60076), *Escherichia coli* ATCC (ATCC 25922), *Salmonella enterica serovar Typhimurium* 14028s, *Staphylococcus aureus* (ATCC 25923), and the methicillin and ofloxacin resistant *Staphylococcus aureus* 272123 clinical isolates were used in the study. Bacterial cultures were grown on standard Mueller-Hinton agar (MH) and horse blood (MHF) plates at 37 °C under aerobic environment.

Determination of antibacterial activity

Screening of antibacterial activity of compounds against standard bacterial strains for their inhibition zones was carried out by standard disc diffusion method[60]. Briefly, the compounds were dissolved in DMSO at concentration 5 (**26** and **27**) and 4 (**28**) mg/mL. The bacterial suspension (inoculums 0.5 McFarland, 1 – 2×10^8 CFU ml^{-1}) was spread on plate and the sterile filter paper discs (6 mm in diameter) impregnated with 10 μL of the compound solution was placed. DMSO served as negative control, and ampicillin, erythromycin, imipenem, cefuroxime and vancomycin were used as positive control. The plates were incubated (35 +/-2 °C for 24 h) under aerobic conditions. The diameters of inhibition zones created by the compounds (including the disc) were measured and recorded.

Determination of minimum inhibitory concentrations by microdilution method

The minimum inhibitory concentrations (MICs) of all tested compounds (**1**-**4**, **21**, and **22**) were determined according to the Clinical and Laboratory Standards Institute (CLSI) guidelines in three independent assays. The compounds were diluted in 100 μL of Mueller–Hinton medium in 96-well flat-bottomed microtiter plates. The starting concentration was 100 μM, and two-fold serial dilutions were prepared in the microplates before the addition of the bacterial culture. Then, a 10^{-4} dilution of an overnight bacterial culture in 100 μL of the medium was added to each well, with the exception of the medium control wells. The

plates were further incubated at 37 °C for 18 h; at the end of the incubation period, MIC values of the tested compounds were determined by naked eye[61].

Testing for anti-inflammatory activity

Cyclooxygenase (COX) inhibitory activity

Based on the fluorometric method described in BioVision's COX-1 inhibitor screening kit leafkit (K548-100, BioVision, CA, USA) and COX-2 inhibitor screening kit leafkit (K547-100, BioVision, CA, USA), respectively, COX-1 and COX-2 inhibitory activities were assessed. The sample solutions were dissolved in DMSO and then in buffer to achieve suitable concentrations. In a 96-well white plate (655,101, F-bottom, Greiner Bio-One, Germany), 80 µL reaction mix (containing 76 µL assay buffer, 1 µL COX Probe, 2 µL COX cofactor, and 1 µL COX enzyme) was added to 10 µL sample solution, DMSO, and assay buffer to obtain test wells assigned for sample screen (S), negative control (N), and blank, respectively. Ten microliters of arachidonic/NaOH solution were added to each well using a multichannel pipette to start the reaction simultaneously, and the fluorescence of each well was measured kinetically at Ex/Em 550/610 nm, at 25 °C for 10 min, using a FluoStar Optima plate reader (BMG Labtech, Ortenberg, Germany). The COX inhibitory activity of SC560 and Celecoxib, standard inhibitors of COX-1 and COX-2, respectively, was also determined.

The change in fluorescence between two points, T_1 and T_2, were determined, and relative inhibition was computed as follows:

$$\text{Inhibition \%} = [(\text{change in N} - \text{change of S}) / \text{change in N}] \times 100$$

5-Lipoxygenase (5-LOX) inhibitory activity

Based on the fluorometric method described in BioVision's 5-LOX inhibitor screening kit leafkit (K980-100, BioVision, CA, USA), measuring the decrease in fluorescence in the presence of potential 5-lipoxygenase inhibitors, 5-LOX inhibitory activity was tested. Briefly, to obtain a sample screen (S), the samples were dissolved in anhydrous DMSO, and 2 µL sample solutions were added to a 96-well white plate (655,101, F-bottom, Greiner Bio-One, Germany). Two microlitres each of assay buffer, anhydrous DMSO, and Zileuton

solution, a standard inhibitor, were added to the corresponding wells to produce a blank, negative control (N), and positive control. Assay buffer (38 µL) was added to all wells and, subsequently, 40 µL reaction mix (containing 34 µL LOX assay buffer, 2 µL LOX probe, and 4 µL LOX enzyme). The reaction was started simultaneously after 10 min using a multichannel pipette to add 20 µL diluted substrate solution to each well, and the fluorescence of each well was determined kinetically at Ex/Em 485/520 nm, at 25 °C for 20 min, using a FluoStar Optima plate reader (BMG Labtech, Ortenberg, Germany).

The change in fluorescence between two points, T_1 (3 min) and T_2 (10 min), was determined, and relative inhibition was computed as follows:

$$\text{Inhibition \%} = [(\text{change in N} - \text{change in S}) / \text{change of N}] \times 100$$

15-Lipoxygenase (15-LOX) inhibitory activity

15-LOX inhibitory activities of the compounds were assessed using Cayman's lipoxygenase inhibitor screening assay kit (760,700, Cayman Chemical, MI, USA), detecting and measuring the hydroperoxides produced in the lipoxygenation reaction using a lipoxygenase enzyme. Briefly, in a 96-well white plate (655,101, F-bottom, Greiner Bio-One, Germany), blank wells contained 100 µL assay buffer; negative-control wells contained 90 µL lipoxygenase standard solution and 10 µL assay buffer; standard inhibitor wells contained 90 µL lipoxygenase standard solution and 10 µL nordihydroguaiaretic acid (NDGA) solution, and sample wells contained 90 µL lipoxygenase standard solution and 10 µL sample solution prepared by dissolving in methanol and then assay buffer until suitable concentrations were achieved. After incubation for 10 min, 10 µL arachidonic/NaOH solution was added to all wells using a multichannel pipette to start the reaction simultaneously, and the plate was placed on a shaker. After 5 min, the reaction was stopped by adding 100 µL of chromogen to all wells, and the absorbance was read at 485 nm. The inhibition % was computed as

$$\text{Inhibition \%} = [(\text{absorbance of control} - \text{absorbance of sample}) / \text{absorbance of control}] \times 100$$

The dose-effect investigations on the most active compounds were employed to measure the concentration, inhibiting 50% of COX-1, COX-2, 5-LOX, and 15-LOX enzyme

activity. The sigmoidal dose–response model was obtained using GraphPad Prism 8.0 (La Jolla, CA, USA), and these were employed to determine the IC_{50} values of the compounds.

RESULTS

Isolation of compounds from the investigated species

Isolation of compounds from *Pholiota populnea*

The fresh mushroom material (4.2 kg) was ground in a blender and then percolated with MeOH (20 L) at room temperature. After concentration, the dry residue (151 g) was dissolved in 600 mL 50% aqueous MeOH and subjected to solvent–solvent partition with *n*-hexane (5 × 500 mL), $CHCl_3$ (5 × 500 mL), and EtOAc (5 × 500 mL) (**Figure 1**).

The *n*-hexane-soluble phase (24 g) was subjected to **NP-FC1** separation. Fractions with similar compositions were combined according to TLC monitoring (H1–H26). Fractions H20 (130 mg), H21 (400 mg), and H22 (200 mg) were further separated by **NP-FC2** and then by **NP-FC3** methods, which led to the isolation of compound **21** (10 mg) and obtaining other 13 fractions (D1–D13). Purification of D9 and D10 fractions was performed by **PTLC1** to give compound **4** (13 mg). Fractions H23 and H24 (1.7 g) were subjected to **NP-FC4**, which resulted 22 fractions (B1–B22). The combined fractions B16 (94 mg) and B17 (294 mg) were purified by **NP-FC5** method to obtain compound **1** (18 mg) and compound **3** (12 mg), respectively. Fractions B10 (95 mg) and B11 (300 mg) were first separated by **RP-FC1**, then by **PTLC2** to isolate compound **2**. Finally, compound **22** (130 mg) was isolated from fractions H10–H12 (2 g) using **NP-FC6**.

The chloroform-soluble phase part A (25.3 g) was subjected to **NP-FC9**. Fractions with similar compositions were combined according to TLC monitoring to fractions C1–C18. Compound **11** (2.1 mg) was obtained by further purification of fraction C5 (390 mg) by **NP-HPLC3** method. Fraction C7 (800 mg) was separated using multiple steps of **NP-FC10**, and **NP-FC11**, affording 14 (C7A a-n) and 12 (C7B a-l) combined fractions. Then, a final purification was conducted on C7Ae (17.5 mg) by **PTLC3** to provide compound **8** (2.5 mg). Finally, compound **20** (5.2 mg) was isolated from fraction C7Bb (5.9 mg) by **RP-HPLC2**.

The chloroform-soluble phase part B (7 g) was subjected to **GFC1**, providing 10 fractions (F1-10). The combined fractions F5 (780 mg) and F6 (320 mg) were further separated by **NP-FC12**. Fractions with similar compositions were combined based on TLC monitoring toG1-21. Fraction G12 (161 mg) was separated by **RP-HPLC3**, which resulted in 5 fractions (K1-5). Purification of fraction K2 (54.6 mg) was conducted by **NP-HPLC4** to isolate compounds **12** (8.2 mg), **19** (8.3 mg), and to obtain 3 other subfractions (L1-3). Subfraction L1 (5.6 mg) was purified by **NP-HPLC5** to yield compound **13** (2 mg). Subfraction L3 (15 mg) was further separated by **RP-HPLC4**, which led to the isolation of compound **14** (1.1 mg) and **16** (1.2 mg). Compound **17** (7.9 mg) was obtained by purification of fraction K4 (8.8 mg) via **PTLC4**. Fraction G11 (250 mg) was first separated by **RP-HPLC5**, affording 3 subfractions (M1-3). **RP-HPLC6** was applied for the final purification of M2 (10.3 mg) to yield compound **15** (1.2 mg).

The EtOAc-soluble phase (16.7 g) was subjected to **NP-FC7**, providing 17 combined fractions (E1–17). Fraction E7 (30 mg) was further separated by **NP-HPLC1**, allowing the isolation of compound **10** (2.7 mg). Fraction E11 (4.2 g) was subjected to **NP-FC8**, which afforded 14 fractions (EA 1–14). To further purify EA3 (370 mg), **NP-HPLC2** was employed, yielding fraction EA3-c (90 mg), which led to the isolation of compounds **5** (25.8 mg), and **6** (3.7 mg), **7** (2.4 mg), **9** (4.7 mg), via **RP-HPLC1**. Compound **18** (1.2 mg) was isolated from fraction EA3-a (90 mg) by **RP-HPLC7**, and then **RP-HPLC8**. Another fraction (E16, 160 mg) was first separated by **GFC2**, then by **RP-HPLC9** to obtain compounds **24** (12 mg) and **25** (3.5 mg).

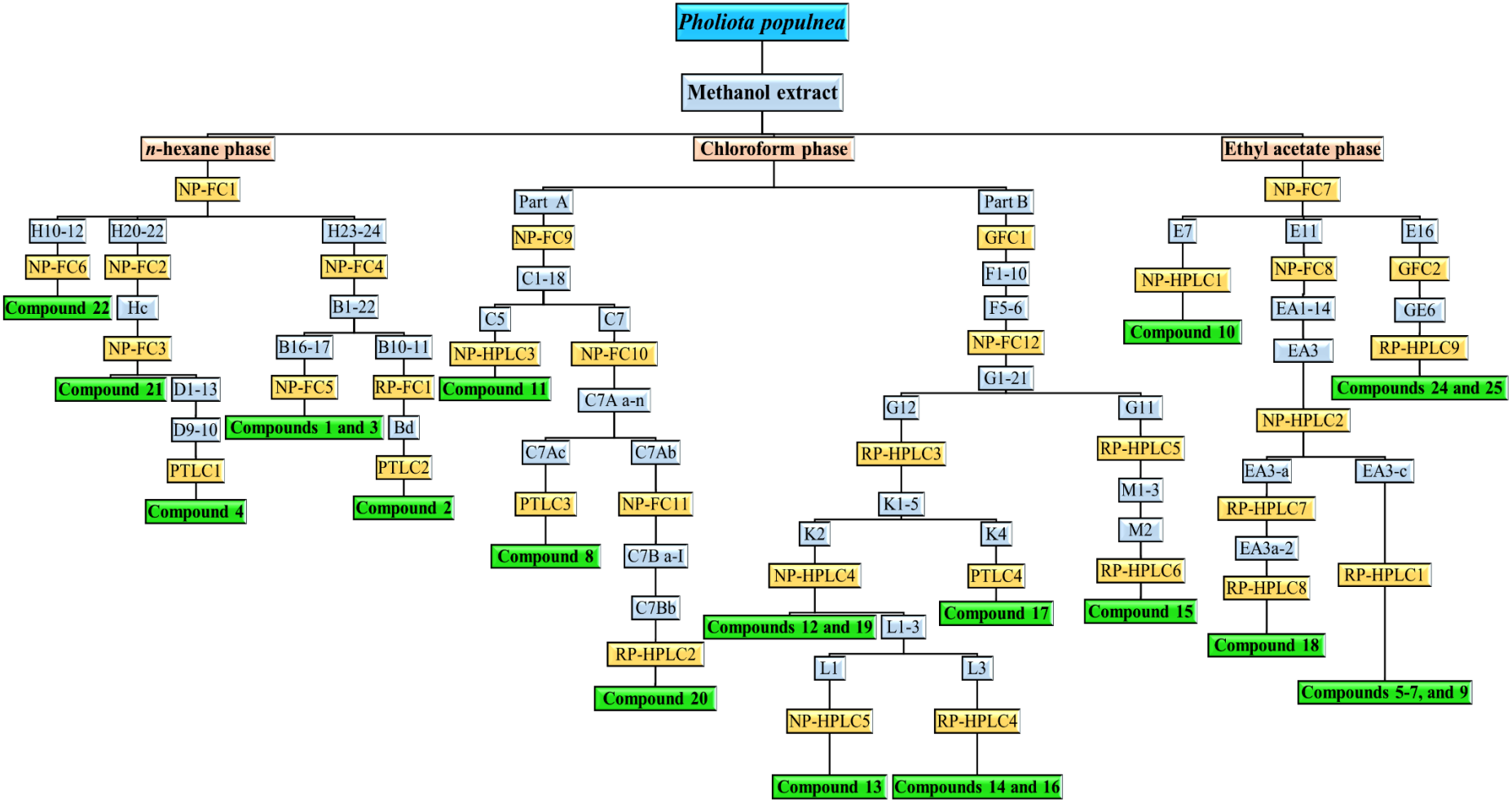

Figure 1. Isolation of compounds from *Pholiota populnea*

Isolation of compounds from *Clitocybe nebularis*

The fresh mushroom material (5.6 kg) was extracted with MeOH (20 L) at room temperature. After concentration, the MeOH extract (54 g) was dissolved in 50% aqueous MeOH and subjected to solvent-solvent partition using *n*-hexane (5 × 500 mL), $CHCl_3$ (5 × 500 mL), and then EtOAc (5 × 500 mL) (**Figure 2**).

The $CHCl_3$ soluble phase (2.12 g) was separated by **NP-FC13**. According to TLC monitoring, fractions with similar compositions were combined to C1-C15. Fractions C7 (142 mg), C8 (108 mg) and C9 (69 mg) were further chromatographed by **RP-FC2**, then by **RP-FC3**, resulting in the isolation of compounds **26** (31 mg) and **27** (2.7 mg).

The EtOAc phase (4.15 g) was separated by **NP-FC14** to obtain 20 major combined fractions (E1–20). Fractions E13 (33 mg), E14 (18 mg) and E15 (20 mg) were further separated by a combination of **NP-FC15**, then **PTLC5** to isolate compound **28** (2 mg).

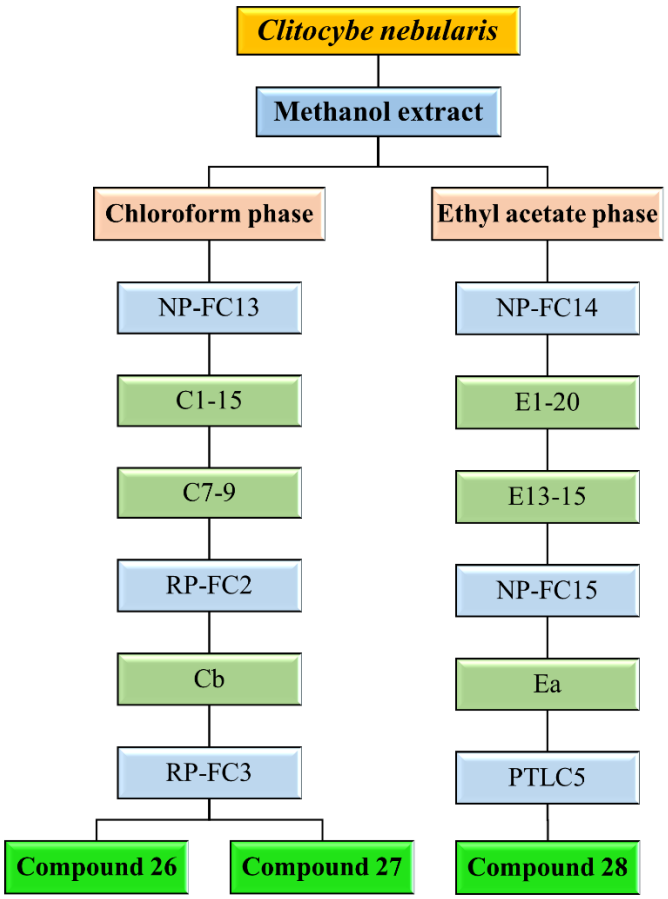

Figure 2. Isolation of compounds from *Clitocybe nebularis*

Characterization and structure determination of the isolated compounds

The structure elucidation of the isolated compounds was performed by means of NMR and MS spectroscopy. HRESIMS measurements revealed the molecular masses and molecular compositions of the compounds. Information from 1D (^{1}H-NMR and JMOD) and 2D (^{1}H-^{1}H COSY, NOESY, ROESY, HSQC and HMBC) NMR experiments provided the most important information for the structure determination. Complete assignments of the ^{1}H and ^{13}C NMR signals, and optical rotation data were provided for the new compounds. In the thesis the structure determinations are presented in the order of the compounds from pholiol A to pholiol S.

Compounds from *Pholiota populnea*

Investigation of the MeOH extract prepared from the edible mushroom *Pholiota populnea* led to the isolation of 25 compounds (**Figure 3**). Structure determination revealed 19 undescribed triterpenes, for which the trivial names pholiols A-S (**1-19**) were given.

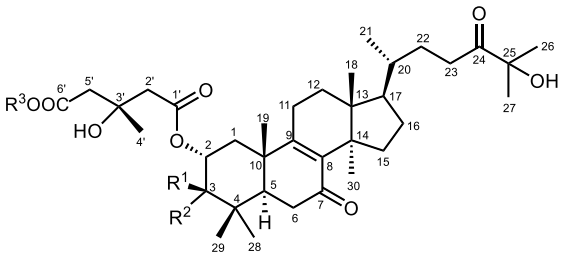

	R^1	R^2	R^3
1	OAc	H	H
2	OAc	H	CH_3
8	OH	H	CH_3
9	O		H

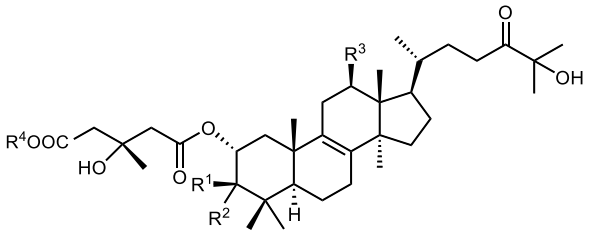

	R^1	R^2	R^3	R^4
3	OAc	H	OH	H
4	OAc	H	OH	CH_3
5	O		H	H
6	OAc	H	H	H
7	OH	H	H	H

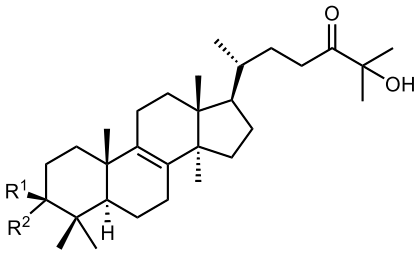

	R^1	R^2
10	OH	H
11	O	

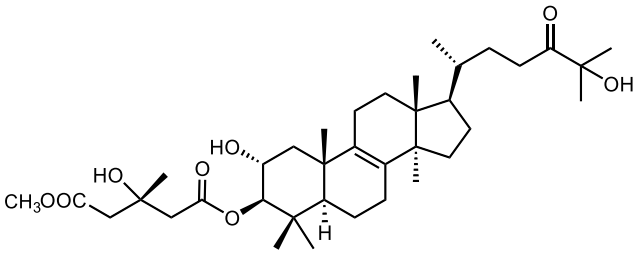

12

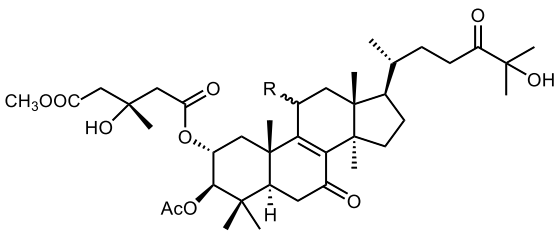

	R
13	*β*OH
14	*α*OH

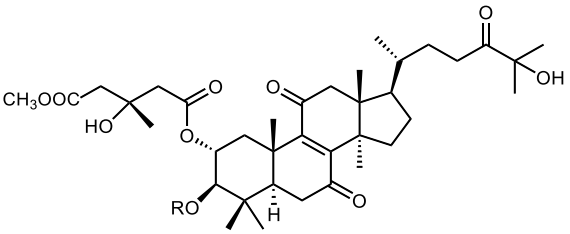

	R
15	Ac
16	H

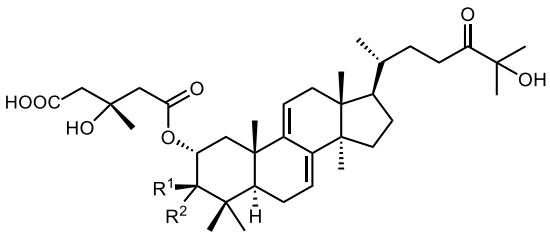

	R^1	R^2
17	OAc	H
18	O	

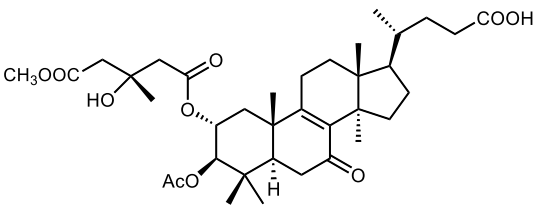

19

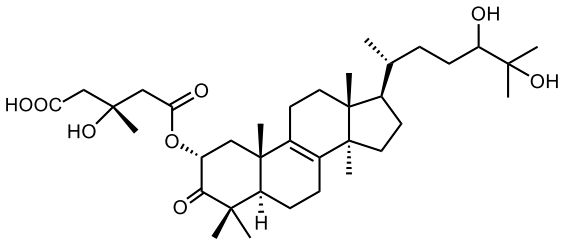

20

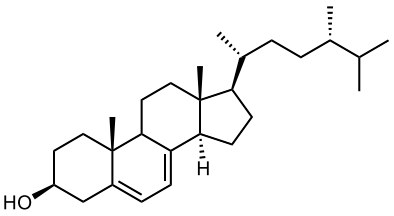

22

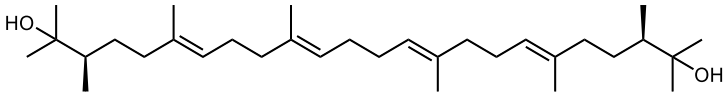

21

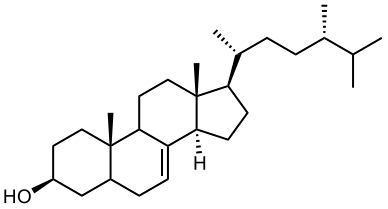

23

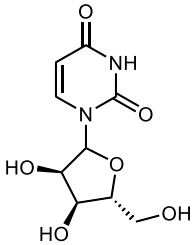

24

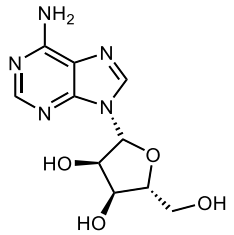

25

Figure 3. Structures of compounds from *Pholiota populnea*

Based on the HRESIMS data, the molecular formulas of compounds **1** and **2** were $C_{38}H_{58}O_{10}$ and $C_{39}H_{60}O_{10}$, respectively, differing only in a methylene group. The ^{1}H and ^{13}C NMR spectra of **1** and **2** (**Table S1** and **S2**) were similar except for a singlet signal with three-proton intensity at δ_H 3.71 appearing in the ^{1}H NMR spectrum and the extra resonance at δ_C 51.7 in the ^{13}C NMR spectrum of **2**. These findings suggested that **2** was the *O*-methyl derivative of **1**. In accordance with the elemental compositions, the ^{13}C NMR spectra presented 38 and 39 resonances in compounds **1** and **2**, respectively. Based on the HSQC spectra, besides the additional methoxy group in **2**, 10 methyl, 10 methylene, and 5 methine groups, and 13 nonprotonated carbons were commonly present in the compounds. Considering the elemental compositions and the chemical shift values of the nonprotonated carbons, two carbonyl groups (δ_C 214.9/214.8 and δ_C 197.9/197.9), three carboxylate moieties (δ_C 173.7/172.1, 170.8/171.2, and 171.4/170.6), an unsaturation (δ_C 139.2/139.1 and δ_C 163.1/163.0), and two sp^3 carbons attached to oxygens (δ_C 76.2/76.2 and 69.6/69.5) were present in **1** and **2**. The remaining four signals (δ_C 39.3/39.2, 40.5/40.5, 44.9/44.9, and 47.8/47.8 for **1**/**2**) could be ascribed to sp^3 nonprotonated carbons. Based on the characteristic HMBC correlations of the angular methyl singlets [H_3-18 with C-12, C-13, C-14, and C-17; H_3-19 with C-1, C-5, C-9, and C-10; H_3-21 with C-17, C-20, and C-22; H_3-29 and H_3-30 with C-3, C-4, and C-5], it was concluded that **1** and **2** are based on a lanostane skeleton. The HMBC correlations of the *O*-methine doublets at δ_H 4.85/4.83 with C-1, C-4, C-29, and C-30 confirmed their assignment to H-3 in **1**/**2**, while HMBC cross-peaks of the *O*-methine groups at δ_C 70.3/69.9 (C-2) with protons at δ_H 4.85/4.83 (H-3) suggested that the lanostane skeleton bears oxygen-containing substituents at both C-2 and C-3. The HMBC correlations of the acetyl CO signal with H-3 and the acetyl methyl signal suggested the presence of an acetate group at C-3, while, based on the HMBC correlations of H-2/C-1′, H-2′/C-1′, H-2′/C-3′, H-2′/C-4′, H-2′/C-5′, H-4′/C-5′, and H-5′/C-6′, a 3-hydroxy-3-methylglutarate moiety was attached to C-2 in compounds **1** and **2**. The additional H-7′/C-6′ HMBC correlation in compound **2** suggested that **2** was the methyl ester of compound **1**. Further to these, the HMBC correlations of the doublet of doublets at δ_H 1.88/1.85 (assigned to H-5) with C-4, C-10, C-19, C-29, and C-30 confirmed this assignment, while long-range correlations of H-5 with the methylene at δ_C 36.2/36.2 and with the carbonyl at δ_C 197.8/197.8 enabled the assignment of C-6 and suggested the presence of a keto group in position 7. In parallel, the HMBC correlations between the diastereotopic protons (H-22) and the methylene group at δ_C 32.6/32.5 (C-23) and carbonyl group at δ_C 214.9/214.8 (C-24) and between the methyl singlets of H_3-26 and H_3-27 and C-24 and nonprotonated carbon

at δ_C 76.2/76.2 (C-25) led to the conclusion that a 24-keto-25-hydroxy side chain was present at C-17. Based on the complete ^{1}H and ^{13}C NMR assignments (**Table S1** and **S2**), compounds **1** and **2** were identified as fasciculic acid A (66, 67) derivatives.

According to the observed NOE correlations of H_3-18 with H-11*β*, H-15*β*, H-16*β*, and H-20, those of H_3-19 with H-1*β*, H-2, H-11*β*, and H_3-29, and of H_3-28 with H-15*α*, H-16*α* and H-17, the relative stereochemistry as depicted in structural formulas **1** and **2** was proposed for the two compounds. Thus, compound **1**, named as pholiol A, was assigned as the 3-*O*-acetyl-7,24-diketo analogue of fasciculic acid A (66, 67), while pholiol B (**2**) was assigned as its methyl ester. The relative configuration of the C-3′ chiral center could not be determined on this basis and is only tentatively given as *S*, based on the close chemical shift values with those of similar compounds (66, 67) and on assuming that similar metabolic pathways led to the formation of the structurally similar compounds in the different fungal species.

The molecular formulas of **3** ($C_{38}H_{60}O_{10}$) and **4** ($C_{39}H_{62}O_{10}$) derived from HRESIMS measurements differed only in a methylene group, similarly to those of compound pair **1** and **2**. As compared to pholiols A (**1**) and B (**2**), compounds **3** and **4** contained two additional hydrogens, nominally corresponding to the saturation of the double bond in **1**/**2**.

The ^{1}H and ^{13}C NMR spectra of **3** and **4** were highly similar to those of compounds **1** and **2**. The most striking differences were the presence of a triplet signal with one hydrogen intensity at δ_H 4.13/4.14 in the ^{1}H NMR spectrum and in parallel the absence of the carbonyl resonance belonging to C-7 and the appearance of resonance at δ_C 72.8/72.8 in the ^{13}C NMR spectrum of **3**/**4**. Thus, at first sight, the reduction of the keto group at C-7 to a hydroxy group was envisaged. The ^{1}H and ^{13}C NMR spectra of **3** and **4** were almost identical, except for the presence of a singlet with a three-hydrogen intensity at δ_H 3.73 in the ^{1}H NMR spectrum and a carbon signal at δ_C 51.7 in the ^{13}C NMR spectrum of **4**. This suggested that **4** was the methyl ester of compound **3**. Analysis of the HSQC and HMBC data showed that a hydroxy group was attached to C-12 ($\delta_{H\text{-}12}$ 4.13/4.14, each 1H, t, J = 7.7 Hz; $\delta_{C\text{-}12}$ 72.8/72.8 for **3**/**4**; HMBC correlation between H-18 and C-12) and a methylene group was present in position 7 based on the HMBC correlation of H-5 and H-6 with C-7. Compound **3**, named as pholiol C, was identified as the 24-keto derivative of fasciculic acid B [63], while pholiol D (**4**) was identified as its methyl ester. The similar chemical shifts and NOE correlations suggested that the relative configurations of the C-2, C-3, C-5, C-10, C-14, C-17, and C-20 (and C-1′) chiral centers of **3** and **4** were identical to those determined for pholiols A (**1**) and

B (**2**). The NOE correlations of H-12 with H-11α, H-17, and H-28 (**Figure S1**) suggested that the hydroxy group occupied the β position (thus, the C-12 chiral center had an *R* configuration) in pholiols C (**3**) and D (**4**).

Compound **5** was isolated as a white amorphous powder with an optical rotation of $[\alpha]_D^{25}$ +49 (*c* 0.1, MeOH). Its protonated molecular ion at *m/z* 617.4063 $[M+H]^+$ (calcd for $C_{36}H_{57}O_8$ 617.4048) in the HRESIMS spectrum offered the molecular formula $C_{36}H_{56}O_8$. The ^{1}H NMR spectrum exhibited the presence of a 3-hydroxy-3-methylglutarate [δ_H 2.80 m (2H), 2.75 m (2H), 1.41 s (CH_3); δ_C2 × 171.6, 2 × 46. 6, 45.8, 70.9, 27. 6] ester group in the molecule characteristic to members of pholiol series (**Table S3** and **S4**). Furthermore, the ^{1}H NMR spectrum demonstrated resonances of seven tertiary (δ_H 1.40, 2 × 1.30, 1.11, 1.18, 0.93, and 0.78, each 3H, s) and one secondary (δ_H 0.94, 3H, d, J = 6.2 Hz) methyl groups as well as one oxymethine (δ_H 5.67, dd, J = 13.6 and 5.6 Hz). From the ^{13}C J-MOD spectrum, two keto groups (δ_C 210.9 and 217.8) and an oxygen-substituted nonprotonated carbon (δ_C 77.9) could be identified. The presence of a tetrasubstituted olefin bond was obvious from the nonprotonated sp^2 carbon signals at δ_C 136.9 and 134.7. The 1D NMR data proposed that compound **5** is a lanostanol-en-dione monoester. Regarding its HMBC correlations with δ_H 2.36 (H-1a), 1.66 (H-1b), 5.67 (H-2), 1.11 (H_3-28), and 1.18 (H_3-29), the keto group at δ_C 210.9 was placed at C-3. The other keto group (δ_C 217.8) was concluded to be at C-24 based on its long-range correlations with δ_H 1.30 (H_3-26, H_3-27) and 2.67 (H_2-23). The HMBC correlations of C-25 (δ_C 77.9) with protons at δ_H 1.30 (H_3-26 and H_3-27) depicted the hydroxy group at C-25, whereas correlations between δ_C 171.6 (C-1′) and δ_H 5.67 (H-2) as well as 2.80 and 2.75 (H_2-2') were indicative of the position of the ester group at C-2. Based on the HMBC cross-peaks of signals at δ_C 136.9 (C-8) with δ_H 0.93 (H_3-30), 2.18 (H_2-7), and 1.73 (H-6) as well as δ_C 134.7 (C-9) with δ_H 1.40 (H_3-19) and 2.18 (H_2-7), the location of the olefin group at C-8–C-9 was determined. The relative configuration of compound **5** was examined using diagnostic Overhauser effects detected in a NOESY spectrum. The NOESY correlations of H-2 (δ_H 5.67) with H_3-19 (δ_H 1.40), H_3-29 (δ_H 1.18), and H-1a (δ_H 2.36) pointed these protons in the β orientation and the ester group in the α orientation. The NOEs between H_3-18/H-20 and H-17/H_3-30 were in line with those of lanostane triterpenes [64]. The above findings were consistent with the proposed structure of compound **5** [2α-(3-hydroxy-3-methylglutaroyloxy)-25-hydroxylanosta-8-en-3,24-dione], which was called pholiol E (**5**) (**Figure 3**).

Compound **6** was obtained as a white amorphous powder with $[\alpha]_D^{25}$ +5 (*c* 0.1, $CHCl_3$). Its molecular formula was deduced to be $C_{38}H_{60}O_9$ from the protonated molecular ion at *m/z* 661.4320 $[M+H]^+$ (calcd for $C_{38}H_{61}O_9$, 661.4310) detected in the HRESIMS spectrum. A comprehensive analysis of ^1H and ^{13}C J-MOD as well as 2D data demonstrated the presence of the same parent system and 3-hydroxy-3-methylglutarate moiety as in compound **5**, except the C-3 keto group, which was replaced by an acetoxy group (**Table S3** and **S4**). The acetoxy group is attached at C-3, as demonstrated by the sequences of the correlated protons in the ^1H–^1H–COSY spectrum: CH_2–CH(OR)–CH(OR)–(δ_H 2.11 m, 1.38 m, 5.19 t (10.8 Hz), 4.79 d). The location of the ester functionalities was corroborated by the HMBC correlations observed between δ_C 171.1 (C-1′) and δ_H 5.19 (H-2), 2.62 and 2.51 (H-2') and δ_C 171.8 (AcCO) and δ_H 4.79 (H-3), and 2.10 (AcMe), showing 3-hydroxy-3-methylglutarate at C-2 and acetate at C-3. The coupling constant of H-2 and H-3 (J = 10.5 Hz) and NOESY correlations between H-3 (δ_H 4.79)/H-1b (δ_H 1.38), H-3/H_3-28 (δ_H 0.92), H-2 (δ_H 5.19)/H-1a (δ_H 2.11), and H-2/H_3-29 (δ_H 0.95) confirmed the opposite orientation of the ester groups. The Overhauser effect of H-2 with H_3-19 (δ_H 1.13) indicated the H-2β and H-3α positions. Thus, the structure of this compound was elucidated as 2α-(3-hydroxy-3-methylglutaroyloxy)-3-acetoxy-25-hydroxylanosta-8-en-24-one (**6**), called pholiol F.

Compound **7**, called pholiol G, was isolated as a white amorphous solid with $[\alpha]_D^{25}$ +4 (*c* 0.1, MeOH). It gave the molecular formula $C_{36}H_{58}O_8$, which was determined *via* HRESIMS using the sodiated molecular ion peak at *m/z* 641.4017 $(M + Na)^+$ (calcd for $C_{36}H_{58}O_8Na$ 641.4029). In the comparison of the ^1H NMR spectra of **6** and **7**, the major differences were the remarkable paramagnetic shifts of H-3 (δ_H **6**: 4.79 d versus **7**: 3.20 d) and the absence of acetyl resonance (**Table S3**). To define the structure of **7**, a complete series of 2D NMR spectra was recorded and analyzed affording the structure 2α-(3-hydroxy-3-methylglutaroyloxy)-3β,25-dihydroxylanosta-8-en-24-one. Regarding the NOESY correlations between H-3/H_3-28, H-3/H-1b (δ_H 1.18 m), H-2/H-1a (δ_H 2.05 m), H-2/H_3-19, H-2/H_3-29, H-18$_3$/H-20, and H-17/H_3-30, the stereochemistry of **7** was found to be the same as that of pholiol F (**6**). The fragmentation behaviour of **7** was investigated by direct-injection electrospray ionization quadrupole Orbitrap high-resolution mass spectrometry. The negative ion HRMS/MS spectrum with the proposed fragmentation pathway of **7** is shown in **Figure S2**. Interestingly, mainly the 3-hydroxy-3-methylglutarate ester group of the precursor ion is involved in the fragmentation process and thus resulting in characteristic fragment ions.

Compound **8** was obtained as a white amorphous solid with optical rotation $[\alpha]_D^{25}$ +16.5 (*c* 0.5, MeOH). Its formula was assigned as $C_{37}H_{58}O_9$ by the protonated molecular ion at *m/z* 647.4166 $[M+H]^+$ (calcd for $C_{37}H_{59}O_9$, 647.4154) in HRESIMS. A detailed ^1H and ^{13}C J-MOD as well as 2D NMR spectroscopic analysis revealed that the difference between **7** and **8** was the replacement of the 7-methylene group in **7** for a keto group in **8** (δ_C 201.3). The position of the 7-keto group was established based on the HMBC correlations between C-7 and H_2-6 protons [δ_H 2.55 dd (16.3, 14.5 Hz), 2.36 m]. Furthermore, in the NMR spectra of **8**, an additional methoxy group could be observed [δ_H 3.68 s (3H), δ_C 52.0], which was assigned to the carboxymethyl ester of 3-hydroxy-3-methylglutarate moiety, as indicated by the HMBC correlation of OCH_3 group with C-6'. Therefore, compound **8** [lanosta-8-ene-3,25-diol-7,24-dione 2*α*-(methyl 3-hydroxy-3-methylglutarate)] was elucidated as depicted in **Figure 3** and named pholiol H.

Compound **9** with optical rotation of $[\alpha]_D^{25}$ +11 (*c* 0.1, MeOH) had the molecular formula of $C_{36}H_{54}O_9$ as deduced from the prominent pseudomolecular ion peak in HRESIMS at *m/z* 631.3844 $[M+H]^+$ (calcd for $C_{36}H_{55}O_9$, 631.3841). The ^1H and ^{13}C NMR spectral data (**Table S3** and **S4**) depicted that **9** was also a lanostane-type triterpene, exhibiting a similar structure to that of pholiol E (**5**). A detailed comparison of these two compounds revealed an additional keto group at δ_C 200.3 in **9** instead of a methylene group, which is bonded at C-7 as displayed by the long-range correlation of C-7 with H-6. The tetrasubstituted $\Delta^{8,9}$ olefin was downfield shifted [δ_C **5**: 136.9 (C-8), 134.7 (C-9); **9**: 140.2 (C-8), 166.6 (C-9)] as a consequence of the emerging enone system. Diagnostic $^1H,^1H$–COSY, HSQC, and HMBC correlations resulted in the assignment of all proton and carbon chemical shifts, and NOESY cross-peaks (**Figure S3**) afforded the stereochemical assignment of compound **9** [2*α*-(3-hydroxy-3-methylglutaroyloxy)-25-hydroxylanosta-8-en-3,7,24-tri-one] named pholiol I.

The molecular formula of compound **10** was determined as $C_{30}H_{50}O_3$ by analyzing the prominent pseudomolecular ion peak at *m/z* 459.3833 $[M+H]^+$ (calcd for $C_{30}H_{51}O_3$ 459.3833) in HRESIMS. Compound **10** was obtained as a colorless amorphous solid with $[\alpha]_D^{25}$ +39 (*c* 0.1, MeOH). It exhibited close similarity to pholiol F (**6**), but the 3-hydroxy-3-methylglutarate ester moiety was absent in **10**. The 3-hydroxy, 8,9-olefin, 24-keto, and 25-hydroxy functionalities of lanostane triterpene were confirmed by the HMBC correlations of C-3 (δ_C 79.7) with H_3-28 (δ_H 0.98 s) and H_3-29 (δ_H 0.81 s); C-8 (δ_C 135.8) with H_3-30 (δ_H 0.92 s); C-9 (δ_C 136.1) with H_3-19 (δ_H 1.01 s) and H_2-7 (δ_H 2.07 m); C-24 (δ_C 217.8) with H_2-23 (δ_H 2.65 m); and C-25 (δ_C 77.9) with H_3-26 (δ_H 1.29 s) and H_3-27 (δ_H 1.29 s),

respectively (**Table S3** and **S4**). Based on the Overhauser effects of H-3/H-5 and H-3/H_3-28 as well as the coupling constants of H-3 (10.1 and 6.3 Hz), the 3*β* orientation of the hydroxy group was determined[65]. Therefore, compound **10**, named pholiol J, was identified as 3*β*,25-dihydroxylanosta-8-en-24-one. This compound was first isolated from natural source, but previously synthesized without assignments of NMR chemical shifts[66]. In the previous experiment, side-chain modified lanosterol derivatives were produced with the aim to develop compounds that reverse protein aggregation in cataracts. Lanosterol analogs with remarkable potency and efficacy in reversing several types of mutant crystalline aggregates were identified.

Compound **11**, named pholiol K, was isolated as a colorless amorphous solid with optical rotation $[\alpha]_D^{25}$ +29 (*c* 0.1, $CHCl_3$). Based on the HRESIMS pseudomolecular ion peak at *m/z* 457.3677 $[M+H]^+$ (calcd for $C_{30}H_{49}O_3$, 457.3676), the molecular formula of compound **11** was deduced to be $C_{30}H_{48}O_3$. The ^{13}C J-MOD spectrum of compound **11** demonstrated the existence of two keto groups (δ_C 215.1 and 217.9) in the molecule; one of them was placed at C-3 (δ_C 215.1) with regard to the HMBC correlations between C-3 and H_3-28 (δ_H 1.10 s), H_3-29 (δ_H 1.07 s), and H-2a (δ_H 2.57 m) whereas the other at C-24 (δ_C 217.9) based on the long-range correlations of C-24 and H_3-26 (δ_H 1.39 s), H_3-27 (δ_H 1.38 s), and H_2-23 (δ_H 2.55 m). The 25-hydroxy functionality was proposed by the carbon chemical shift value of $\delta_{C\text{-}25}$ 76.4. NOESY cross-peaks between H_3-18/H-20, H_3-28/H-5, and H-17/H_3-30 were consistent with the suggested structure of compound **11** [25-dihydroxylanosta-8-en-3,24-dione] (**Figure 3**).

Compound **12**, named pholiol L, was obtained as a colorless amorphous solid with $[\alpha]^{23}_D$ −11.6 (*c* 0.1, $CHCl_3$). Its HRESIMS spectrum exhibited a protonated molecular ion at *m*/*z* 647.4147 $[M + H]^+$ (calcd for $C_{37}H_{59}O_9^+$ 647.4154), indicating the molecular formula of $C_{37}H_{58}O_9$. The ^1H NMR and ^{13}C-JMOD spectra indicated a 3-hydroxy-3-methylglutaric acid 6-methyl ester (MeHMG) derivative [δ_H 2.75 m, 2.57 m (H_2-2′), 2.92 m, 2.27 m (H_2-5′), 1.42 s (H_3-4′), 3.72 s (OCH_3-7′); δ_C 171.4 (1′), 173.3 (C-6′), 46.3 (C-2′), 43.7 (C-5′), 70.4 (C-3′), 28.3 (C-4′), 52.1 (OCH_3-7′)], substituted with two keto groups (δ_C 198.3 and 215.0); the presence of two hydroxy groups was suggested by the carbon resonances of a methine group at δ_C 66. 9 (C-2) and a quaternary carbon at δ_C 76.3 (C-25). A sequence of the correlated protons in the ^1H–^1H COSY spectrum –CH_2–CH(OR)–CH(OR)– (δ_H 2.21 dd (12.5, 3.8 Hz), 1.44 m, 3.92 dt (3.8, 11.1 Hz), 4.60 d (9.9 Hz) could be assigned to the C-1–C-3 part of the molecule, with regard to the HMBC correlations between H_2-1 and C-10; H_3-19 and C-10;

H-3 and C-4; H_3-28 and H_3-29 and C-4; H-1a, H_3-28, H_3-29, and H_3-19 with C-5 (**Figure 4**). NMR data of compound **12** were very similar to those of the previously isolated pholiol H, with the major differences in chemical shifts of H-2, H-3 (**12**: $\delta_{H\text{-}2}$ 3.92 dt, $\delta_{H\text{-}3}$ 4.60 d versus pholiol H: $\delta_{H\text{-}2}$ 5.07 dt, $\delta_{H\text{-}3}$ 3.24 d), and C-2 and C-3 (**12**: $\delta_{C\text{-}2}$ 66.9, $\delta_{C\text{-}3}$ 84.5 versus pholiol H: $\delta_{C\text{-}2}$ 73.4, $\delta_{C\text{-}3}$ 80.0) demonstrating the connection of the ester group at position C-3 and hydroxyl group at C-2 in **12**. The relative configuration of **12** was determined based on the Overhauser effects detected in the NOESY spectrum. The NOESY correlation of H-3 (δ_H 4.60) with H-1α (δ_H 1.44), H_3-28 (δ_H 0.91), and H-5 (δ_H 1.82) showed these protons in the α orientation, while correlations of H-2 (δ_H 3.92) with H-1β (δ_H 2.21), H_3-19 (δ_H 1.24), and H_3-29 (δ_H 0.96) indicated the β orientation of H-2 and the 19- and 29-methyl groups (**Figure 4**). The Overhauser effect between H_3-18 and H-20 was indicative for their β position, similar to the previously isolated pholiol compounds. All of the above evidence confirmed the structure of pholiol L (**12**), as depicted in **Figure 3**.

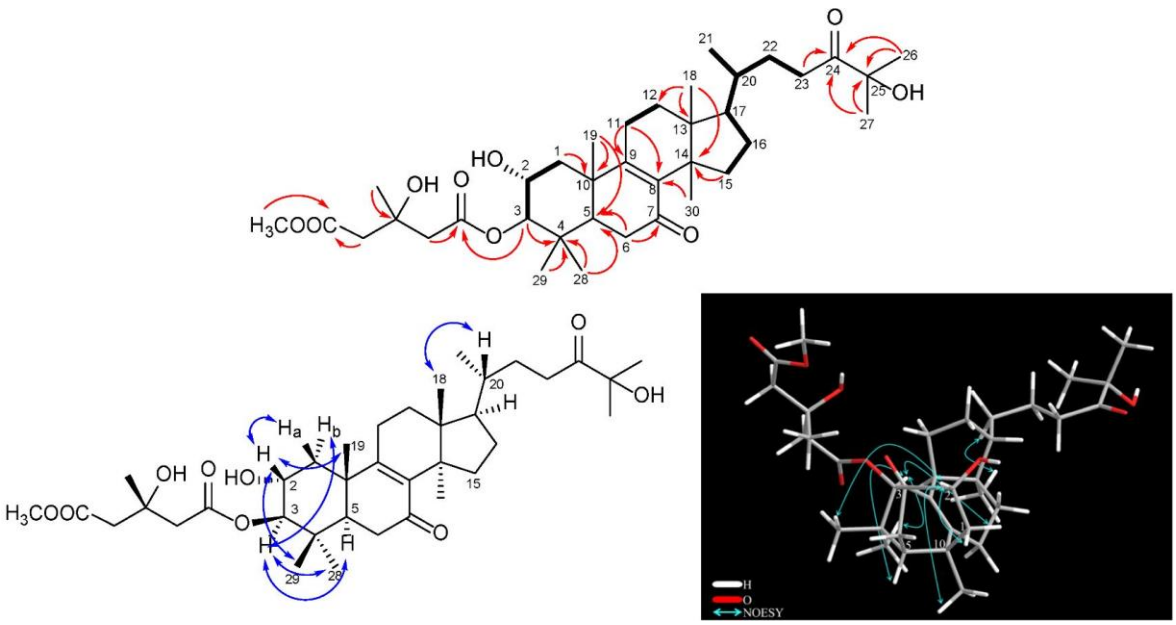

Figure 4. Key COSY (–), HMBC (→), and NOESY (H↔H) correlations of pholiol L (**12**).

Compound **13** (pholiol M) was obtained as a colorless amorphous solid with an optical rotation of $[\alpha]^{23}_D$ −10.9 (*c* 0.05, $CHCl_3$). Its molecular formula was assigned as $C_{39}H_{60}O_{11}$ by the deprotonated molecular ion at *m*/*z* 703.4078 $[M\text{-}H]^-$ (calcd for $C_{39}H_{59}O_{11}^-$ 703.4063) in HRESIMS. The ^{1}H NMR and ^{13}C-JMOD spectrum showed that compound **13** is a lanostane diester esterified with an acetic acid [δ_H 2.07 s (3H); δ_C 170.8 (CO), 21.1 (CH_3)], and a 3-hydroxy-3-methylglutaryl 6-methyl ester [δ_H 2.68 m, 2.54 m (H_2-2′), 2.70 m, 2.62 m (H_2-5′), 1.35 s (H_3-4′), 3.71 s (OCH_3-7′); δ_C 171.4 (1′), 172.3 (C-6′), 45.0 (C-2′), 45.0 (C-

5′), 69.7 (C-3′), 27.7 (C-4′), 51.9 (OCH_3-7′)] (**Table S5** and **S6**). Similarly to pholiol L (**12**), compound **13** contained the 8,9-en-7-one moiety [δ_C 139.7 (C-8), 160.5 (C-9), 199.7 (C-7)] and C_8 aliphatic chain at C-17 substituted with a keto [δ_C 214.9 (C-24)] and a hydroxy group [δ_C 76.4 (C-25)]. The ^{1}H NMR and JMOD spectra exhibited an additional *O*-substituted methine at δ_H 4.57 br t (5.7 Hz), δ_C 67.3, which was placed at C-11 with regard to the ^{1}H-^{1}H COSY [δ_H 2.28 m, 1.88 m, 4.57 br t; –CH_2–CH(OH)–; C-12–C-11] and HMBC correlations of H-11 with C-8 and C-13; and H-12 with C-14. The assignment of C-11 (δ_C 67.3) and C-12 (δ_C 42.9) were in agreement with literature data [67]. The ^{1}H-^{1}H COSY spectrum defined the structural fragment with correlated protons –CH_2–CH(OR)–CH(OR)– (δ_H 2.87 dd, 1.70 t, 5.29 dt, and 4.83 d) (C-1–C-3). The positions of the ester groups were established via the HMBC experiment. The correlations of the carbonyl signals at δ_C 171.4 (1′) and 170.8 (AcCO) with the proton signals at δ_H 5.29 (H-2) and δ_H 4.83 (H-3) indicated the presence of the 3-hydroxy-3-methylglutaryl 6-methyl ester (MeHMG) and acetyl groups at C-2 and C-3, respectively. The relative configuration was determined with the use of a NOESY measurement. The Overhauser effects between H-5/H-3, H-3/H_3-28, H-3/H-1α, and H-1α/H-11 pointed these protons in the α position, while those between H-1β/H-2, H-2/H_3-19, H_3-19/H-1β, and H-2/H_3-29 indicated their β position. The above findings were consistent with the proposed structure of **12** as depicted in **Figure 3**.

Compound **14**, named pholiol N, was isolated as a white amorphous powder with an optical rotation of $[\alpha]^{23}_D$ −8.9 (*c* 0.05, $CHCl_3$). Its molecular composition was determined as $C_{39}H_{60}O_{11}$ based on the sodiated molecular ion peak at *m*/*z* 727.4041 $[M + Na]^+$ (calcd for $C_{39}H_{60}O_{11}Na^+$ 727.4028) detected in the HRESIMS spectrum. Careful evaluation of the 1D and 2D NMR spectra of **14** resulted in the elucidation of the same planar structure as that of compound **13**. The main differences were found in the chemical shift values of carbons C-11–C-12 [δ_C 65.6 (C-11), 44.4 (C-12) for **14**; δ_C 67.3 (C-11), 42.9 (C-12) for **13**], indicating that the orientation of 11-OH group may be different. This was confirmed by the NOESY correlations of **14**; the Overhauser effects between H_3-18 (δ_H 0.65 s) and H-12β (δ_H 2.46 m); H-12β and H-11 (δ_H 4.49 m); H-12α (δ_H 1.84 m) and H_3-30 (δ_H 1.12 s) proved the α position of the 11-hydroxy group. NOEs of H-2 with H_3-19 and H_3-28; and that of H-3 with H_3-29; H_3-18 with H-20 corroborated the stereostructure of compound **14**, as depicted in **Figure 3**.

Compound **15**, named pholiol O, was obtained as a colorless amorphous solid with an optical rotation of $[\alpha]^{27}_D$ +11.8 (*c* 0.05, $CHCl_3$). It gave the molecular formula $C_{39}H_{58}O_{11}$, determined from the HRESIMS by the sodiated molecular ion peak at *m*/*z* 725.3877 (M +

Na)$^+$, (calcd for $C_{39}H_{58}O_{11}Na^+$ 725.3871). Analysis of ^{1}H NMR and ^{13}C-JMOD spectra of **15** indicated the presence of the same esterification pattern and aliphatic chain at C-17 as in compound **13** (**Table S5** and **S6**). The main differences were the remarkable difference in chemical shifts of C-8 (**13**: δ_C 139.7; **15**: δ_C 152.2), and C-9 (**13**: δ_C 160.5; **15**: δ_C 151.9), and the presence of an additional keto group (δ_C 203.6) at C-11 in compound **15**. The position of this keto group was established based on its HMBC correlations with H_2-12 [δ_H 2.87 d, 2.58 d (J = 16.1 Hz)]. NOESY correlations between H-3 and H-5, and H_3-28, H-1α; between H-2 and H-1β, and H_3-19; between H-12β and H_3-18; between H-12α and H-30; and between H-30 and H-20 allowed the stereochemical features identical with those of compounds **12** and **13** to be assigned for **15** (**Figure 3**).

Compound **16** (pholiol P) was obtained as a white amorphous solid with an optical rotation of $[\alpha]^{23}$ −1.6 (*c* 0.05, MeOH). Its molecular formula was deduced to be $C_{39}H_{56}O_{10}$ from HRESIMS sodium adduct ion peak at *m*/*z* 683.3767 $[M + Na]^+$ (calcd for $C_{37}H_{56}O_{10}Na^+$ 683.3766). Comprehensive analysis of ^{1}H NMR, ^{13}C JMOD and 2D NMR data of **15** and **16** indicated the presence of the same 2,3,25-trihydroxy-7,11,24-triketo-triterpene core and MeHMG esterification at C-2 as discussed at compound **15**, with the exception of the acetoxy group at C-3, which was replaced by a hydroxy group. This was clearly shown by the H-3 signal at δ_H 3.28 d (J = 11.0 Hz) for **16**, instead of H-3 at δ_H 3.28 d (J = 11.0 Hz) for **15** (**Table S5** and **S6**). NOESY correlations between H-2/H_3-19, H-3/H_3-28, H-11α/H_3-30, and H_3-28/H-6α permitted the same stereochemistry of **16** as that of **15**.

Compound **17**, pholiol Q, was isolated as a colorless amorphous solid with an optical rotation of $[\alpha]^{27}_D$ +5.0 (*c* 0.1, MeOH). Its molecular formula was determined to be $C_{38}H_{58}O_9$ based on the HRESIMS ion peak at *m*/*z* 657.4010 $[M–H]^-$ (calcd for $C_{38}H_{57}O_9^-$, 657.4008). Analysis of ^{1}H NMR and ^{13}C–JMOD as well as 2D NMR data demonstrated the presence of a 3-hydroxy-3-methyl glutarate and an acetate group in **17**, and the same side chain at C-17 as in pholiols L–N (**12**–**16**) (**Table S5** and **S6**). NMR signals of **17** at δ_H 5.53 t (H-7) and 5.39 d (H-11), and δ_C121.2 (C-7), 143.9 (C-8), 146.3 (C-9), 118.3 (C-11) suggested two trisubstituted olefin groups which were placed at C-7–C-8, and C-9–C-11 considering the HMBC correlations of C-9 with H-7, H-12b, H-1b, H_3-19, and those of C-8 with H-11, H-6, and H_3-30. NOESY cross-peaks between H-2/H_3-29, H-2/H-1β, H-1β/H_3-19, H-3/H-1α, and H_3-30/H-17 afforded the same stereochemical assignment of compound **17** as that of **12**–**16**.

Compound **18**, pholiol R, was isolated as a white amorphous solid with an optical rotation of $[\alpha]^{22}_D$ +24.9 (*c* 0.05, MeOH). Its HRESIMS spectrum exhibited a molecular ion

peak at *m*/*z* 613.3768 $[M–H]^-$ (calcd for $C_{36}H_{53}O_8^-$, 613.3746) indicating the molecular formula of $C_{36}H_{54}O_8$. ^1H and ^{13}C NMR assignments of **7(18)**, prepared by analysis of the ^1H-^1H COSY, HSQC and HMBC spectra, showed that chemical shifts of **18** were very similar to that of **17** differing only in the resonances of ring A protons and carbons (**Table S5** and **S6**). In case of **18** a carbonyl group (δ_C 210.6) can be found at position C-3, as it was confirmed by the HMBC correlation between C-3 and H_3-28 and H_3-29. Cross-peaks in the NOESY spectrum of **18** between H-2/H_3-29, H-2/H_3-19, H-20/H_3-18, H_3-30/H-17, H-5/H_3-28, H-5/H-6*α*, and H-6*β*/H-19 were in agreement with the stereostructure of **18**, as depicted in **Figure 3**.

Compound **19** (pholiol S) was a colorless amorphous solid and had an optical rotation of $[\alpha]^{23}_D$ −14.2 (*c* 0.1, $CHCl_3$). Its HRESIMS spectrum exhibited sodium adduct ion peak at 669.3623 $[M + H]^+$ (calcd for $C_{36}H_{54}O_{10}Na^+$ 669.3609), indicating the molecular formula of $C_{36}H_{54}O_{10}$. The ^1H NMR and ^{13}C JMOD spectra evidenced the presence of one acetate and one MeHMG group in the molecule, and a 27 carbon atom containing basic skeleton (**Table S5** and **S6**). The chemical shifts of skeletal protons and carbons were very similar to those of pholiol B, with exception of the resonances of the C-17 side chain. The ^1H-^1H COSY spectrum of **19** indicated a structural fragment with correlated protons at δ_H 1.43 m, 0.92 d (3H), 1.85 m, 1.35 m, 2.40 m, 2.27 m [–CH(CH_3)–CH_2–CH_2–] which was assigned as C-20–C-23 part of **19**. This structural fragment was coupled with a carboxyl group (δ_C 178.7, C-24) with help of its HMBC correlations with H_2-22 (δ_H 1.85 m), and H_2-23 (δ_H 2.40 m, 2.27 m), and connected to C-17 as showed by the long-range correlation of C-17 (δ_C 48.9) with H_3-21 (δ_H 0.92 d). NOESY correlations between H-2/H_3-29, H-2/H_3-19, H-2/H-1*β*, H-3/H_3-28, H-3/H-1*α*, H_3-19/H-1*β*, and H_3-18/H-20 proved the stereochemistry of compound **19**, as shown in **Figure 3**.

Compound **20** was identical in all of its spectral characteristics with (+)-clavaric acid. This compound was reported to be a specific inhibitor of human farnesyl protein transferase (FPTase) (IC_{50} 1.3 μM)[68] and was first isolated from the fungus *Clavariadelphus truncatus* [69]. The ^1H and ^{13}C NMR assignments of compound **20** were published in $CDCl_3$, but in our experiment, these data were determined in CD_3OD (**Table S3** and **S4**). The NOESY correlations between H-2/H_3-19, H-2/H_3-28, H_3-18/H-20, H-2/H-1a (δ_H 2.36), H-1a/H-11a (δ_H 2.16), and H-20/H-22a (δ_H 1.82) matched the relative stereostructure of (+)-clavaric acid.

Compound **21** was identified as (6*E*,10*E*,14*E*,18*E*)-2,3,22,23-tetrahydroxy-2,6,10,15,19,23-hexamethyl-6,10,14,18-tetracosatetraene regarding its ^1H and ^{13}C NMR

chemical shift values, identical with literature data[70]. The 3*S*,22*S* configuration of **21** can be suggested based on the opposite optical rotation data than that of the 3*R*,22*R* isomer[71]. Compound **22** was found to be identical in all of its spectroscopic characteristics with that of ergosterol[72]. 3*β*-Hydroxyergosta-7,22-diene (**23**) was detected in the *n*-hexane fraction with the use of an authentic standard.

Moreover, in the EtOAc extract, uridine (**24**) and adenosine (**25**) were isolated and identified.

All compounds (**1**-**25**) were isolated and identified for the first time from this species.

Compounds from *Clitocybe nebularis*

Processing the sample of *Clitocybe nebularis* allowed to isolate 3 compounds, which were found for the first time form this species. The compounds were characterized on the basis of HRMS, MS-MS and 1D and 2D NMR data compared to those reported in the literature[73–75]. Compounds **26–28** were identified as 5*α*-ergosta-7,22-diene-3*β*,5,6*β*-triol (=cerevisterol) (**26**), (22*E*,24*S*)-5*α*-ergosta7,22-diene-3*β*,5,6*β*,9*α*-tetraol (**27**), and indole-3-carboxylic acid (**28**) (**Figure 5**).

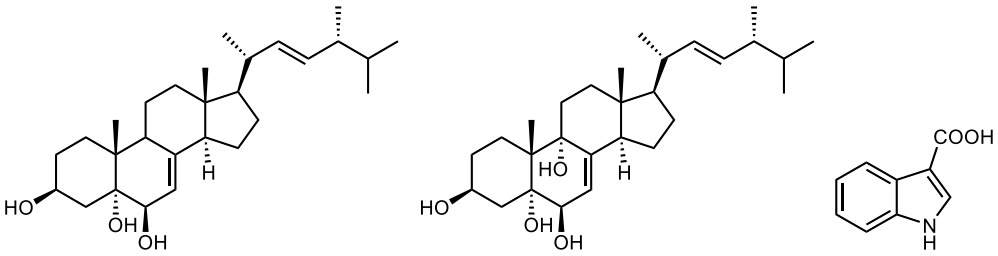

26 **27** **28**

Figure 5. Structures of compounds isolated from *Clitocybe nebularis*

Pharmacological activities of the isolated compounds

Antiproliferative assay of the compounds from *Pholiota populnea*

Pholiols L, M, O, Q, and S (**12**, **13**, **15**, **17**, and **19**), compounds isolated in good yield and high purity, were investigated for their antiproliferative activity *in vitro* by MTT assay in human colon adenocarcinoma cell lines, both sensitive (Colo205) and resistant (Colo320) ones, hormone-responsive breast cancer (MCF-7), human non-small cell lung cancer (A549), and human embryonic lung fibroblast cell line (MRC-5). The anticancer drug doxorubicin was used as a reference agent. The results, obtained as the concentration of the compound that produced half of the inhibition (IC_{50}), are shown in **Table 1**. The highest

antiproliferative effects were observed for pholiols M (**13**) and O (**15**) against the MCF-7 cell line, with IC_{50} values of 2.48 and 9.95 μM, respectively. These compounds were also potent against Colo205 cells, but to a lower extent [IC_{50} 23.91 (**13**), and 23.30 μM (**15**)], while pholiol L (**12**) was moderately active on the MRC-7 cell line (IC_{50} 21.74 μM). All other compounds exhibited weaker activity on the viability of the treated cancer cells, displaying IC_{50} values ranging from 28.07 to 89.84 μM. Compounds **12**, **13**, **15**, **17**, and **19** were tested for their antiproliferative activity in the non-cancerous human embryonic lung fibroblast cell line as well, and on the basis of these results, selectivity indexes (SI) were calculated. The relatively high SI values of pholiol M (**13**) indicated its strong and moderate tumor cell selectivity regarding the MCF-7 (SI > 40) and Colo205 (SI = 4.18) cell lines. SI values of 4.3 and 1.8 of pholiol O (**15**) indicated this compound to be moderately or slightly selective towards Colo205 cells[76]. Compounds **12**, **17**, and **19** did not display selectivity to cancerous cell lines over normal cells.

Table 1. Antiproliferative activity (IC_{50} μM) of pholiols L, M, O, Q, and S (**12**, **13**, **15**, **17**, and **19**) in human sensitive (Colo205) and resistant (Colo320) colon adenocarcinoma cells and normal embryonal fibroblast (MRC-5) cell line.

Comp	Colo205		Colo320		MCF-7		A549		MRC-5	
	Mean	SD	Mean	SD	Mean	SD	Mean	SD	Mean	SD
12	32.41	0.89	28.07	4.62	**21.74**	0.88	53.73	1.27	70.86	1.22
13	**23.91**	0.026	32.51	2.97	**2.48**	0.16	>100	–	>100	–
15	**23.39**	0.060	42.14	0.15	**9.95**	0.37	51.53	1.61	42.89	1.34
17	49.97	0.52	69.19	2.67	46.28	1.86	51.21	1.04	>100	–
19	59.87	0.55	68.54	4.40	35.33	3.03	89.84	0.75	>100	–
Dox*	0.0617	0.0128	0.25	0.06	0.155	0.0027	1.04	0.097	0.52	0.018
DMSO	>2%	–	>2%	–	>2%	–	>2%	–	>2%	–

*Dox = doxorubicin.

Cytotoxic effect of the compounds from *Pholiota populnea*

The compounds (**1**–**4**, **12**, **13**, **15**, **17**, **19**, **21**, and **22**) isolated in good yield were tested for their cytotoxic activity on sensitive Colo205 and resistant Colo320 cell lines and on the normal MRC-5 embryonal fibroblast cell line using the MTT assay with doxorubicin as a positive control. Five compounds (**12**, **13**, **15**, **17**, **19**) were tested on MCF-7 and A549 cell lines, too. In the cytotoxic assay a higher cell population and a shorter exposure were used than in the antiproliferative test. Under these conditions, the direct killing effect can be

measured instead of the cell growth inhibitory activity. Among the studied compounds, ergosterol (**22**) showed substantial cytotoxic activity against the tumor cell lines with IC_{50} values of 4.9 μM (Colo205) and 6.5 μM (Colo320) (**Table 2**). Unfortunately, this compound was more potent against the MRC-5 cell line (IC_{50} 0.50 μM). Pholiols B (**2**), D (**4**), L (**12**), M (**13**), O (**15**), Q (**17**), S (**19**) and 2,3,22,23-tetrahydroxy-2,6,10,15,19,23-hexamethyl-6,10,14,18-tetracosatetraene (**21**) possessed weak inhibitory activities (IC_{50} values between 26–93 μM) against the tested cell lines without any selectivity.

Table 2. Cytotoxic activity in human sensitive (Colo205) and resistant (Colo320) colon adenocarcinoma cells and relative resistance ratio of pholiols A–D, L, M, O, Q, S (**1**–**4**, **12**, **13**, **15**, **17**, and **19**), compound **21**, and ergosterol (**22**)

Compd	**IC_{50} (μM)**				**RR[a]**	**IC_{50} (μM)**					
	Colo205 (A)		**Colo320** (B)		B/A	**MCF-7**		**A549**		**MRC-5**	
	Mean	**SD**	**Mean**	**SD**		**Mean**	**SD**	**Mean**	**SD**	**Mean**	**SD**
1	>100	-	>100	-	-	-	-	-	-	>100	-
2	67.92	0.39	61.5	4.7	**0.90**	-	-	-	-	89.96	0.01
3	>100	-	>100	-	-	-	-	-	-	>100	-
4	51.36	0.1	48.94	0.65	**0.95**	-	-	-	-	54.18	3.00
12	40.33	1.64	33.92	1.84	**0.84**	43.69	0.03	93.61	1.94	66.08	1.36
13	35.93	0.44	67.22	3.86	1.87	>100	–	58.12	0.70	>100	–
15	31.52	0.91	91.52	4.96	2.90	>100	–	56.86	1.53	57.99	0.82
17	56.12	0.84	34.73	1.24	**0.62**	43.78	0.18	85.88	2.41	>100	–
19	57.50	0.96	57.52	2.36	1.0	42.99	0.61	83.65	6.06	55.27	0.41
21	26.7	0.33	27.48	1.56	1.03	-	-	-	-	29.06	2.2
22	**4.88**	0.57	**6.48**	0.22	1.33	-	-	-	-	**0.50**	0.09
Dox	3.32	0.08	11.96	0.88	3.60	5.73	1.02	10.22	0.07	3.60	0.35
DMSO	>2%	–	>2%	–		>2%	–	>2%	–	>2%	–

[a] RR (relative resistance ratio) = IC_{50} resistant/IC_{50} sensitive; Dox = doxorubicin

Comparing the antiproliferative and cytotoxic effects of the compounds remarkable difference displayed selectivity for the growing cell population without directly killing the exposed cells. Such a result was exhibited by pholiols M (**13**) and O (**15**), for which, no cytotoxic effect could be detected on MCF-7 cells (IC_{50} > 100 μM), proving their action exclusively on tumor cell proliferation.

Comparison of the cytotoxic activities on drug-resistant (Colo320) and sensitive (Colo205) cells allowed for the detection of relative resistance (RR), which was calculated as the ratio of the IC_{50} value in the resistant and in sensitive cancer cell lines. Compounds with RR < 1 show selectivity against resistant cells, whereas RR ≤ 0.5 indicate that the compounds have a collateral sensitivity (CS) effect[77]. The calculated RR values of the tested compounds showed selectivity against the resistant Colo320 cells of pholiols B (**2**) (RR 0.90), D (**4**) (RR 0.95), L (**12**) (RR 0.84) and Q (**17**) (RR 0.62) (**Table 2**).

Rhodamine 123 accumulation assay of the compounds from *Pholiota populnea*

The inhibitory activities of compounds **1**–**3**, **21**, and **22** on efflux function were evaluated by measuring the intracellular accumulation of rhodamine 123, a well-known P-glycoprotein substrate fluorescent dye, within the Colo320 MDR cells. Tariquidar, a strong P-gp inhibitor, was used as positive control. All tested compounds were dissolved in DMSO, and the final concentration (2.00%) of the solvent was investigated for any effect on the retention of rhodamine 123. The results revealed inhibition of P-gp MDR efflux pump activity manifested by pholiols A (**1**) and B (**2**) and aliphatic triterpene **21** (**Table 3**). In the literature, compounds with FAR values greater than 1 were considered to be active P-gp inhibitors, while compounds with FAR values greater than 10 were considered to be strong MDR modulators. The pholiol B (**2**) and the polyhydroxy-squalene derivative (**21**) exerted the highest anti-MDR effect in this bioassay with FAR values of 6.880 and 6.638, respectively.

Table 3. P-gp efflux pump inhibitory activity of compounds **1**–**3**, **21**, and **22** against MDR Colo320 cell line

Sample	**conc. µM**	**FAR**
tariquidar[a]	0.2	5.533
pholiol A (**1**)	20	3.418
pholiol B (**2**)	20	**6.880**
pholiol C (**3**)	20	0.967
compound **21**	20	**6.638**
ergosterol (**22**)	2	1.053
DMSO	2.00%	0.828

[a]Positive control.

Checkerboard combination assay of the compounds from *Pholiota populnea*

Compounds **2**, **4**, **21**, and **22** were tested for their capacity to reduce the resistance of the MDR Colo320 cell line to doxorubicin. A checkerboard microplate combination assay was accomplished, which is a well-known *in vitro* method for the assessment of drug interactions. Experimental data were analyzed using CompuSyn software, which enabled the determination of the most effective ratios of combined agents and calculation of combination indices (CI). Based on the combination indices, the type of interaction could be determined according to the literature[78]. **Table 4** reveals that pholiols B (**2**) and D (**4**), and **21** interacted in a synergistic manner, and CI values at 50% of the ED_{50} were found to be 0.348, 0.660, and 0.082, respectively. The outstanding potency of **21**, designated as very strong synergism (CI = 0.082), is favorable. In this assay ergosterol (**22**) was found to have an additive effect in combination with doxorubicin.

Table 4. Chemosensitizing activity of compounds **2**, **4**, **21**, and **22** on Colo320 adenocarcinoma cells

compound	best ratio[a]	CI at ED_{50}[b]	SD	interaction
pholiol B (**2**)	23.2:1	0.348	0.051	synergism
pholiol D (**4**)	139.2:1	0.660	0.03	Synergism
compound **21**	2.9:1	0.082	0.057	very strong synergism
ergosterol (**22**)	3.6:1	1.03	0.12	nearly additive

[a]Best ratio: the best combination ratio between compound and doxorubicin. [b]CI at ED50: combination index value at the 50% growth inhibition dose.

Antimicrobial assay of the compounds from *Pholiota populnea*

Compounds **1–4**, **21**, and **22** were tested and found to be inactive against *Escherichia coli* (ATCC 25922), *Salmonella enterica serovar Typhimurium* (14028s), *Staphylococcus aureus* (ATCC 25923), and *S. aureus* (27213) strains.

Antimicrobial assay of the compounds from *Clitocybe nebularis*

The antimicrobial activity of compounds cerevisterol (**26**), (22*E*,24*S*)-5α-ergosta7,22-diene-3β,5,6β,9α-tetraol (**27**), and indole-3-carboxylic acid (**28**) was tested against bacterial strains of *Streptococcus agalactiae* (ATCC 13813), *Staphylococcus epidermidis* (ATCC 12228), *Moraxella catarrhalis* (ATCC 25238), *Haemophilus influenzae* (ATCC 49766), and *Proteus mirabilis* (HNCMB 60076) by disc diffusion method. Compounds **27** and **28** exhibited

marginal inhibition on the growth of *M. catarrhalis*, while this strain showed resistance against compound **26**.

Anti-inflammatory assay of the compounds from *Pholiota populnea*

The anti-inflammatory activity of compounds **3**, **5-11**, and **20**, was evaluated using COX-1, COX-2, 5-LOX, and 15-LOX assays, and the results are presented in **Table 5** and **Table 6**.

At a concentration of 50 μM, the compounds showed moderate-to-weak inhibition of COX enzymes. Dose-response experiments revealed that pholiols F (**6**) and (+)-clavaric acid (**20**) exhibited moderate anti-inflammatory activity against COX-2, with IC_{50} values of 439.8 and 766.7 μM, respectively. The other compounds had inhibition below 50% at the highest concentration tested (2.5 mM). Among the compounds, pholiols C (**3**), F (**6**), G (**7**), and I (**9**) exhibited the best inhibitory activity against 5-LOX, with IC_{50} values ranging from 194.5 to 519.7 μM. Pholiol F (**6**) was the most active against 5-LOX, with an IC_{50} value of 194.5 μM. However, all compounds were inactive against 15-LOX at the tested concentrations.

Table 5. COX-1 and COX-2 inhibitory activities of the triterpenes of *P. populnea*.

Compound	COX-1			COX-2		
	Inhibitory (%)[a]	S.D.	IC_{50} (μM)	Inhibitory (%)	S.D.	IC_{50} (μM)
Pholiol C (**3**)	17.7	0.64	-	3.28	36.76	-
Pholiol E (**5**)	−10.42	9.43	-	7.00	4.59	-
Pholiol F (**6**)	20.32	0.19	-	35.74	10.67	439.8
Pholiol G (**7**)	−0.56	6.87	-	2.82	3.89	-
Pholiol H (**8**)	6.65	1.487	-	−2.50	4.99	-
Pholiol I (**9**)	4.89	17.26	-	−3.26	3.95	-
Pholiol J (**10**)	−16.16	13.84	-	−5.26	6.60	-
Pholiol K (**11**)	−37.13	3.20	-	−8.40	2.27	-
(+)-Clavaric acid (**20**)	20.96	9.99	-	37.27	8.54	766.7
Standard	50.94[b]	2.13	-	79.02	3.071	0.45[b]

[a]Relative percentage inhibition was assessed at 50 μM of the compounds and in triplicates. Dose–response investigations were conducted in duplicates with 2.5 mM as the highest concentration. [b]Standards: SC560 for COX-1, Celecoxib for COX-2.

Table 6. 5-LOX and 15-LOX inhibitory activities of the triterpenes of *P. populnea*.

Compound	5-LOX			15-LOX		
	Inhibitory (%)[a]	S.D.	IC_{50} (μM)	Inhibitory (%)	S.D.	IC_{50} (μM)
Pholiol E (**5**)	−35.25	3.05	-	−23.22	11.2	-
Pholiol F (**6**)	−7.91	16.28	194.5	−16.19	15.27	-
Pholiol G (**7**)	15.11	2.04	519.7	−77.38	24.05	-
Pholiol H (**8**)	−55.04	23.91	-	−94.87	11.21	-
Pholiol I (**9**)	0.72	4.07	480.5	−50.72	24.91	-
Pholiol J (**10**)	−102.2	19.33	-	−79.45	30.41	-
Pholiol K (**11**)	−302.5	8.65	-	−58.33	28.85	-
(+)-Clavaric acid (**20**)	−35.61	5.60	-	−39.6	22.47	-
Pholiol C (**3**)	17.27	9.16	370.1	−112.1	15.97	-
Standard	50.72	2.54	0.53[b]	103.5[b]	18.59	-

[a]Relative percentage inhibition was assessed at 100 μM of the compounds and in triplicates. Dose–response investigations were conducted in duplicates with 3 mM as the highest concentration. [b]Standards: Zileuton for 5-LOX, NDGA for 15-LOX.

DISCUSSION

Investigation of *Pholiota populnea* and *Clitocybe nebularis*

The goal of our study was to reveal the chemical and pharmacological potency of two mushroom species that are native to Hungary. Although in Hungary more than 3000 species of mushrooms occur, there have been only a few comprehensive studies that have explored the pharmacological effects of these fungi.

The investigated fungal species were collected from the surrounding areas of Szeged, Hungary. The mushroom samples were extracted using an amphipolar solvent (methanol), allowing the isolation of lipophilic and polar components. The liquid-liquid partition between the aqueous methanol extract and *n*-hexane, $CHCl_3$, and EtOAc afforded fractions with different polarities. The richest composition was shown by the *n*-hexane and $CHCl_3$ extracts, from which the compound isolation was carried out.

Isolation of the bioactive compounds

Multiple FC methods were applied to separate and purify compounds **1**, **3, 21**, and **22** from the *n*-hexane fraction of *Pholiota populnea*. Preparative TLC was used for final purification of compounds **2** and **4** using a mixture of $CHCl_3$-MeOH and *n*-hexane-acetone, respectively.

Due to the large quantity of the chloroform fraction, we decided to divide it into smaller parts, namely A, B, C, and D. After monitoring the TLC results, we selected parts A and B for further separation as they appeared to be more interesting. In the initial step of separation, the EtOAc and chloroform (part A) fractions of *Pholiota populnea*, FC methods were used. However, after reviewing the results, for chloroform part B, the GFC1 method was applied first. Subsequently, various chromatographic techniques, such as OCC, FC, GFC, preparative TLC, and HPLC, were used to purify compounds **5**-**20** and **23**-**25**.

To study *Clitocybe nebularis* metabolites, the chloroform phase was fractionated using NP-FC, and the combined fractions were analyzed using repeated RP-FC, which resulted in compounds **26** and **27**. Purification was carried out by multiple NP-FC followed by PTLC of the EtOAc extract, leading to the isolation of a compound **28**.

Structure elucidation

Various spectroscopic methods were used to elucidate the structures of the isolated compounds (**1**-**28**). Molecular masses and molecular compositions were obtained from HRESIMS investigations. The structures were further determined using 1D and 2D NMR spectroscopy, which provided the most useful information. The constitutions and planar structures of the compounds were elucidated from the ^{1}H and ^{13}C NMR, ^{1}H-^{1}H COSY, HSQC, and HMBC experiments, and then the relative configurations of the chiral centers were determined with the aid of NOESY and ROESY spectra. As a result of our NMR studies, we complete ^{1}H- and ^{13}C assignments were accomplished to characterize the new compounds and to supplement previously published data for some known compounds where the data were incomplete.

Triterpenes and nucleosides from *Pholiota populnea*

The investigation of the chemical composition of *Pholiota populnea* resulted in the isolation of 19 undescribed triterpenes, which were named pholiol A to S, in addition to 6 known components. Among the 19 compounds, 18 had lanostane skeletons (pholiol A-R) (**1**-**18**), while 1 had a trinorlanostane skeleton (pholiol S) (**19**). Structure elucidation of pholiols revealed the presence of two unique moieties, a 3-hydroxy-3-methylglutarate methyl ester (MeHMG) and a 3-hydroxy-3-methylglutarate (HMG). MeHMG was found to be linked to either at C-2 (**2**, **4**, **8**, **13**-**16**, and **19**) or C-3 (**12**), while HMG was attached only at C-2 (**1**, **3**, **5**-**7**, **9**, **17**, and **18**). Our research afforded the first discovery of a lanostane triterpene containing either MeHMG or HMG moiety from the *Pholiota* genus. In 2004, fasciculol E,

a lanostane triterpenoid conjugated to a HMG containing depsipeptide unit was isolated for the first time from the genus *Pholiota*[79]. Further structural characteristic of pholiol series (**1-19**) is the presence of a keto group at C-24. (+)-Clavaric acid (**20**) is a triterpenoid compound that is structurally related to fasciculic acid, which is a calmodulin inhibitor produced by *Naematoloma* (syn. *Hypholoma*) *fasciculare*[63,80]. Compound **21** was identified as (3*S*,6*E*,10*E*,14*E*,18*E*,22*S*)-2,3,22,23-tetrahydroxy-2,6,10,15,19,23-hexamethyl-6,10,14,18-tetracosatetraene, which is a linear triterpene polyol. While the compound **21** was first isolated from the dried bark of *Ekebergia capensis*[70] and later from the seeds of *Alpinia katsumadai*[81] in 2012, our study represents the first isolation of this compound from a mushroom.

Ergosterol (**22**) and 3*β*-hydroxyergosta-7,22-diene (**23**) are both sterols with broad distribution in fungal species[82–84]. Ergosterol (**22**) is a sterol that is similar in structure to cholesterol, which is found in animal organisms[85]. It is a major component of fungal cell membranes and plays an important role in maintaining their integrity and fluidity[86]. Ergosterol (**22**) is also a precursor of vitamin D2, which is produced when it is exposed to ultraviolet light[87].

In the EtOAc extract of the species, uridine (**24**) and adenosine (**25**) were detected. Both are nucleosides, which are building blocks of nucleic acids such as DNA and RNA[88]. Adenosine[89–91] and uridine[82,89,92] have been identified in various species of mushrooms.

Triterpenes and an organic acid from *Clitocybe nebularis*

Processing the extract of *C. nebularis* provided the isolation of three compounds, which had not previously been isolated from this species. With regard to their structures, the components can be divided into two groups: cerevisterol (**26**) and (22*E*,24*S*)-5*α*-ergosta-7,22-diene-3*β*,5,6*β*,9*α*-tetraol (**27**) belong to the group of triterpenes, while indole-3-carboxylic acid (**28**) is an organic acid. Cerevisterol (**26**), which was found for the first time in the yeast *Saccharomyces cerevisiae*[93], was identified in the chloroform fraction of *C. nebularis*. Morelli et al. analyzed the steroids of *C. nebularis* and found cyclolaudenol, 31-norcyclolaudenol, portensterol, ergosterol, and campesterol[94]. Interestingly, these steroids were not identified in our experiment. Cyclolaudenol and 31-norcyclolaudenol are based on the 19-cyclolanostane skeleton, while portensterol, ergosterol, and campesterol have the ergostane scaffold, which is also present in our isolated compounds (**26**) and (**27**). Senatore conducted a study on the steroids of *C. nebularis* using GC-MS measurements and found

that the main sterols are C_{28} with smaller amounts of C_{27} and C_{29} sterols. Ergosterol was identified to be the sterol with the highest concentration, comprising 62-68% of the total sterol content. Additionally, small or insignificant quantities of other closely related sterols, including cholesterol, desmosterol, *β*-sitosterol, stigmasterol, and fucosterol, were identified[95]. Our study provided the first documentation of indole 3-carboxylic acid (**28**) in the *Clitocybe* genus. In the past, only closely related indole derivatives (indole 3-carbaldehyde) had been isolated from a *Clitocybe* species[96]. Indole derivatives were identified as the dominant odorous constituents responsible for the complex odor of the taxonomically related *Tricholoma* species[97].

Biological activities of the compounds of investigated species

Pholiota populnea

The detailed chemical investigation of *Pholiota populnea* extracts yielded the isolation of 25 compounds. The isolated compounds **1–4**, **21**, and **22** did not show any antimicrobial activity against selected bacterial strains. The antiproliferative activity of the compounds isolated from the $CHCl_3$ fraction (**12**, **13**, **15**, **17**, and **19**) was investigated using MTT assay on Colo205, Colo320, MCF-7, A549, MRC-5 cell lines. Pholiols M (**13**) and O (**15**) showed the highest antiproliferative effects and tumor cell selectivity against the MCF-7 cell line. In terms of their chemical structure, compounds **13** and **15** belong to the class of lanostane triterpenes with 2,3-diester-7-on-8(9)-en functionalities. Additionally, compound **15** contains a 11-keto group while compound **13** has a 12-hydroxy group. Based on the results of the cytotoxicity tests conducted on the metabolites **1**–**4**, **12**–**19**, **21**, and **22**, ergosterol (**22**) was found to exhibit substantial cytotoxic activity against the Colo205, Colo320, and MRC-5 cell lines without any selectivity towards tumor cells. In contrast, pholiols B (**2**), D (4), L (**12**), and Q (**17**) demonstrated selective cytotoxicity against the resistant Colo320 cells compared to the sensitive Colo205 cells. Based on the results of the MDR efflux pump inhibitory assay, compounds (**1**), (**2**), and (**21**) were found to have the capacity to inhibit the efflux-pump overexpressed in the cell. In addition, compound **21** demonstrated very strong synergistic activity with doxorubicin on the Colo320 cell line, while pholiols B (**2**) and D (**4**) showed synergistic effects using a checkerboard combination assay.

It is noteworthy that the tetrahydroxysqualene derivative (**21**) has the capacity to potentiate the effect of doxorubicin in Colo320 cells by P-gp modulation and strong synergism with doxorubicin, and therefore it represents a promising new class of potential

adjuvants of cancer chemotherapy. With regard to the moderate P-gp inhibitory activity and strong synergism of **21** in combination with doxorubicin, the mechanism of its chemosensitizing effect should have another P-gp-independent mechanism.

Anti-inflammatory activity of the compounds was tested using COX-1, COX-2, 5-LOX, and 15-LOX inhibitory assays. The results revealed that pholiol F (**6**) and clavaric acid (**20**) have COX-2 inhibitory activity, while pholiols C (**3**), F (**6**), G (**7**), and I (**9**) have moderate 5-LOX inhibitory activity. Zhang et al. reported a protein from the edible fungus *Pholiota nameko* that modulated cytokine secretion in mice bearing MCF-7 xenografts and induced apoptosis of MCF-7 cells *in vivo*[98]. Choi et al. investigated the acyclic triterpenoid **21**, which was isolated from the seeds of *Alpinia katsumadai*. They found that this compound was responsible for inhibiting acyl-CoA: cholesterol acyltransferase (ACAT) activities in rat liver microsomes, with IC_{50} values of 47.9 μM. Additionally, it decreased cholesteryl ester formation with IC_{50} values of 26 μM in human hepatocyte HepG2 cells[81]. Clavaric acid (**20**) was obtained from the mushroom *Clavariadelphus truncates* and *Naematoloma* (syn. *Hypholoma*) *spp*.[68,69,99–101]. This compound is a potent inhibitor of Ras farnesyl transferase. The human Ras (P21) protein is involved in the regulation of cell division, and ras oncogenic mutations result in uncontrolled cell proliferation in a wide variety of human tumors, including colorectal carcinoma, exocrine pancreatic carcinoma and myeloid leukemias[99]. Zhou et al., reported that polysaccharides, specifically SPAP2-1, obtained from *Pholiota adiposa* showed significant interference of the cell cycle of HeLa cells and induced apoptosis[102]. The polysaccharides and triterpenoids derived from *Ganoderma lucidum* were found to be highly effective in inhibiting tumor growth both in vitro and in vivo[103]. Additionally, extracts from *G. lucidum* and *G. tsugae* were observed to have the ability to suppress the growth of colorectal cancer cells in vitro[104].

Clitocybe nebularis

As part of our study, compounds **26**–**28** detected in *Clitocybe nebularis* were evaluated for their antimicrobial activity using the agar disc diffusion assay. The growth of *M. catarrhalis* strain was slightly affected by compounds **27** and **28**, while it was resistant to compound **26**. In earlier studies, it was shown that cerevisterol (**26**) could inhibit the growth of certain bacteria, including *S. aureus, S. typhi*, and *A. niger*, with a MIC value of 25 μg/mL, and *E. faecalis*, with a MIC value of 50 μg/mL[105]. However, when tested using the disk diffusion method at a concentration of 20 μg/mL, cerevisterol (**26**) was found to be inactive against *Bacillus subtilis, B. pumilus, M. luteus, S. aureus, C. albicans*, and *A. niger*[106]. Indole-3-

carboxylic acid (**28**) was previously tested against various pathogenic fungi and bacteria, including *Fusarium avenaceum*, *F. graminearum*, *F. culmorum*, *Pyricularia oryzae*, *S. aureus*, *E. coli*, and *B. subtilis*. However, no antifungal or antibacterial activity was observed[107]. There is no information in the literature regarding the antibacterial activity of (22*E*,24*S*)-5*α*-ergosta-7,22-diene-3*β*,5,6*β*,9*α*-tetraol (**27**). In another investigation, an extract of *Clitocybe nebularis* showed significant antiproliferative and cytotoxic activities[108,109]

SUMMARY

Our study aimed to highlight the chemical and pharmacological potential of mushrooms *Pholiota populnea* and *Clitocybe nebularis*, focusing on previously undescribed compounds with cytotoxic, antiproliferative, and anti-inflammatory activity.

The isolation process involved grinding the samples, followed by percolation with methanol. The fractions with different polarities were then roughly separated using liquid-liquid extractions, resulting in *n*-hexane, chloroform, and EtOAc phases. The composition of these extracts was monitored by TLC investigations. Subsequently, various chromatographic methods, such as OCC, FC, PTLC, and HPLC, were employed for further separation, affording the isolation of 28 compounds in pure form. The structures of the isolated compounds were determined by means of spectroscopic methods, mainly MS and NMR spectroscopy.

In case of *Pholiota populnea*, solvent-solvent extraction and different chromatographic separations of the extracts led to the isolation of nineteen novel triterpenes, named pholiol A-S (**1**-**19**), together with 6 know compounds, a lanostane type triterpene, (+)-clavaric acid (**20**), an acyclic triterpene, (3*S*,6*E*,10*E*,14*E*,18*E*,22*S*)-2,3,22,23-tetrahydroxy-2,6,10,15,19,23-hexamethyl-6,10,14,18-tetracosatetraene (**21**), two ergostane-type triterpenes, ergosterol (**22**), and 3*β*-hydroxyergosta-7,22-diene (**23**), and two nucleosides, uridine (**24**) and adenosine (**25)**. The new compounds, pholiol A–S, are lanostane-type triterpenes (with exception of **10** and **11)** substituted with 3-hydroxy-3-methylglutaric acid and its 6-methyl ester. Characteristic structural features are the 24-keto group, 8/9 double bond, and in some compounds, 7- or/and 11-keto groups. Pholiol S (**19**) is an unusual compound with a trinor-triterpene structure, and pholiols Q (**17**), and R (**18**) with 7(8),9(11)-diene structure. All compounds (**1**–**25**) were isolated for the first time from this species. Pholiols M (**13**) and O (**15**) displayed antiproliferative activity against the MCF-7 cell line

with IC_{50} of 2.48 and 9.95 μM, respectively. Furthermore, these compounds demonstrated tumor cell selectivity on MCF-7 cells [SI values of >40 (**13**) and 4.3 (**15**)]. The isolated metabolites (**1**–**4**, **12-19**, **21**, and **22**) were investigated for cytotoxic activity against Colo205, Colo320, A549, MCF-7, and nontumoral MRC-5 cell lines. Among the tested compounds, ergosterol (**22**) showed substantial cytotoxic activity against all cell lines with IC_{50} values of 4.9 μM (Colo205), 6.5 μM (Colo320), and 0.50 μM (MRC) with no tumor cell selectivity. However, pholiols B (**2**) (RR 0.90), D (**4**) (RR 0.95), L (**12**) (RR 0.84), and Q (**17**) (RR 0.62) were found to have selective cytotoxicity against the resistant Colo320 cells compared to the sensitive Colo320 cells. A P-glycoprotein efflux pump modulatory test on resistant Colo320 cells revealed that pholiols A (**1**), B (**2**), and the acyclic triterpene **21** have the capacity to inhibit the efflux-pump overexpressed in the cells. Moreover, the drug interactions of triterpenes with doxorubicin were studied by the checkerboard method on Colo320 cells. Pholiols B (**2**) (CI 0.348) and D (**4**) (CI 0.660) interacted in synergistic and acyclic triterpene **21** (CI 0.082) in a very strong synergistic manner. The anti-inflammatory activity of the isolated compounds (**3**, **5-11**, and **20**) was screened using COX-1, COX-2, 5-LOX, and 15-LOX inhibitory assays. The results showed that the lanostane derivatives exhibited moderate inhibitory activity against 5-LOX and COX-2 enzymes. Among the tested compounds, pholiol F (**6**) demonstrated the highest potency, with IC_{50} values of 194.5 μM and 439.8 μM against 5-LOX and COX-2, respectively. The isolated compounds were ineffective as antimicrobial agents.

For the first time, two steroids (cerevisterol (**26**) and (22*E*,24*S*)-5*α*-ergosta7,22-diene-3*β*,5,6*β*,9*α*-tetraol (**27**)) and an organic acid (indole-3-carboxylic acid (**28**)) were obtained from the chloroform and EtOAc fractions of *Clitocybe nebularis*. Their antimicrobial activity was assessed against human pathogen strains using the agar disc diffusion method. The susceptibility assay exhibited that compounds **27** and **28** have weak antimicrobial activity against *M. catarrhalis*.

Our findings indicate that mushrooms native to Hungary are a rich source of biologically active metabolites with great structural diversity. Especially, *P. populnea* is a promising source for discovery of new triterpenes with significant antiproliferative, and chemosensitizing activities on cancer cells. Therefore, understanding the mechanism of action of these compounds can provide a strong foundation for developing new, effective agents for the treatment of different types of cancer.

REFERENCES

1. Chang, S. T., Miles, P. G. & Chang, S. T. *Mushrooms: cultivation, nutritional value, medicinal effect, and environmental impact*. CRC Press, **2004**.
2. Patra, A. & Mukherjee, A. K. Mushroom mycetism – A neglected and challenging medical emergency in the Indian subcontinent: A road map for its prevention and treatment. *Toxicon*. **2022**, 217, 56–77.
3. Blackwell, M. The Fungi: 1, 2, 3 … 5.1 million species? *Am.J. Bot*. **2011**, 98, 426–438.
4. Wasser, S. Medicinal mushrooms as a source of antitumor and immunomodulating polysaccharides. *Appl. Microbiol. Biotechnol*. **2002**, 60, 258–274.
5. Kalač, P. A review of chemical composition and nutritional value of wild-growing and cultivated mushrooms: Chemical composition of edible mushrooms. *J. Sci. Food Agric.* **2013**, 93, 209–218.
6. Friedman, M. Mushroom polysaccharides: chemistry and antiobesity, antidiabetes, anticancer, and antibiotic properties in cells, rodents, and humans. *Foods*. **2016**, 5, 80.
7. Bräse, S., Encinas, A., Keck, J. & Nising, C. F. Chemistry and biology of mycotoxins and related fungal metabolites. *Chem. Rev.* **2009**, 109, 3903–3990.
8. Keller, N. P. Fungal secondary metabolism: regulation, function and drug discovery. *Nat. Rev. Microbiol*. **2019**, 17, 167–180.
9. González-Medina M, Owen JR, El-Elimat T, Pearce CJ, Oberlies NH, Figueroa M. et. al. Scaffold diversity of fungal metabolites. *Front. Pharmacol*. **2017**, 8, 180.
10. Esheli, M., Thissera, B., El-Seedi, H. R. & Rateb, M. E. Fungal metabolites in human health and diseases—an overview. *Encyclopedia*. **2022**, 2, 1590–1601.
11. Öztürk, M., Tel-Çayan, G., Muhammad, A., Terzioğlu, P. & Duru, M. E. Mushrooms. *Stud. Nat. Prod. Chem.* **2015**, 45, 363–456.
12. Jin,Y.,Chi, M., Wei, W., Zhao, Y., Wang, G., Freng, T. Tricholosterols A–D, four new ergosterol derivatives from the mushroom *Tricholoma terreum*. *Steroids*. **2023**, 191, 109157.
13. Zhang, H., Dong, X., Ji, H., Yu, J. & Liu, A. Preparation and structural characterization of acid-extracted polysaccharide from *Grifola frondosa* and antitumor activity on S180 tumor-bearing mice. *Int. J. Biol. Macromol*. **2023**, 234, 123302.
14. Thimmaraju, A. & Seedevi, P. Purification, chemical, structural characterization and biological activity of polysaccharide from blue oyster mushroom *Hypsizygus* ulmarius. *Biomass Conv. Bioref.* **2023**. doi:10.1007/s13399-023-04025-y.

15. Krishnasamy, G., Azahar, M.-S., Rahman, S.-N. S. A., Vallavan, V., Zin, N. M., Latif, M. A., et. al. Activity of aurisin A isolated from *Neonothopanus nambi* against methicillin-resistant *Staphylococcus* aureus strains. *Saudi Pharm. J*. **2023**, 31, 617-625.
16. Ruan, Y., Han, C., Wang, D., Inoue, Y., Amen, Y., Othman, A., et. al. New benzaldehyde derivatives from the fruiting bodies of *Hericium erinaceus* with cytotoxic activity. *Nat. Prod. Res*. **2023**, 1–10.
17. Chinthanom, P., Choowong, W., Thummarukcharoen, T., Chen, H.-P., Liu, J.-K., & Isaka, M. Lanostane triterpenoids from mycelial cultures of the basidiomycete *Ganoderma weberianum*. *Phytochem. Lett*. **2022**, 51, 12–17.
18. Sheng, Z., Wen, L. & Yang, B. Structure identification of a polysaccharide in mushroom Lingzhi spore and its immunomodulatory activity. *Carbohydr. Polym*. **2022**, 278, 118939.
19. Sung, H., Ferlay, J., Siegel, R. L., Laversanne, M., Soerjomataram, I., Jemal, A., et. al. Global cancer statistics 2020: globocan estimates of incidence and mortality worldwide for 36 cancers in 185 countries. *CA: Cancer J. Clin*. **2021**, 71, 209–249.
20. Marć, M. A., Kincses, A., Rácz, B., Nasim, M. J., Sarfraz, M., Lázaro-Milla, C., et. al. Antimicrobial, anticancer and multidrug-resistant reversing activity of novel oxygen-, sulfur- and selenoflavones and bioisosteric analogues. *Pharmaceuticals*. **2020**, 13, 453.
21. Zhou, B., Xiao, X., Xu, L., Zhu, L., Tan, L., Tang, H., et al. A dynamic study on reversal of multidrug resistance by ginsenoside Rh2 in adriamycin-resistant human breast cancer MCF-7 cells. *Talanta*. **2012**, 88, 345–351.
22. Chen, H.-P., Zhao, Z.-Z., Li, Z.-H., Huang, Y., Zhang, S.-B., Tang, Y., et al. Anti-proliferative and anti-inflammatory lanostane triterpenoids from the polish edible mushroom *Macrolepiota procera*. *J. Agric. Food Chem.* **2018**, 66, 3146–3154.
23. Bao, T.-R.-G., Long, G.-Q., Wang, Y., Wang, Q., Liu, X.-L., Hu, G.-S., et al. New lanostane-type triterpenes with anti-inflammatory activity from the epidermis of *Wolfiporia cocos*. *J. Agric. Food Chem.* **2022**, 70, 4418–4433.
24. Ványolós, A., Muszyńska, B., Chuluunbaatar, B., Gdula-Argasińska, J., Kała, K., & Hohmann, J. Extracts and steroids from the edible mushroom *Hypholoma lateritium* exhibit anti-inflammatory properties by inhibition of COX-2 and activation of Nrf2. *Chem. Biodivers*. **2020**, 17, e2000391.
25. Lee, J. W., Park, M. S., Park, J.-H., Cho, Y., Kim, C., Kim, C. S., et al. Taxonomic study of the genus *Pholiota* (Strophariaceae, Basidiomycota) in Korea. *Mycobiology*. **2020**, 48, 476–483.

26. Zhu, Z.-Y., Pan, L.-C., Han, D., Sun, H. & Chen, L.-J. Structural properties and antioxidant activities of polysaccharide from fruit bodies of *Pholiota nameko*. *Nat. Prod. Res*. **2019**, 33, 1563–1569.
27. Zhang, X., Liu, J., Wang, X., Hu, H., Zhang, Y., Liu, T., et al. Structure characterization and antioxidant activity of carboxymethylated polysaccharide from *Pholiota nameko*. *J. Food Biochem*. **2022**, 46, e14121.
28. Qu, Y., Yan, J., Zhang, X., Song, C., Zhang, M., Mayo, K. H., et al. Structure and antioxidant activity of six mushroom-derived heterogalactans. *Int. J. Biol. Macromol*. **2022**, 209, 1439–1449.
29. Fan, Y., Chun, Z., Wang, G., Pu, S., Pan, Y., Ma, J., et al. Isolation, structural characteristics, and in vitro and in vivo antioxidant activity of the acid polysaccharide isolated from *Pholiota nameko*. *Phcog Mag*. **2020**, 16, 738.
30. Zhang, X., Liu, T., Wang, X., Zhou, L., Qi, J., & An, S. Structural characterization, antioxidant activity and anti-inflammatory of the phosphorylated polysaccharide from *Pholiota nameko. Front. Nutr.* **2022**, 9, 976552.
31. Guo, G.-Y., Sun, R.-G., Guo, Q., Zhang, X.-F. & Dou, P.-J. Preparation and structural characterization of wPNP-a1 from *Pholiota nameko*. *Plant Sci. J.* **2012**, 30, 423.
32. Abreu, H., Smiderle, F. R., Sassaki, G. L., Sovrani, V., Cordeiro, L. M. C., & Iacomini, M. Naturally methylated mannogalactans from the edible mushrooms *Pholiota nameko* and *Pleurotus eryngii*. *J. Food Compos. Anal*. **2021**, 102, 103985.
33. Nei, Y., Jiang, H., Su, Y., Zhuo, C. & Wen, F. Isolation,purification and determination of the structure of polysaccharide PAP2 from *Pholiota adiposa*. *Food and Fermentation Industries*. **2011**, 37, 21–24.
34. Wang, X., Jiang, S. & Liu, Y. Anti-diabetic effects of fungal ergosta-4, 6, 8(14), 22-tetraen-3-one from *Pholiota adiposa*. *Steroids*. **2023**, 192, 109185.
35. Wang, C. R., Zhou, R., Ng, T. B., Wong, J. H., Qiao, W. T., & Liu, F. First report on isolation of methyl gallate with antioxidant, anti-HIV-1 and HIV-1 enzyme inhibitory activities from a mushroom (*Pholiota adiposa*). *Environ. Toxicol. Pharmacol*. **2014**, 37, 626–637.
36. Chung, I. M., Kong, W. S., Lee, O. K. & Park, J. S. Cytotoxic chemical constituents from the mushroom of *Pholiota adiposa*. *Food Sci. Biotechnol*. **2006**, 14, 255–258.
37. Liu, D.-Z., Jia, R.-R., Wang, F. & Liu, J.-K. A new spiroaxane sesquiterpene from cultures of the basidiomycete *Pholiota adiposa*. *Z. Naturforsch. B*. **2008**, 63, 111–113.

38. Lin, J., Huo, R.-Y., Hou, L., Jiang, S., Wang, S.-L., Deng, Y.-L., et al. New polyketides from the basidiomycetous fungus *Pholiota* sp. *J. Asian Nat. Prod. Res*. **2022**, 1–9.
39. He, Y., Wang, R., Huang, B., Dai, Q. & Lin, J. Pholiotone A, a new polyketide derivative from *Pholiota* sp. *Nat. Prod. Res*. **2020**, 34, 1957–1961.
40. Kazutosh, S., Yukiko, K. & Mizuki, M. Antimicrobial activities of bisnoryangonin contained in *Pholiota aurivella*. *J. Home Econ*. **2007**, 58, 563–568.
41. Kirk PM, Cannon PF, Minter DW, Stalpers JA. *Dictionary of the fungi (10th ed.)*. CABI, **2008**.
42. Pohleven, J., Kos, J. & Sabotic, J. Medicinal properties of the genus *Clitocybe* and of lectins from the clouded funnel cap mushroom, *C. nebularis* (Agaricomycetes): A review. *Int. J. Med. Mushrooms*. **2016**, 18, 965–975.
43. Ahamed, M., Singh, S., Mayirnao, H.-S., Mehmood, T., Verma, K., Kapoor, R., et al. Morphological and molecular characterization of two species of *Pholiota* from North-western Himalaya, India. *Ind. Phytopathol*. **2023**, 76, 273–280.
44. Becker, U., Anke, T. & Sterner, O. A novel bioactive illudalane sesquiterpene from the fungus *Pholiota destruens*. *Nat. Prod. Lett*. **1994**, 5, 171–174.
45. Mleczek, M., Gąsecka, M., Budka, A., Siwulski, M., Mleczek, P., Magdziak, Z., et al. Mineral composition of elements in wood-growing mushroom species collected from of two regions of Poland. *Environ. Sci. Pollut. Res*. **2021**, 28, 4430–4442.
46. Knudsen, H., Vesterholt, J. *Funga Nordica: agaricoid, boletoid, clavarioid, cyphelloid and gastroid genera*. Nordsvamp, **2012**.
47. Desjardin, D. E., Wood, M. & Stevens, F. A. *California mushrooms: the comprehensive identification guide*. Timber Press, **2015**.
48. Löfgren, N., & Lüning, B. On the structure of nebularine. *Acta Chem. Scand.* **1953**, 7, 225–225.
49. Pang, Z., Anke, H., & Sterner, O. A chemical investigation of the fruit bodies of *Lepista nebularis*. *Acta Chem. Scand.* **1994**, 48, 408–410.
50. Fogedal, M., Mickos, H. & Norberg, T. Isolation of *N*-2′-hydroxyhexadecanoyl-1-O-β-D-glucopyranosyl-9-methyl-4,8-D-erythro-sphingadienine from fruiting bodies of two Basidiomycetes fungi. *Glycoconj. J*. **1986**, 3, 233–237.
51. Brzin, J., Rogelj, B., Popovič, T., Štrukelj, B. & Ritonja, A. Clitocypin, a new type of cysteine proteinase inhibitor from fruit bodies of mushroom *Clitocybe nebularis*. *J. Biol. Chem*. **2000**, 275, 20104–20109.

52. Kim, Y.-S., Lee, I.-K., Seok, S.-J. & Yun, B.-S. Chemical constituents of the fruiting bodies of *Clitocybe nebularis* and their antifungal activity. *Mycobiology*. **2008**, 36, 110–113.
53. Schrey, H., Scheele, T., Ulonska, C., Nedder, D. L., Neudecker, T., Spiteller, P., et al. Alliacane-type secondary metabolites from submerged cultures of the basidiomycete *Clitocybe nebularis*. *J. Nat. Prod.* **2022**, 85, 2363–2371.
54. Kemami Wangun, H. V., Dörfelt, H. & Hertweck, C. Nebularic acids and nebularilactones, novel drimane sesquiterpenoids from the fungus *Lepista nebularis*. *Eur. J. Org. Chem.* **2006**, 2006, 1643–1646.
55. Dizeci, N., Onar, O., Karaca, B., Demirtas, N., Cihan, A. C., & Yildirim, O. Comparison of the chemical composition and biological effects of *Clitocybe nebularis* and *Infundibulicybe geotropa*. *Mycologia*. **2021**, 113, 1156-1168.
56. Onar, O., Telkoparan-Akillilar, P. & Yildirim, O. *Clitocybe nebularis* extract and 5-fluorouracil synergistically inhibit the growth of HT-29 colorectal cancer cells by inducing the S phase arrest. *3 Biotech*. **2023**, 13, 48.
57. Dimitrijevic, M. V., Mitic, V. D., Nikolic, J. S., Djordjevic, A. S., Mutic, J. J., Stankov Jovanovic, V. P., et al. First report about mineral content, fatty acids composition and biological activities of four wild edible mushrooms. *Chem. Biodivers*. **2019**, 16, e1800492.
58. Chou, T.-C. Theoretical basis, experimental design, and computerized simulation of synergism and antagonism in drug combination studies. *Pharmacol. Rev*. **2006**, 58, 621–681.
59. Chou, T.-C. Drug combination studies and their synergy quantification using the chou-talalay method. *Cancer Res*. **2010**, 70, 440–446.
60. Bauer, A. W., Kirby, W. M., Sherris, J. C. & Turck, M. Antibiotic susceptibility testing by a standardized single disk method. *Am. J. Clin. Pathol*. **1966**, 45, 493–496.
61. Béni, Z., Dékány, M., Sárközy, A., Kincses, A., Spengler, G., Papp, V., et al. Triterpenes and phenolic compounds from the fungus *Fuscoporia torulosa*: isolation, structure determination and biological activity. *Molecules*. **2021**, 26, 1657.
62. Kim, K. H., Moon, E., Choi, S. U., Kim, S. Y. & Lee, K. R. Lanostane triterpenoids from the mushroom *Naematoloma fasciculare*. *J. Nat. Prod.* **2013**, 76, 845–851.
63. Takahashi, A., Kusano, G., Ohta, T., Ohizumi, Y. & Nozoe, S. Fasciculic acids A,B and C as calmodulin antagonists from the mushroom *Naematoloma fasciculare*. *Chem. Pharm. Bull*. **1989**, 37, 3247–3250.
64. Aichour, S., Haba, H., Benkhaled, M., Harakat, D. & Lavaud, C. Terpenoids and other constituents from *Euphorbia bupleuroides*. *Phytochem. Lett*. **2014**, 10, 198–203.

65. Nakamura, S., Iwami, J., Matsuda, H., Mizuno, S. & Yoshikawa, M. Absolute stereostructures of inoterpenes A–F from sclerotia of *Inonotus obliquus*. *Tetrahedron*. **2009**, 65, 2443–2450.

66. Yang, X., Chen, X.-J., Yang, Z., Xi, Y.-B., Wang, L., Wu, Y., et al. Synthesis, evaluation, and structure–activity relationship study of lanosterol derivatives to reverse mutant-crystallin-induced protein aggregation. *J. Med. Chem.* **2018**, 61, 8693–8706.

67. Zhao, Z.-Z., Chen, H.-P., Huang, Y., Li, Z.-H., Zhang, L., Feng, T., et al. Lanostane triterpenoids from fruiting bodies of *Ganoderma leucocontextum*. *Nat. Prod. Bioprospect.* **2016**, 6, 103–109.

68. Lingham, R. B., Silverman, K. C., Jayasuriya, H., Kim, B. M., Amo, S. E., Wilson, F. R., et al. Clavaric acid and steroidal analogues as Ras- and FPP-directed inhibitors of human farnesyl-protein transferase. *J. Med. Chem.* **1998**, 41, 4492–4501.

69. Jayasuriya, H., Silverman, K. C., Zink, D. L., Jenkins, R. G., Sanchez, M., Pelaez, F., et al. Clavaric acid: A triterpenoid inhibitor of farnesyl-protein transferase from *Clavariadelphus t runcatus*. *J. Nat. Prod.* **1998**, 61, 1568–1570.

70. Nishiyama, Y., Moriyasu, M., Ichimaru, M., Tachibana, Y., Kato, A., Mathenge, S. G., et al. Acyclic triterpenoids from *Ekebergia capensis*. *Phytochemistry*. **1996**, 42, 803–807.

71. Nishiyama, Y., Moriyasu, M., Ichimaru, M., Kato, A., Mathenge, S. G., Nganga, J. N., et al. Absolute configurations of two acyclic triterpenoids from *Ekebergia capensis*. *Phytochemistry*. **1999**, 52, 1593–1596.

72. Alexandre, T. R., Lima, M. L., Galuppo, M. K., Mesquita, J. T., do Nascimento, M. A., dos Santos, A. L., et al. Ergosterol isolated from the basidiomycete *Pleurotus salmoneostramineus* affects *Trypanosoma cruzi* plasma membrane and mitochondria. *J. Venom. Anim. Toxins Incl. Trop. Dis*. **2017**, 23, 30.

73. Valisolalao, J., Luu, B. & Ourisson, G. Steroides cytotoxiques de polyporus versicolor. *Tetrahedron*. **1983**, 39, 2779–2785.

74. Jinming, G. A novel sterol from Chinese truffles *Tuber indicum*. *Steroids*. **2001**, 66, 771–775.

75. Burton, G., Ghini, A. A. & Gros, E. G. ^{13}C NMR spectra of substituted indoles. *Magn. Reson. Chem.* **1986**, 24, 829–831.

76. Acton, E. M., Narayanan, V. L., Risbood, P. A., Shoemaker, R. H., Vistica, D. T., & Boyd, M. R. Anticancer specificity of some ellipticinium salts against human brain tumors in vitro. *J. Med. Chem.* **1994**, 37, 2185–2189.

77. Hall, M. D., Handley, M. D. & Gottesman, M. M. Is resistance useless? Multidrug resistance and collateral sensitivity. *Trends Pharmacol. Sci*. **2009**, 30, 546–556.
78. Spengler, G., Gajdács, M., Marć, M., Domínguez-Álvarez, E. & Sanmartín, C. Organoselenium compounds as novel adjuvants of chemotherapy drugs—A promising approach to fight cancer drug resistance. *Molecules*. **2019**, 24, 336.
79. Clericuzio, M., Piovano, M., Chamy, M. C., Garbarino, J. A., Milanesio, M., Viterbo, D., et al. Structural characterisation of metabolites from *Pholiota spumosa* (Basidiomycetes). *Croat. Chem. Acta*. **2004**, 77, 605-611.
80. Nozoe, S., Takahashi, A. & Ohta, T. Chirality of the 3-Hydroxy-3-methylglutaric acid moiety of fasciculic acid A, a calmodulin antagonist isolated from *Naematoloma fasciculare*. *Chem. Pharm. Bull.* **1993**, 41, 1738–1742.
81. Choi, S.-Y., Lee, M. H., Choi, J. H. & Kim, Y. K. 2,3,22,23-Tetrahydroxyl-2,6,10,15,19,23-hexamethyl-6,10,14,18-tetracosatetraene, an acyclic triterpenoid isolated from the seeds of *Alpinia katsumadai*, inhibits Acyl-CoA: Cholesterol acyltransferase activity. *Biol. Pharm. Bull*. **2012**, 35, 2092–2096.
82. Chuluunbaatar, B., Béni, Z., Dékány, M., Kovács, B., Sárközy, A., Datki, Z., et al. Triterpenes from the mushroom *Hypholoma lateritium*: isolation, structure determination and investigation in bdelloid rotifer assays. *Molecules*. **2019**, 24, 301.
83. Sárközy, A., Kúsz, N., Zomborszki, Z. P., Csorba, A., Papp, V., Hohmann, J., et al. Isolation and characterization of chemical constituents from the poroid medicinal mushroom *Porodaedalea chrysoloma* (Agaricomycetes) and their antioxidant activity. *Int. J. Med. Mushrooms*. **2020**, 22, 125–131.
84. Sárközy, A., Béni, Z., Dékány, M., Zomborszki, Z. P., Rudolf, K., Papp, V., et al. Cerebrosides and steroids from the edible mushroom *Meripilus giganteus* with antioxidant potential. *Molecules*. **2020**, 25, 1395.
85. Yokokawa, H. & Mitsuhashi, T. The sterol composition of mushrooms. *Phytochemistry*. **1981**, 20, 1349–1351.
86. Lees, N. D., Skaggs, B., Kirsch, D. R. & Bard, M. Cloning of the late genes in the ergosterol biosynthetic pathway of *Saccharomyces cerevisiae*—A review. *Lipids*. **1995**, 30, 221–226.
87. Kaur, K., Bindra, P., Mondal, S., Li, W.-P., Sharma, S., Sahu, B. K., et al. Up conversion nanodevice-assisted healthy molecular photocorrection. *ACS Biomater. Sci. Eng.* **2021**, 7, 291–298.

88. Zhang, S., Chen, Q., Li, Q., Huang, H., Zhu, Q., Ma, J., et al. The chemistry of purine nucleoside-based antibiotics. in *Comprehensive Natural Products III*, Elsevier, **2020**. doi:10.1016/B978-0-12-409547-2.14709-2.

89. Maľučká, L. U., Uhrinová, A. & Lysinová, P. Medicinal mushrooms Ophiocordyceps sinensis and Cordyceps militaris. *Ceska Slov. Farm.* **2022**, 71, 259–265.

90. Çayan, F., Tel-Çayan, G., Deveci, E., Duru, M. E. & Öztürk, M. Isolation and identification of compounds from truffle *Reddellomyces westraliensis* and their antioxidant, cytotoxic and enzyme inhibitory activities. *Process Biochem.* **2022**, 121, 553–562.

91. Kovács, B., Béni, Z., Dékány, M., Orbán-Gyapai, O., Sinka, I., Zupkó, I., et al. Chemical analysis of the edible mushroom *Tricholoma populinum*: Steroids and sulfinyladenosine compounds. *Nat. Prod. Commun.* **2017**, 12, 1583-1584.

92. Papaspyridi, L.-M., Aligiannis, N., Christakopoulos, P., Skaltsounis, A.-L. & Fokialakis, N. Production of bioactive metabolites with pharmaceutical and nutraceutical interest by submerged fermentation of *Pleurotus ostreatus* in a batch stirred tank bioreactor. *Procedia Food Sci*. **2011**, 1, 1746–1752.

93. Bills, C. E. & Honeywell, E. M. Antiricketic substances. *J. Biol. Chem*. **1928**, 80, 15–23.

94. Morelli, I., Pistelli, L. & Catalano, S. Some constituents of *Clitocybe nebularis* and of *Hydnum repandum*. *Fitoterapia*. **1981**, 52, 45–47.

95. Senatore, F. Chemical constituents of some mushrooms. *J. Sci. Food Agric.* **1992**, 58, 499–503.

96. Chen, J.-T., Su, H.-J. & Huang, J.-W. Isolation and identification of secondary metabolites of *Clitocybe nuda* responsible for inhibition of zoospore germination of Phytophthora capsici. *J. Agric. Food Chem.* **2012**, 60, 7341–7344.

97. Fons, F., Rapior, S., Fruchier, A., Saviuc, P. & Bessiere, J. M. Volatile composition of *Clitocybe amoenolens*, *Tricholoma caligatum* and *Hebeloma radicosum*. *Cryptogam. Mycol.* **2006**, 27, 45–55.

98. Zhang, Y., Zhang, Y. N., Gao, W., Zhou, R., Liu, F., & Ng, T. B. A novel antitumor protein from the mushroom *Pholiota nameko* induces apoptosis of human breast adenocarcinoma MCF-7 cells in vivo and modulates cytokine secretion in mice bearing MCF-7 xenografts. *Int. J. Biol. Macromol*. **2020**, 164, 3171–3178.

99. Godio, R. P. & Martín, J. F. Modified oxidosqualene cyclases in the formation of bioactive secondary metabolites: Biosynthesis of the antitumor clavaric acid. *Fungal Genet. Biol*. **2009**, 46, 232–242.

100. Godio, R. P., Fouces, R., Gudiña, E. J., & Martín, J. F. Agrobacterium tumefaciens-mediated transformation of the antitumor clavaric acid-producing basidiomycete *Hypholoma sublateritium*. *Curr. Genet*. **2004**, 46, 287–294.
101. Godio, R. P., Fouces, R. & Martín, J. F. A squalene epoxidase is involved in biosynthesis of both the antitumor compound clavaric acid and sterols in the basidiomycete *H. sublateritium*. *Chem. Biol*. **2007**, 14, 1334–1346.
102. Zhou, J., Gong, J., Chai, Y., Li, D., Zhou, C., Sun, C., et al. Structural analysis and in vitro antitumor effect of polysaccharides from *Pholiota adiposa*. *Glycoconj. J*. **2022**, 39, 513–523.
103. Min, B.-S., Gao, J.-J., Nakamura, N. & Hattori, M. Triterpenes from the spores of *Ganoderma lucidum* and their cytotoxicity against Meth-A and LLC tumor cells. *Chem. Pharm. Bull.* **2000**, 48, 1026–1033.
104. Hsu, S.-C., Ou, C.-C., Li, J.-W., Chuang, T.-C., Kuo, H.-P., Liu, J.-Y., et al. *Ganoderma tsugae* extracts inhibit colorectal cancer cell growth via G2/M cell cycle arrest. *J. Ethnopharmacol*. **2008**, 120, 394–401.
105. Appiah, T., Agyare, C., Luo, Y., Boamah, V. E. & Boakye, Y. D. Antimicrobial and resistance modifying activities of cerevisterol isolated from *Trametes* Species. *Curr. Bioact. Compd*. **2020,** 16, 115–123.
106. Guo, K., Fang, H., Gui, F., Wang, Y., Xu, Q., & Deng, X. Two new ring *A* -Cleaved lanostane-type triterpenoids and four known steroids isolated from endophytic fungus *Glomerella* sp. F00244. *Helv. Chim. Acta*. **2016**, 99, 601–607.
107. Tian, S., Yang, Y., Liu, K., Xiong, Z., Xu, L., & Zhao, L. Antimicrobial metabolites from a novel halophilic actinomycete *Nocardiopsis terrae* YIM 90022. *Nat. Prod. Res*. **2014**, 28, 344–346.
108. Bézivin, C., Lohézic, F., Sauleau, P., Amoros, M. & Boustie, J. Cytotoxic activity of Tricholomatales determined with murine and human cancer cell lines. *Pharm. Biol*. **2002**, 40, 196–199.
109. Pohleven, J., Obermajer, N., Sabotič, J., Anžlovar, S., Sepčić, K., Kos, J., et al. Purification, characterization and cloning of a ricin B-like lectin from mushroom *Clitocybe nebularis* with antiproliferative activity against human leukemic T cells. *Biochim. Biophys. Acta - Gen. Subj*. **2009**, 1790, 173–181.

Acknowledgments

First and foremost, I am deeply grateful to my supervisors, *Prof. Dr. Judit Hohmann* and *Dr. Attila Ványolós*, for their exceptional guidance, expertise, and unwavering support throughout my research journey. Their mentorship and invaluable insights have shaped my scientific growth and contributed to the successful completion of this dissertation.

I would like to extend my sincere appreciation to *Prof. Dr. Judit Hohmann*, *Dr. Zoltán Béni*, *Dr. Miklós Dékány*, *Dr. Anita Barta*, and *Dr. Anasztázia Hetényi* for their collaboration and expertise in conducting the NMR investigations. Their technical assistance and insightful discussions have greatly enhanced the quality and reliability of my research findings.

A special acknowledgment goes to *Dr. Róbert Berkecz* for his expertise and contributions in performing the mass spectrometry measurements. His guidance and meticulous approach have been instrumental in obtaining accurate and meaningful analytical data.

I am grateful to *Orinamhe Godwin Agbadua* for his valuable assistance in conducting the anti-inflammatory assay. His expertise and collaboration have significantly contributed to the evaluation of the anti-inflammatory properties of the compounds under investigation.

I would like to express my appreciation to *Dr. Gabriella Spengler* and *Dr. Nikoletta Szemerédi* for their involvement in assessing the antiproliferative and cytotoxic activities. Their expertise and contributions have provided valuable insights into the biological effects of the compounds studied.

I extend my sincere gratitude to *Dr. Attila Sándor* and the Hungarian Mushroom Society for their invaluable help in the identification and collection of mushroom samples. Their support has played a vital role in obtaining the necessary research materials.

I would like to acknowledge my colleagues in the Department of Pharmacognosy for their collaboration, discussions, and support throughout my research. Their collective expertise and camaraderie have enriched my academic experience.

I would also like to express my deep gratitude to my family for their unwavering love, encouragement, and support. Their belief in my abilities has been a constant source of motivation and strength.

Furthermore, I would like to thank the Stipendium Hungaricum scholarship program for their financial support and the opportunity they provided me. Their assistance has been

instrumental in pursuing my research and academic goals. This work was supported by the project ELKH-USZ Biologically Active Natural Products Research Group.

Lastly, I would like to express my sincere appreciation to the Iranian government, including its agencies such as the Ministry of Health and Medical Education, the Organization of Student Affairs, the General Department of Exchange and Student Dispatch, and the Iranian Embassy in Hungary. Their support and coordination have been invaluable in facilitating my studies and research abroad.

Annex

Table S1. ^{1}H NMR data (800 MHz) of compounds **1**–**4** in $CDCl_3$

	δ_H, mult (*J* in Hz)			
Atom	**1**	**2**	**3**	**4**
1β	2.25, dd (12.2, 4.1)	2.22, dd (12.3, 4.3)	2.12, dd (12.1, 4.2)	2.15, dd (12.2, 4.4)
1α	1.57, t (12.2)	1.54, t (12.3)	1.37, m	1.40, m
2	5.22, td (10.8, 4.1)	5.20, td (10.8, 4.3)	5.17, td (10.8, 4.2)	5.18, td (10.8, 4.4)
3	4.85, d (10.8)	4.83, d (10.8)	4.79, d (10.8)	4.81, d (10.8)
5	1.88, dd (13.3, 4.0)	1.85, dd (13.3, 4.0)	1.26, m	1.30, m
6β	2.46, m (2H)	2.44, m (2H)	1.55, m	1.57, m
6α	-	-	1.70, m	1.72, m
7	-	-	2.06, m	2.06, m
11β	2.31, m (2H)	2.30, m (2H)	1.78, m	1.79, m
11α	-	-	2.49, m	2.52, m
12	1.81, m	1.79, m	4.13, t (7.7)	4.14, t (7.7)
15β	1.75, m	1.74, m	1.70, m	1.73, m
15α	2.10, m	2.07, m	1.21, m	1.25, m
16β	1.41, m	1.40, m	1.56, m	1.58, m
16α	2.01, m	2.01, m	1.89, m	1.91, m
17	1.47, m	1.44, m	1.87, m	1.89, m
18	0.67, s	0.65, s	0.72, s	0.74, s
19	1.32, s	1.30, m	1.14, s	1.16, s
20	1.43, m	1.40, m	1.66, m	1.67, m
21	0.93, d (6.6)	0.92, d (6.6)	1.01, d (6.6)	1.04, d (6.6)
22	1.85, m	1.83, m	1.28, m	1.31, m
22	1.33, m	1.31, m	1.92, m	1.95, m
23	2.59, m	2.57, ddd (17.1, 9.8, 5.1)	2.56, m	2.60, dd (9.5, 5.4)
23	2.51, m	2.49, ddd (17.1, 9.3, 6.1)	-	-
26	1.41, s	1.38, s	1.39, s	1.41, s
27	1.41, s	1.39, s	1.38, s	1.40, s
28	0.94, s	0.92, m	0.90, s	0.93, s
29	1.03, s	1.00, s	0.94, s	0.95, s
30	0.93, s	0.91, m	0.91, s	0.93, m
2′	2.57, m	2.54, AB (15.4)	2.53, m	2.56, AB (15.6)
2′	2.70, m	2.68, AB (15.4)	2.68, m	2.70, AB (15.6)
4′	1.40, s	1.35, s	1.38, s	1.36, s
5′a	2.55, br m	2.62, AB (15.4)	2.64, m	2.73, AB (14.9)
5′b	2.72, br m	2.71, AB (15.4)	2.68, m	2.64, AB (14.9)
7′	-	3.71, s	-	3.73, s
3-OAc	2.09, s	2.07, s	2.06, m	2.08, s
25-OH	-	3.82, s	-	3.83, s
3′-OH	-	3.91, s	-	3.96, s

Table S2. ^{13}C NMR data (200 MHz) of compounds **1**–**4** in $CDCl_3$

	δ_C			
Atom	**1**	**2**	**3**	**4**
1	40.1	40.1	41.0	41.1
2	70.3	69.9	71.2, CH	70.7
3	79.0	78.9	80.1, CH	80.0
4	39.3	39.2	39.3, C	39.3
5	49.3	49.3	49.9	50.0
6	36.2	36.2	17.9	17.9
7	197.8	197.8	25.8	25.9
8	139.2	139.1	134.8	134.7
9	163.1	163.0	134.2	134.2, C
10	40.5	40.5	37.8	37.9
11	23.8	23.8	33.8	34.0
12	29.9	29.9	72.8	72.8
13	44.9	44.9	49.0	49.0
14	47.8	47.8	52.2	52.2
15	31.8	31.8	31.2	31.1
16	28.6	28.6	25.1	25.2
17	48.9	48.9	50.5	50.6
18	15.8	15.7	9.9	9.8
19	19.4	19.4	20.0	20.0
20	35.9	35.9	33.8	33.8
21	18.5	18.5	21.2	21.2
22	30.1	30.0	29.1	29.1
23	32.6	32.5	33.7	33.6
24	214.9	214.8	215.2	215.1
25	76.2	76.2	76.3	76.2
26	26.5	26.6	26.5	26.5
27	26.5	26.5	26.5	26.5
28	25.0	25.0	24.2	24.1
29	17.3	17.2	17.4	17.4
30	27.6	27.6	28.2	28.2
1′	170.8	171.2	171.5	171.4
2′	44.9	44.8	44.7	44.9
3′	69.6	69.5	69.7	69.5
4′	27.1	27.3	27.2	26.5
5′	44.8	44.7	45.0	44.7
6′	173.7	172.1	173.5	172.1
7′		51.7		51.7
3-OAc	171.4	170.6	171.1	170.8
	20.9	20.9	21.0	21.0

Table S3. ^{1}H NMR data of compounds **5–11**, and **20** (500 MHz, δ ppm, J = Hz).

H	5[a]	6[b]	7[a]	8[a]	9[a]	10[a]	11[b]	20[a]
1	2.36 dd (12.3, 5.6), 1.66 m	2.11 m, 1.38 m	2.05 m, 1.18 m	2.20 dd (12.3, 4.3), 1.45 m	2.50 m, 1.93 t (13.1)	1.76 m, 1.22 m	1.98 m, 1.61 m	2.36 dd (12.3, 5.6), 1.66 m
2	5.67 dd (13.6, 5.6)	5.19 dt (3.4, 10.5)	4.92 dt (3.9, 10.6)	5.07 dt (4.3, 11.5)	5.72 dd (13.5, 5.8)	1.63 m (2H)	2.57 m, 2.41 ddd (15.8, 6.7, 3.5)	5.66 dd (13.4, 5.6)
3	-	4.79 d (10.5)	3.20 d (10.1)	3.24 d (10.1)	-	3.17 dd (10.1, 6.3)	-	-
5	1.53 m	1.51 m	1.53 m	1.77 m	2.10 dd (14.6, 3.2)	1.06 m	1.60 m	1.53 m
6	1.80 m, 1.73 m	1.69 m, 1.56 m	1.74 m, 1.57 m	2.55 dd (16.3, 14.5), 2.36 m	2.73 m, 2.32 dd (16.6, 3.2)	1.71 m, 1.54 m	1.61 m (2H)	1.80 m, 1.72 m
7	2.18 m (2H)	2.09 m (2H)	2.10 m (2H)	-	-	2.07 m (2H)	2.08 m (2H)	2.17 m (2H)
11	2.16 m, 2.09 m	2.00 m (2H)	2.04 m (2H)	2.38 m (2H)	2.47 m (2H)	2.06 m (2H)	2.04 m (2H)	2.16 m, 2.10 m
12	1.79 m (2H)	1.73 m (2H)	1.74 m (2H)	1.84 m (2H)	1.87 m (2H)	1.78 m, 1.72 m	1.75 m, 1.70 m	1.81 m (2H)
15	1.78 m, 1.23 m	1.61 m, 1.21 m	1.65 m, 1.22 m	2.01 m, 1.72 m	2.03 m, 1.76 m	1.67 m, 1.21 m	1.62 m, 1.22 dd (13.7, 2.5)	1.69 m, 1.25 m
16	2.01 m, 1.46 m	1.97 m, 1.39 m	1.98 m, 1.41 m	2.00 m, 1.42 m	2.02 m, 1.45 m	1.98 m, 1.42 m	1.97 m, 1.38 m	2.01 m, 1.43 m
17	1.56 m	1.30 m	1.53 m	1.47 m	1.49 m	1.53 m	1.50 m	1.57 m
18	0.78 s	0.70 s	0.74 s	0.71 s	0.74 s	0.74 s	0.72 s	0.79 s
19	1.40 s	1.13 s	1.12 s	1.32 s	1.57 s	1.01 s	1.12 s	1.40 s
20	1.45 m	1.40 m	1.42 m	1.42 m	1.44 m	1.43 m	1.40 m	1.46 m
21	0.94 d (6.2)	0.89 d (6.4)	0.92 d (6.4)	0.95 d (6.1)	0.96 d (6.2)	0.93 d (6.2)	0.91 d (6.4)	0.96 d (6.4)
22	1.70 m, 1.27 m	1.82 m, 1.30 m	1.76 m, 1.21 m	1.77 m, 1.23 m	1.78 m, 1.30 m	1.77 m, 1.22 m	1.81 m, 1.31 m	1.82 m, 1.01 m
23	2.67 m (2H)	2.54 m, 2.50 m	2.66 m (2H)	2.66 m (2H)	2.69 m (2H)	2.65 m (2H)	2.55 m, 2.48 m	1.74 m, 1.14 m
24	-	-	-	-	-	-	-	3.17 d (9.9)
26	1.30 s	1.39 s	1.29 s	1.29 s	1.29 s	1.29 s	1.39 s	1.16 s
27	1.30 s	1.39 s	1.29 s	1.29 s	1.29 s	1.29 s	1.38 s	1.16 s
28	1.11 s	0.92 s	1.06 s	1.05 s	1.09 s	0.98 s	1.10 s	1.10 s
29	1.18 s	0.95 s	0.89 s	0.96 s	1.24 s	0.81 s	1.07 s	1.18 s
30	0.93 s	0.89 s	0.93 s	0.95 s	0.94 s	0.92 s	0.90 s	0.93 s
2’	2.80 m, 2.75 m	2.62 m, 2.51 m	2.51 m, 2.33 m	2.71 m (2H)	2.70 m, 2.65 m			2.75 m, 2.71 m
4’	1.41 s	1.39 s	1.33 s	1.41 s	1.37 s			1.41 s
5’	2.69 m (2H)	2.62 m, 2.51 m	2.66 m, 2.50 m	2.71 s (2H)	2.70 m, 2.65 m			2.75 m, 2.71 m
7’	–			3.68 s				
OAc	–	2.10 s						

[a] recorded in CD_3OD; [b] recorded in $CDCl_3$

Table S4. ^{13}C NMR data of compounds **5–11**, and **20** in CD_3OD (125 MHz, δ ppm).

Atom	5[a]	6[b]	7[a]	8[a]	9[a]	10[a]	11[b]	20[a]
1	43.7	41.3	42.2	41.1	42.4	37.0	36.2	43.7
2	73.7	71.9	74.6	73.4	73.0	28.5	34.8	73.9
3	210.9	80.5	80.6	80.0	208.5	79.7	215.1	210.9
4	49.00	39.6	40.6	40.7	49.1	40.0	47.5	49.1
5	54.0	50.6	51.8	51.1	52.6	52.0	51.4	54.0
6	20.0	18.2	19.4	37.5	37.7	19.4	19.6	20.0
7	27.2	26.4	27.4	201.3	200.3	27.7	26.5	27.2
8	136.9	135.2	136.1	139.9	140.2	135.8	135.4	136.9
9	134.7	133.5	135.2	167.2	166.6	136.1	133.3	134.8
10	39.1	38.4	39.4	42.1	41.7	38.3	37.1	39.1
11	22.6	21.4	22.2	24.9	25.3	22.1	21.2	22.5
12	32.2	31.0	32.2	31.2	31.2	32.4	31.0	32.2
13	51.0	44.8	51.0	49.1	46.2	45.8	44.7	51.0
14	45.8	50.0	45.7	46.1	49.7	51.1	50.1	45.8
15	31.1	30.9	31.8	33.2	33.2	31.9	31.1	31.8
16	29.0	28.2	29.1	41.1	29.6	29.1	28.2	29.2
17	51.8	50.3	51.8	50.4	50.3	51.9	50.6	51.9
18	16.3	16.0	16.3	16.3	16.4	16.4	16.0	16.3
19	20.2	20.2	20.4	19.5	19.5	19.6	18.8	20.2
20	37.3	36.2	37.3	37.2	37.2	37.4	36.3	38.1
21	19.0	18.6	19.0	19.1	19.0	19.0	18.6	19.4
22	31.8	30.4	31.1	31.0	31.0	31.1	30.3	34.9
23	34.0	32.8	34.0	33.9	33.9	34.0	32.8	29.3
24	217.8	215.0	217.8	217.8	217.8	217.8	217.9	80.6
25	77.9	76.4	78.1	77.9	77.9	77.9	76.4	73.7
26	26.8	26.7	26.8	26.7	26.7	26.8	26.7	25.6
27	26.8	26.7	26.7	26.8	26.8	26.8	26.7	25.6
28	25.1	28.4	29.0	28.3	24.5	28.6	26.4	25.1
29	21.5	17.6	17.2	16.9	21.3	16.1	21.4	21.5
30	24.6	24.4	24.2	25.3	25.3	24.6	24.4	24.7
1’	171.6	171.1	180.3	172.5	171.5			171.7
2’	46.6	44.8	47.5	46.2	47.2			46.8
3’	70.9	n.d.	71.3	71.0	73.0			71.0
4’	27.6	26.7	28.0	27.9	27.7			27.6
5’	45.8	44.8	48.7	46.6	47.2			46.8
6’	171.6	171.1	172.6	173.2	172.8			171.7
7’	-	-	-	52.0	-	-	-	-
OAc-CH_3		21.1						
OAc-CO		171.8						

[a] recorded in CD_3OD; [b] recorded in $CDCl_3$

Table S5. ^{1}H NMR data of compounds **12**–**19** [(500 MHz, δ ppm (J = Hz)]

No.	**12**[a]	**13**[a]	**14**[a,c]	**15**[b]	**16**[b,c]	**17**[b]	**18**[b]	**19**[a]
1α	1.44 m	1.70 t (12.1)	2.18 t (11.6)	1.40 m	1.31 m	1.49 m	1.81 m	1.53 t (12.3)
1β	2.21 dd (12.5, 3.8)	2.87 dd (12.1, 4.1)	2.26 dd (11.6, 4.3)	3.25 dd (13.0, 4.6)	3.23 dd (12.8, 4.6)	2.39 m	2.64 m	2.21 dd (12.5, 4.3)
2	3.92 dt (3.8, 10.5)	5.29 dt (4.1, 10.9)	5.17 dt (4.3, 10.9)	5.24 dt (4.6, 11.0)	5.14 dt (4.6, 11.0)	5.24 dt (4.3, 10.6)	5.74 dd (13.9, 5.5)	5.19 dt (4.3, 10.9)
3	4.60 d (10.5)	4.83 d (10.9)	4.87 d (10.9)	4.81 d (11.0)	3.28 d (11.0)	4.75 d (10.6)	-	4.83 d (10.9)
5	1.82 m	1.81 m	2.01 m	1.83 dd (14.9, 2.3)	1.75 dd (14.9, 2.2)	1.30 m	1.51 m	1.85 m
6α	2.42 m (2H)	2.44 m	2.48 m (2H)	2.46 dd (15.7, 2.3)	2.50 dd (15.4, 2.2)	2.14 m (2H)	2.14 m	2.43 m (2H)
6β		2.54 m		2.66 m	2.71 m		2.34 m	
7	-	-	-	-	-	5.53 t (3.9)	5.59 d (6.7)	-
11α	2.32 m (2H)	4.57 br t (5.7)		-	-	5.39 d (6.1)	5.49 d (6.1)	2.29 m (2H)
11β			4.49 m					
12α	1.79 m (2H)	2.28 m	2.46 m	2.87 d (16.1)	2.90 d (16.2)	2.25 d (17.5)	2.30 d (17.9)	1.78 m (2H)
12β		1.88 m	1.84 m	2.58 d (16.1)	2.62 d (16.2)	2.14 dd (17.5, 6.1)	2.18 dd (17.9, 6.1)	
15	2.07 m, 1.74 m	2.08 m, 1.83 m	2.08 m, 1,65 m	2.13 m, 1.82 m	2.17 m, 1.82 m	1.66 m, 1.43 m	1.70 m, 1.47 m	2.07 m, 1.73 m
16	2.00 m, 1.37 m	2.04 m, 1.45 m	2.00 m, 1.33 m	2.04 m, 1.46 m	2.08 m, 1.49 m	2.03 m, 1.42 m	2.06 m, 1.45 m	2.00 m, 1.38 m
17	1.42 m	1.43 m	1.55 m	1.76 m	1.80 m	1.63 m	1.66 m	1.43 m
18	0.66 s	0.89 s	0.65 s	0.84 s	0.88 s	0.61 s	0.67 s	0.65 s
19	1.24 s	1.50 s	1.34 s	1.44 s	1.47 s	1.14 s	1.40 s	1.30 s
20	1.40 m	1.43 m	1.36 m	1.44 m	1.49 m	1.44 m	1.45 m	1.43 m
21	0.91 d (6.2)	0.94 d (6.2)	0.91 d (6.3)	0.92 d (7.1)	0.97 d (6.6)	0.93 d (6.6)	0.95 d (6.7)	0.92 d (6.7)
22	1.83 m, 1.31 m	1.83 m, 1.31 m	1,82 m, 1.30 m	1.80 m, 1.25 m	1.82 m, 1.33 m	1.77 m, 1.23 m	1.79 m, 1.26 m	1.85 m, 1.35 m
23	2.52 m (2H)	2.53 m (2H)	2.55 m, 2.49 m	2.68 m (2H)	2.72 m (2H)	2.67 m (2H)	2.67 m (2H)	2.40 m, 2.27 m
26	1.38 s	1.38 s	1.38 s	1.29 s	1.34 s	1.29 s	1.31 s	
27	1.38 s	1.38 s	1.39 s	1.29 s	1.34 s	1.29 s	1.31 s	
28	0.91 s	0.90 s	0.92 s	0.93 s	1.11 s	0.91 s	1.11 s	0.90 s
29	0.96 s	1.03 s	1.01 s	1.04 s	1.00 s	1.03 s	1.26 s	1.00 s
30	0.92 s	0.86 s	1.12 s	0.84 s	1.25 s	0.93 s	0.94 s	0.91 s
2’	2.75 m, 2.57 m	2.68 m, 2.54 m	2.63 m, 2.53 m	2.63 m (2H)	2.78 m, 2.73 m	2.66 m, 2.54 m	2.81 m, 2.74 m	2.67 m, 2.52 m
4’	1.42 s	1.35 s	1.35 s	1.35 s	1.44 s	1.33 s	1.44 s	1.33 s
5’	2.92 m, 2.27 m	2.70 m, 2.62 m	2.68 m, 2.62 m	2.68 m (2H)	2.76 m (2H)	2.54 m, 2.39 m	2.81 m, 2.74 m	2.70 m, 2.61 m
7’	3.72 s	3.71 s	3.71 s	3.67 s	3.73 s	-	-	-
OAc	-	2.07 s		2.06 s		2.06 s	-	2.06 s

[a] measured in $CDCl_3$; [b] in CD_3OD; Signal of H-12 in the ^{1}H NMR spectrum measured in CD_3OD was 4.48 dd (J = 9.1, 5.5 Hz); [c] measured at 600 MHz.

Table S6. ^{13}C NMR data of compounds **12**–**19** (125 MHz, δ ppm)

Position	**12**[a]	**13**[a]	**14**[a,c]	**15**[b]	**16**[b,c]	**17**[b]	**18**[b]	**19**[a]
1	42.8	39.5	39.9	40.5	40.4	42.5	43.7	40.4
2	66.9	69.9	70.4	70.6	73.2	71.1	73.4	70.1
3	84.5	79.4	79.1	80.6	79.8	81.7	210.6	79.2
4	38.9	39.6	39.5	40.2	40.6	40.3	49.0	39.4
5	49.8	50.3	49.7	50.9	51.4	50.4	53.0	49.5
6	36.6	36.6	36.8	37.1	37.4	23.9	24.6	36.4
7	198.3	199.7	199.2	202.8	203.5	121.2	123.2	198.0
8	139.1	139.7	141.7	152.2	152.1	143.9	144.0	139.3
9	164.1	160.5	159.1	151.9	152.1	146.3	145.5	163.3
10	40.7	40.8	40.6	41.5	41.7	39.7	39.5	40.7
11	24.0	67.3	65.5	203.6	203.9	118.3	118.7	24.0
12	30.3	42.9	44.6	52.5	52.5	39.0	38.9	30.1
13	45.1	43.6	44.6	48.6	48.9	45.0	44.8	45.1
14	48.0	49.1	48.3	50.4	50.3	51.5	51.6	48.0
15	32.1	32.1	32.8	33.3	33.3	32.6	32.6	32.0
16	28.9	28.9	27.7	28.1	28.1	28.7	28.7	28.7
17	49.1	48.4	49.9	50.3	50.3	52.3	52.3	48.9
18	15.9	17.4	17.0	17.3	17.2	16.3	16.3	15.9
19	19.9	21.2	21.2	19.1	18.9	23.9	23.2	19.6
20	36.1	36.1	36.0	37.1	37.0	37.1	37.1	36.0
21	18.7	18.8	18.5	18.8	18.8	18.8	18.8	18.5
22	30.2	30.2	30.1	30.8	30.8	31.0	31.0	31.1
23	32.7	32.7	32.7	33.8	33.8	34.0	34.0	31.0
24	215.1	214.9	214.8	217.6	217.9	217.8	217.7	178.7
25	76.3	76.4	76.2	77.9	78.0	77.9	77.9	-
26	26.7	26.7	26.7	26.7	26.7	26.8	26.8	-
27	26.7	26.7	26.7	26.8	26.8	26.7	26.7	-
28	28.0	28.1	27.9	28.4	28.6	29.0	25.3	27.8
29	17.5	17.5	17.4	17.7	17.1	18.2	22.2	17.4
30	25.2	25.3	25.4	26.0	26.0	26.1	26.1	25.2
1’	171.4	171.4	171.7	171.9	172.5	172.2	171.7	171.4
2’	46.3	45.0	45.1	46.3	46.6	47.2	46.8	45.1
3’	70.4	69.7	69.8	70.6	70.9	70.8	71.1	69.7
4’	28.3	27.7	27.7	28.0	27.9	27.8	27.6	27.6
5’	43.7	45.0	45.1	46.0	46.0	47.7	46.8	44.9
6’	173.3	172.3	172.1	173.1	173.4	171.7	171.7	172.2
7’	52.0	51.9	52.0	51.9	52.0			
Ac*C*O		170.8	170.7	172.5	-	172.6		170.7
Ac*C*H$_3$		21.1	21.1	21.0	-	21.1		21.0

[a] measured in $CDCl_3$; [b] in CD_3OD; [c] measured at 150 MHz.

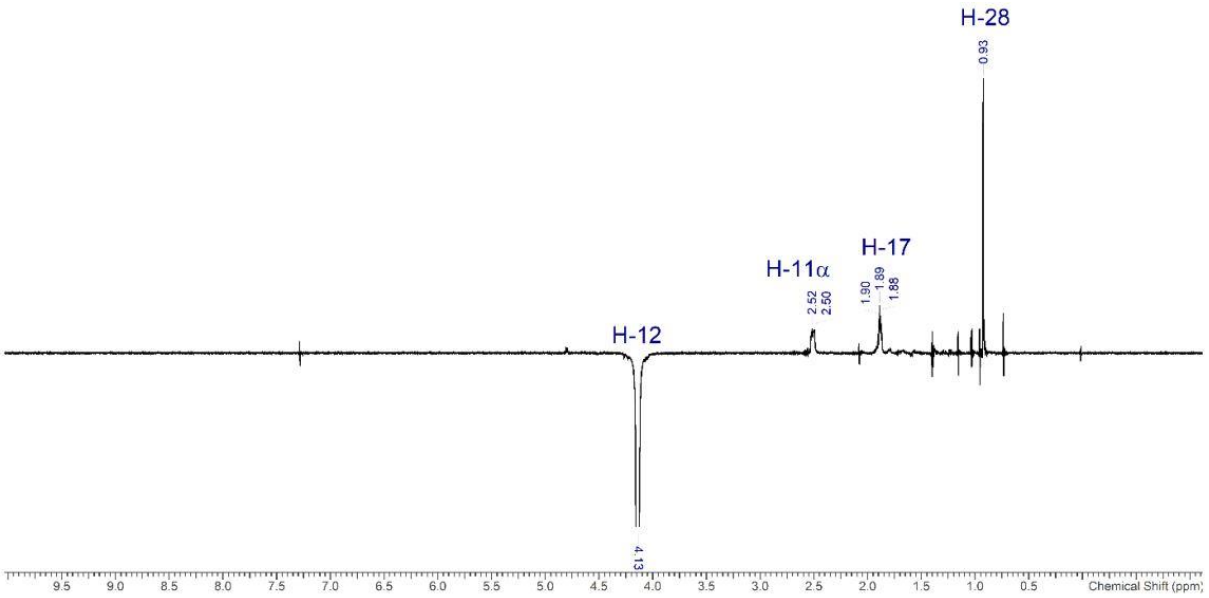

Figure S1. 1D ROESY spectrum of compound **3**

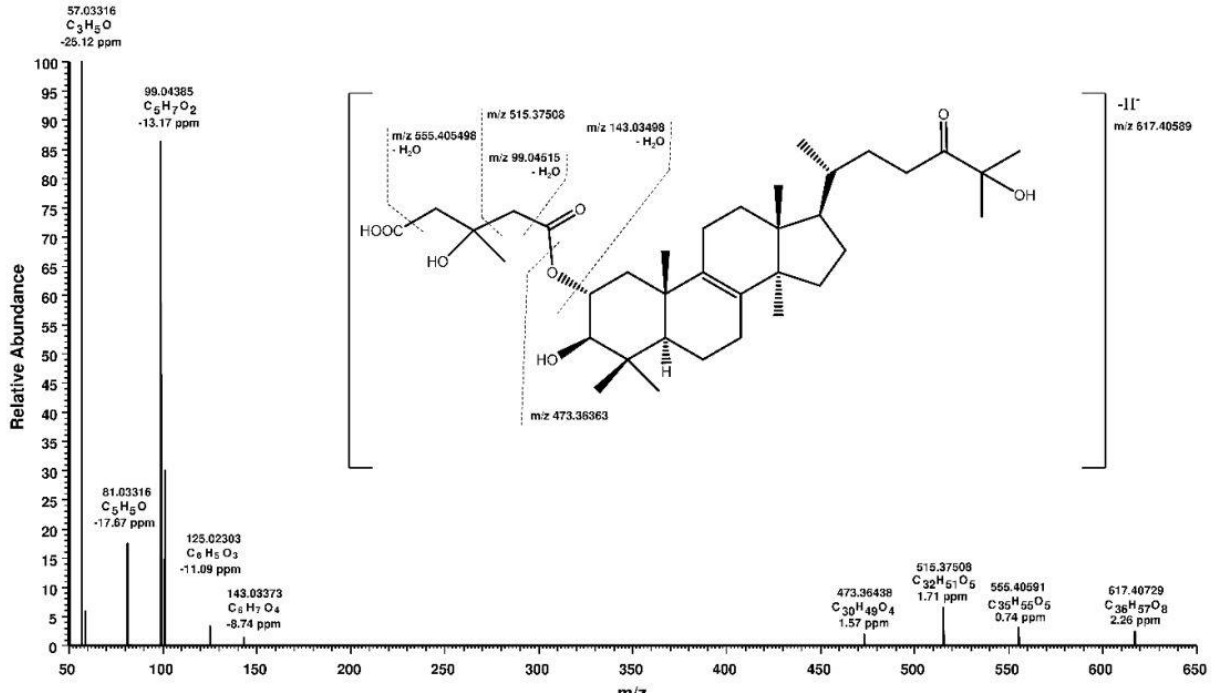

Figure S2. Negative ion HRMS/MS spectrum with proposed fragmentation pathway of compound **7** with main HRMS/MS data of precursor and fragment ions such as molecular formula, mass error in ppm, theoretical and measured *m*/*z* values.

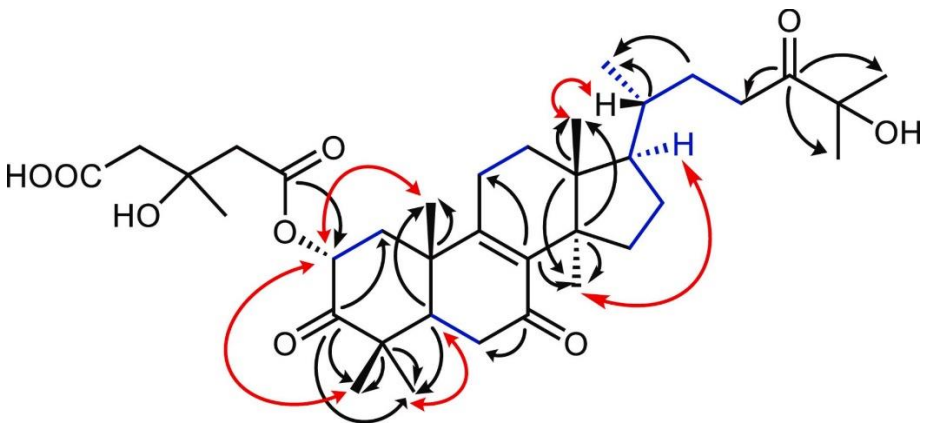

Figure S3. Diagnostic ^{1}H,^{1}H–COSY, HMBC and NOESY correlations of pholiol I (**9**)

I.

JOURNAL OF NATURAL PRODUCTS

pubs.acs.org/jnp

Article

Triterpenes from *Pholiota populnea* as Cytotoxic Agents and Chemosensitizers to Overcome Multidrug Resistance of Cancer Cells

Morteza Yazdani, Zoltán Béni, Miklós Dékány, Nikoletta Szemerédi, Gabriella Spengler, Judit Hohmann,* and Attila Ványolós*

Cite This: *J. Nat. Prod.* 2022, 85, 910−916

Read Online

ACCESS | Metrics & More | Article Recommendations | Supporting Information

ABSTRACT: The detailed mycochemical analysis of the *n*-hexane extract of *Pholiota populnea* led to the isolation of four new lanostane diesters, named pholiols A−D (**1**−**4**), together with an acyclic triterpene, (3*S*,6*E*,10*E*,14*E*,18*E*,22*S*)-2,3,22,23-tetrahydroxy-2,6,10,15,19,23-hexamethyl-6,10,14,18-tetracosatetraene (**5**), ergosterol (**6**), and 3β-hydroxyergosta-7,22-diene (**7**). The isolation was carried out by multistep flash chromatography, and the structures were elucidated using extensive spectroscopic analyses, including 1D and 2D NMR and MS measurements. The isolated metabolites (**1**−**6**) were investigated for cytotoxic activity against Colo205 and Colo320 colon adenocarcinoma and nontumoral MRC-5 cell lines. Among the tested compounds, ergosterol (**6**) showed substantial cytotoxic activity against all cell lines with IC_{50} values of 4.9 μM (Colo 205), 6.5 μM (Colo 320), and 0.50 μM (MRC) with no tumor cell selectivity. A P-glycoprotein efflux pump modulatory test on resistant Colo320 cells revealed that pholiols A (**1**) and B (**2**) and linear triterpene polyol **5** have the capacity to inhibit the efflux-pump overexpressed in the cells. Moreover, the drug interactions of triterpenes with doxorubicin were studied by the checkerboard method on Colo 320 cells. Pholiols B (**2**) and D (**4**) interacted in synergistic and acyclic triterpene **5** in a very strong synergistic manner; the combination index (CI) values at 50% of the growth inhibition dose (ED_{50}) were found to be 0.348, 0.660, and 0.082, respectively. Our results indicate that *P. populnea* is a promising source for finding new triterpenes with significant chemosensitizing activity on cancer cells.

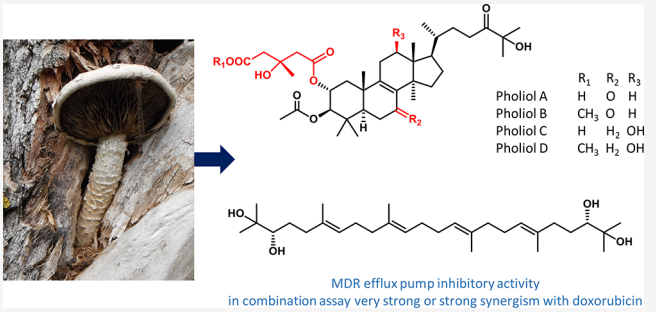

Cancer is among the leading causes of morbidity and mortality worldwide. According to Global Cancer Statistics, an estimated 19.3 million new cancer cases, among them 1.148 million new colon cancer instances (representing 6.0% of all cases), were registered worldwide in 2020.[1] A major problem in clinical cancer therapy is the multidrug resistance (MDR) toward cytotoxic drugs. MDR is associated with cellular pharmacokinetic alterations, such as decreased drug accumulation, increased efflux and detoxification capacity, and subcellular redistribution. One of the most widespread mechanisms of resistance involves the efflux of drug molecules out of the cells. In particular, ATP-binding cassette (ABC) transporters have received great interest; one such transporter that has been investigated in detail is P-glycoprotein (P-gp).[2] Triterpenoids were reported to be able to reverse cell resistance to chemotherapy due to P-gp inhibition. Ginsenoside Rh2, isolated from red ginseng, exerts such activity in doxorubicin-resistant human breast cancer MCF-7 cells.[3] Oleanolic acid was reported to be an inhibitor of certain efflux transporters, including P-gp35, and thus was found to increase the intracellular concentration of paclitaxel.[4] Maslinic acid, a natural triterpene from *Olea europaea* L., has attracted increasing interest in recent years because of its promising anticancer activity and dose-dependent enhancing potency of docetaxel (DOC) sensitivity and cellular drug accumulation in MDA-MB-231/DOC cells in a combination treatment.[5] The tetracyclic triterpene alcohol euphol was reported to have cytotoxicity (IC_{50} < 10 μM) against 27 cell lines when screened against a panel of 71 human cancer cells from 15 tumor types. This compound also exhibited antitumoral and antiangiogenic activity *in vivo*, with synergistic temozolomide interactions in most cell lines.[6] The pentacyclic terpenoid boswellic acid was studied in combination with doxorubicin for the antitumor effects against solid tumors of Ehrlich's ascites carcinoma grown in mice. The results showed that boswellic acid synergized the antitumor activity of doxorubicin.[7] The fungal metabolite ergosta-7,22-diene-3-one was found to be effective against sensitive (Colo 205) and resistant (Colo 320) human colon adenocarcinoma cells with IC_{50} values 11.6 ± 1.7 μM and 8.4 ± 1.1 μM, respectively, and in a combination assay

Received: October 28, 2021
Published: March 16, 2022

synergism was detected between ergosta-7,22-diene-3-one and doxorubicin with CI index 0.521 ± 0.15 at the 50% growth inhibition dose (ED_{50}).[8]

Pholiota populnea (Pers.) Kuyper & Tjall.-Beuk. (syn. *Pholiota destruens* (Brond.) Quel., *Hemipholiota populnea*) is member of the Strophariaceae family, distributed worldwide wherever cottonwood occurs. This mushroom species is usually saprophytic, but sometimes parasitic, and grows on broad-leaved woods, mainly on various poplars, but also on willow and birch, playing an important role in decomposing the deadwood of cottonwoods. The chemistry and pharmacology of *P. populnea* were poorly studied previously, with only pholiotic acid, 3,5-dichloro-4-methoxybenzaldehyde, and 3,5-dichloro-4-methoxybenzyl alcohol, with weak antifungal and cytostatic activities, identified.[9] In a recent paper the mineral element composition of this species was reported.[10]

In the current study, the detailed mycochemical analysis of a methanolic extract of *H. populnea*, isolation, structure determination, and pharmacological evaluation of its chemical compounds are highlighted. The present paper reports four new lanostane diesters (**1**−**4**), one acyclic triterpene tetraol (**5**), and the known compounds ergosterol (**6**) and 3*β*-hydroxyergosta-7,22-diene (**7**). The isolated compounds **1**−**6** were investigated for cytotoxic activity against human colon adenocarcinoma cells (Colo205, Colo320) and the MRC-5 cell line. The combination with doxorubicin and efflux pump inhibitory activity of the compounds on drug-resistant Colo 320 cells were also assayed. In addition, antimicrobial activity against different bacterial strains was evaluated by the microdilution method.

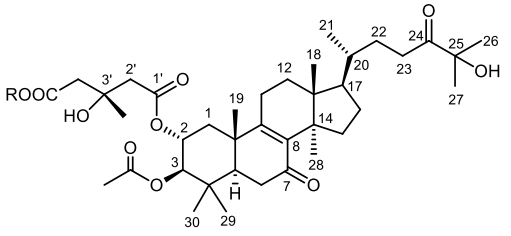

	R
1	H
2	CH_3

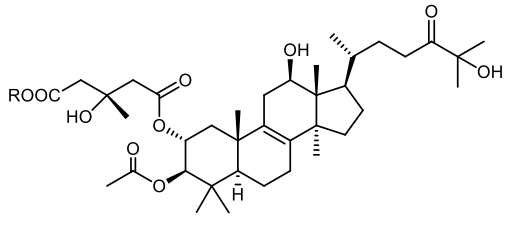

	R
3	H
4	CH_3

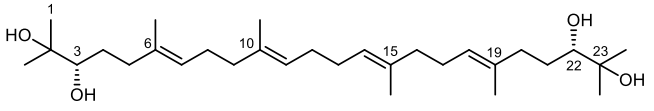

5

RESULTS AND DISCUSSION

Four lanostane triterpenes (**1**−**4**) and an acyclic triterpene tetraol (**5**) were isolated from the *n*-hexane-soluble phase of the MeOH extract prepared from the mushroom *P. populnea* by a combination of multiple flash chromatography steps. The structure elucidation was carried out by extensive spectroscopic analysis, including 1D and 2D NMR (^{1}H−^{1}H COSY, HSQC, HMBC, and ROESY) and HRESIMS experiments.

Based on the HRESIMS data, the molecular formulas of compounds **1** and **2** were $C_{38}H_{58}O_{10}$ and $C_{39}H_{60}O_{10}$, respectively, differing only in a methylene group. The ^{1}H and ^{13}C NMR spectra of **1** and **2** (Tables 1 and 2) were similar except for a singlet signal with three-proton intensity at δ_H 3.71 appearing in the ^{1}H NMR spectrum and the extra resonance at δ_C 51.7 in the ^{13}C NMR spectrum of **2**. These findings suggested that **2** was the *O*-methyl derivative of **1**. In accordance with the elemental compositions, the ^{13}C NMR spectra presented 38 and 39 resonances in compounds **1** and **2**, respectively. Based on the HSQC spectra, besides the additional methoxy group in **2**, 10 methyl, 10 methylene, and 5 methine groups, and 13 nonprotonated carbons were commonly present in the compounds. Considering the elemental compositions and the chemical shift values of the nonprotonated carbons, two carbonyl groups (δ_C 214.9/214.8 and δ_C 197.9/197.9), three carboxylate moieties (δ_C 173.7/172.1, 170.8/171.2, and 171.4/170.6), an unsaturation (δ_C 139.2/139.1 and δ_C 163.1/163.0), and two sp^3 carbons attached to oxygens (δ_C 76.2/76.2 and 69.6/69.5) were present in **1** and **2**. The remaining four signals (δ_C 39.3/39.2, 40.5/40.5, 44.9/44.9, and 47.8/47.8 for **1**/**2**) could be ascribed to sp^3 nonprotonated carbons. Based on the characteristic HMBC correlations of the angular methyl singlets [H-18 with C-12, C-13, C-14, and C-17; H-19 with C-1, C-5, C-9, and C-10; H-21 with C-17, C-20, and C-22; H-29 and H-30 with C-3, C-4, and C-5], it was concluded that **1** and **2** are based on a lanostane skeleton. The HMBC correlations of the *O*-methine doublets at δ_H 4.85/4.83 with C-1, C-4, C-29, and C-30 confirmed their assignment to H-3 in **1**/**2**, while HMBC cross-peaks of the *O*-methine groups at δ_C 70.3/69.9 (C-2) with protons at δ_H 4.85/4.83 (H-3) suggested that the lanosterol skeleton bears oxygen-containing substituents at both C-2 and C-3. The HMBC correlations of the acetyl CO signal with H-3 and the acetyl methyl signal suggested the presence of an acetate group at C-3, while, based on the HMBC correlations of H-2/C-1′, H-2′/C-1′, H-2′/C-3′, H-2′/C-4′, H-2′/C-5′, H-4′/C-5′, and H-5′/C-6′, a 3-hydroxy-3-methylglutarate moiety was attached to C-2 in compounds **1** and **2**. The additional H-7′/C-6′ HMBC correlation in compound **2** suggested that **2** was the methyl ester of compound **1**. Further to these, the HMBC correlations of the doublet of doublets at δ_H 1.88/1.85 (assigned to H-5) with C-4, C-10, C-19, C-29, and C-30 confirmed this assignment, while long-range correlations of H-5 with the methylene at δ_C 36.2/36.2 and with the carbonyl at δ_C 197.8/197.8 enabled the assignment of C-6 and suggested the presence of a keto group in position 7. In parallel, the HMBC correlations between the diastereotopic protons (H-22) and the methylene group at δ_C 32.6/32.5 (C-23) and carbonyl group at δ_C 214.9/214.8 (C-24) and between the methyl singlets of H-26 and H-27 and C-24 and nonprotonated carbon at δ_C 76.2/76.2 (C-25) led to the conclusion that a 24-keto-25-hydroxy side chain was present at C-17. Based on the complete ^{1}H and ^{13}C NMR assignments

https://doi.org/10.1021/acs.jnatprod.1c01024
J. Nat. Prod. 2022, 85, 910−916

Table 1. ^{1}H NMR Data (800 MHz) of Compounds 1−4 in $CDCl_3$

	δ_H, mult (J in Hz)			
atom#	1	2	3	4
1β	2.25, dd (12.2, 4.1)	2.22, dd (12.3, 4.3)	2.12, dd (12.1, 4.2)	2.15, dd (12.2, 4.4)
1α	1.57, t (12.2)	1.54, t (12.3)	1.37, m	1.40, m
2	5.22, td (10.8, 4.1)	5.20, td (10.8, 4.3)	5.17, td (10.8, 4.2)	5.18, td (10.8, 4.4)
3	4.85, d (10.8)	4.83, d (10.8)	4.79, d (10.8)	4.81, d (10.8)
5	1.88, dd (13.3, 4.0)	1.85, dd (13.3, 4.0)	1.26, m	1.30, m
6β	2.46, m (2H)	2.44, m (2H)	1.55, m	1.57, m
6α			1.70, m	1.72, m
7			2.06, m	2.06, m
11β	2.31, m (2H)	2.30, m (2H)	1.78, m	1.79, m
11α			2.49, m	2.52, m
12	1.81, m	1.79, m	4.13, t (7.7)	4.14, t (7.7)
15β	1.75, m	1.74, m	1.70, m	1.73, m
15α	2.10, m	2.07, m	1.21, m	1.25, m
16β	1.41, m	1.40, m	1.56, m	1.58, m
16α	2.01, m	2.01, m	1.89, m	1.91, m
17	1.47, m	1.44, m	1.87, m	1.89, m
18	0.67, s	0.65, s	0.72, s	0.74, s
19	1.32, s	1.30, m	1.14, s	1.16, s
20	1.43, m	1.40, m	1.66, m	1.67, m
21	0.93, d (6.6)	0.92, d (6.6)	1.01, d (6.6)	1.04, d (6.6)
22	1.85, m	1.83, m	1.28, m	1.31, m
22	1.33, m	1.31, m	1.92, m	1.95, m
23	2.59, m	2.57, ddd (17.1, 9.8, 5.1)	2.56, m	2.60, dd (9.5, 5.4)
23	2.51, m	2.49, ddd (17.1, 9.3, 6.1)		
26	1.41, s	1.38, s	1.39, s	1.41, s
27	1.41, s	1.39, s	1.38, s	1.40, s
28	0.94, s	0.92, m	0.90, s	0.93, s
29	1.03, s	1.00, s	0.94, s	0.95, s
30	0.93, s	0.91, m	0.91, s	0.93, m
2′	2.57, m	2.54, AB (15.4)	2.53, m	2.56, AB (15.6)
2′	2.70, m	2.68, AB (15.4)	2.68, m	2.70, AB (15.6)
4′	1.40, s	1.35, s	1.38, s	1.36, s
5′a	2.55, br m	2.62, AB (15.4)	2.64, m	2.73, AB (14.9)
5′b	2.72, br m	2.71, AB (15.4)	2.68, m	2.64, AB (14.9)
7′		3.71, s		3.73, s
3-OAc	2.09, s	2.07, s	2.06, m	2.08, s
25-OH		3.82, s		3.83, s
3′-OH		3.91, s		3.96, s

Table 2. ^{13}C NMR Data (200 MHz) of Compounds 1−4 in $CDCl_3$

	δ_C, type			
atom#	1	2	3	4
1	40.1, CH_2	40.1, CH_2	41.0, CH_2	41.1, CH_2
2	70.3, CH	69.9, CH	71.2, CH	70.7, CH
3	79.0, CH	78.9, CH	80.1, CH	80.0, CH
4	39.3, C	39.2, C	39.3, C	39.3, C
5	49.3, CH	49.3, CH	49.9, CH	50.0, CH
6	36.2, CH_2	36.2, CH_2	17.9, CH_2	17.9, CH_2
7	197.8, C	197.8, C	25.8, CH_2	25.9, CH_2
8	139.2, C	139.1, C	134.8, C	134.7, C
9	163.1, C	163.0, C	134.2, C	134.2, C
10	40.5, C	40.5, C	37.8, C	37.9, C
11	23.8, CH_2	23.8, CH_2	33.8, CH_2	34.0, CH_2
12	29.9, CH_2	29.9, CH_2	72.8, CH_2	72.8, CH_2
13	44.9, C	44.9, C	49.0, C	49.0, C
14	47.8, C	47.8, C	52.2, C	52.2, C
15	31.8, CH_2	31.8, CH_2	31.2, CH_2	31.1, CH_2
16	28.6, CH_2	28.6, CH_2	25.1, CH_2	25.2, CH_2
17	48.9, CH	48.9, CH	50.5, CH	50.6, CH
18	15.8, CH_3	15.7, CH_3	9.9, CH_3	9.8, CH_3
19	19.4, CH_3	19.4, CH_3	20.0, CH_3	20.0, CH_3
20	35.9, CH	35.9, CH	33.8, CH	33.8, CH
21	18.5, CH_3	18.5, CH_3	21.2, CH_3	21.2, CH_3
22	30.1, CH_2	30.0, CH_2	29.1, CH_2	29.1, CH_2
23	32.6, CH_2	32.5, CH_2	33.7, CH_2	33.6, CH_2
24	214.9, C	214.8, C	215.2, C	215.1, C
25	76.2, C	76.2, C	76.3, C	76.2, C
26	26.5, CH_3	26.6, CH_3	26.5, CH_3	26.5, CH_3
27	26.5, CH_3	26.5, CH_3	26.5, CH_3	26.5, CH_3
28	25.0, CH_3	25.0, CH_3	24.2, CH_3	24.1, CH_3
29	17.3, CH_3	17.2, CH_3	17.4, CH_3	17.4, CH_3
30	27.6, CH_3	27.6, CH_3	28.2, CH_3	28.2, CH_3
1′	170.8, C	171.2, C	171.5, C	171.4, C
2′	44.9, CH_2	44.8, CH_2	44.7, CH_2	44.9, CH_2
3′	69.6, C	69.5, C	69.7, C	69.5, C
4′	27.1, CH_3	27.3, CH_3	27.2, CH_3	26.5, CH_3
5′	44.8, CH_2	44.7, CH_2	45.0, CH_2	44.7, CH_2
6′	173.7, C	172.1, C	173.5, C	172.1, C
7′		51.7, CH_3		51.7, CH_3
3-OAc	171.4, C	170.6, C	171.1, C	170.8, C
	20.9, CH_3	20.9, CH_3	21.0, CH_3	21.0, CH_3

(Tables 1 and 2), compounds **1** and **2** were identified as fasciculic acid A[11,12] derivatives.

According to the observed NOE correlations of H-18 with H-11β, H-15β, H-16β, and H-20, those of H-19 with H-1β, H-2, H-11β, and H-29, and of H-28 with H-15α, H-16α and H-17, the relative stereochemistry as depicted in structural formulas **1** and **2** was proposed for the two compounds. Thus, compound **1**, named as pholiol A, was assigned as the 3-*O*-acetyl-7,24-diketo analogue of fasciculic acid A,[11,12] while pholiol B (**2**) was assigned as its methyl ester. The relative configuration of the C-3′ chiral center could not be determined on this basis and is only tentatively given as *S*, based on the close chemical shift values with those of similar compounds[11,12] and on assuming that similar metabolic pathways led to the formation of the structurally similar compounds in the different fungal species.

The molecular formulas of **3** ($C_{38}H_{60}O_{10}$) and **4** ($C_{39}H_{62}O_{10}$) derived from HRESIMS measurements differed only in a methylene group, similarly to those of compound pair **1** and **2**. As compared to pholiols A (**1**) and B (**2**), compounds **3** and **4** contained two additional hydrogens, nominally corresponding to the saturation of the double bond in **1**/**2**. The ^{1}H and ^{13}C NMR spectra of **3** and **4** were highly similar to those of compounds **1** and **2**. The most striking differences were the presence of a triplet signal with one hydrogen intensity at δ_H 4.13/4.14 in the ^{1}H NMR spectrum and in parallel the absence of the carbonyl resonance belonging to C-7 and the appearance of resonance at δ_C 72.8/72.8 in the ^{13}C

https://doi.org/10.1021/acs.jnatprod.1c01024
J. Nat. Prod. 2022, 85, 910−916

NMR spectrum of **3**/**4**. Thus, at first sight, the reduction of the keto group at C-7 to a hydroxy group was envisaged. The ^{1}H and ^{13}C NMR spectra of **3** and **4** were almost identical, except for the presence of a singlet with a three-hydrogen intensity at δ_H 3.73 in the ^{1}H NMR spectrum and a carbon signal at δ_C 51.7 in the ^{13}C NMR spectrum of **4**. This suggested that **4** was the methyl ester analogue of compound **3**. Analysis of the HSQC and HMBC data showed that a hydroxy group was attached to C-12 ($\delta_{H\text{-}12}$ 4.13/4.14, each 1H, t, J = 7.7 Hz; $\delta_{C\text{-}12}$ 72.8/72.8 for **3**/**4**; HMBC correlation between H-18 and C-12) and a methylene group was present in position 7 based on the HMBC correlation of H-5 and H-6 with C-7. 2D NMR experiments allowed the complete ^{1}H and ^{13}C NMR assignments of **3** and **4** as listed in Tables 1 and 2. Compound **3**, named as pholiol C, was identified as the 24-keto derivative of fasciculic acid B,[11] while pholiol D (**4**) was identified as its methyl ester. The similar chemical shifts and NOE correlations suggested that the relative configurations of the C-2, C-3, C-5, C-10, C-14, C-17, and C-20 (and C-1′) chiral centers of **3** and **4** were identical to those determined for pholiols A (**1**) and B (**2**). The NOE correlations of H-12 with H-11α, H-17, and H-28 (Figure S26) suggested that the hydroxy group occupied the β position (thus, the C-12 chiral center had an *R* configuration) in pholiols C (**3**) and D (**4**).

Compound **5** was identified as (6*E*,10*E*,14*E*,18*E*)-2,3,22,23-tetrahydroxy-2,6,10,15,19,23-hexamethyl-6,10,14,18-tetracosatetraene regarding its ^{1}H and ^{13}C NMR chemical shift values, identical with literature data.[13] The 3*S*,22*S* configuration of **5** can be suggested based on the opposite optical rotation data than that of the 3*R*,22*R* isomer.[14] Compound **6** was found to be identical in all of its spectroscopic characteristics with that of ergosterol.[15] 3β-Hydroxyergosta-7,22-diene was detected in the *n*-hexane fraction with the use of an authentic standard.

Cytotoxic Activity. The isolated compounds (**1**−**6**) were tested for their cytotoxic activity on sensitive Colo 205 and resistant Colo 320 cell lines and on the normal MRC-5 embryonal fibroblast cell line using the 3-(4,5-dimethylthiazol-2-yl)-2,5-diphenyltetrazolium bromide (MTT) assay with doxorubicin as a positive control. Among the studied compounds, ergosterol (**6**) showed substantial cytotoxic activity against the tumor cell lines with IC_{50} values of 4.9 μM (Colo 205) and 6.5 μM (Colo320) (Table 3). This compound was more potent against the MRC-5 cell line (IC_{50} 0.50 μM). Pholiols B (**2**) and D (**4**) and compound **5** possessed weak inhibitory activities (IC_{50} > 25 μM) against the tested cell lines without any selectivity (Table S2).

Table 3. Cytotoxic Effect of the Compound 6

	Colo205 (IC_{50} μM)		Colo320 (IC_{50} μM)		MRC-5 (IC_{50} μM)	
compound	mean	SD	mean	SD	mean	SD
ergosterol (**6**)	**4.9**	0.6	**6.5**	0.2	**0.5**	0.1
doxorubicin	2.5	0.3	7.4	0.2	>20	

MDR Efflux Pump Inhibitory Activity. The inhibitory activities of compounds **1**−**3**, **5**, and **6** on efflux function were evaluated by measuring the intracellular accumulation of rhodamine 123, a well-known P-glycoprotein substrate fluorescent dye, within the Colo320 MDR cells. Tariquidar, a strong P-gp inhibitor, was used as positive control. All tested compounds were dissolved in DMSO, and the final concentration (2.00%) of the solvent was investigated for any effect on the retention of rhodamine 123. The results revealed inhibition of P-gp MDR efflux pump activity manifested by pholiols A (**1**) and B (**2**) and triterpene **5**. In general, compounds with fluorescence activity ratio (FAR) values greater than 1 were considered to be active P-gp inhibitors, while compounds with FAR values greater than 10 were considered to be strong MDR modulators. The sterol compounds with methyl ester functionality (**2**) and the polyhydroxy-squalene derivative (**5**) exerted the highest anti-MDR effect in this bioassay with FAR values of 6.880 and 6.638, respectively.

Table 4. P-gp Efflux Pump Inhibitory Activity of Compounds 1−3, 5, and 6 against MDR COLO 320 Colon Adenocarcinoma Cells

sample	conc., μM	FAR
tariquidar[a]	0.2	5.533
pholiol A (**1**)	20	3.418
pholiol B (**2**)	20	**6.880**
pholiol C (**3**)	20	0.967
compound **5**	20	**6.638**
ergosterol (**6**)	2	1.053
DMSO	2.00%	0.828

[a]Positive control.

Combination Studies with Doxorubicin. Compounds **2** and **4**−**6** were tested for their capacity to reduce the resistance of the MDR Colo 320 cell line to doxorubicin. A checkerboard microplate combination assay was performed, which is a widely used *in vitro* method for the assessment of drug interactions. Experimental data were analyzed using CompuSyn software, which enabled the determination of the most effective ratios of combined agents and calculation of combination indices (CI). Based on the combination indices, the type of interaction could be defined according to the literature.[16] Pholiols B (**2**) and D (**4**), with a 3-hydroxy-3-methyl-glutarate methyl ester moiety, and **5** interacted in an synergistic manner, and CI values at 50% of the ED_{50} were found to be 0.348, 0.660, and 0.082, respectively. The outstanding potency of **5**, designated as very strong synergism (CI = 0.082), is promising. In this assay ergosterol (**6**) was found to have an additive effect in combination with doxorubicin.

It is noteworthy that the tetrahydroxy-squlene derivative (**5**) has the capacity to potentiate the effect of doxorubicin in Colo 320 adenocarcinoma cells by P-gp modulation and strong synergism with doxorubicin, and therefore it represents a promising new class of potential adjuvants of cancer chemotherapy. With regard to the moderate P-gp inhibitory activity and strong synergism of **5** in combination with doxorubicin, the mechanism of its chemosensitizing effect should have another P-gp-independent mechanism.

Antibacterial Effect. Compounds **1**−**6** were inactive against *Escherichia coli* ATCC 25922, *Salmonella enterica* serovar Typhimurium 14028s, *Staphylococcus aureus* ATCC 25923, and *S. aureus* 27213.[8]

EXPERIMENTAL SECTION

General Experimental Procedures. The chemicals used in the experiments were supplied by Sigma-Aldrich Hungary and Molar Chemicals, Hungary. An InsMark IP-Digi1 polarimeter (Shanghai InsMark Instrument Technology Co., Ltd., Shanghai, China) was applied for optical rotation measurements. Flash chromatography

https://doi.org/10.1021/acs.jnatprod.1c01024
J. Nat. Prod. 2022, 85, 910−916

Table 5. Chemosensitizing Activity of Compounds 2 and 4−6 on Colo 320 Adenocarcinoma Cells

compound	best ratio[a]	CI at ED_{50}[b]	SD	interaction
pholiol B (**2**)	23.2:1	0.348	0.051	synergism
pholiol D (**4**)	139.2:1	0.660	0.03	Synergism
compound **5**	2.9:1	0.082	0.057	very strong synergism
ergosterol (**6**)	3.6:1	1.03	0.12	nearly additive

[a]Best ratio: the best combination ratio between compound and doxorubicin. [b]CI at ED_{50}: combination index value at the 50% growth inhibition dose.

(FC) was carried out on a CombiFlash Rf+ Lumen Instrument with integrated UV, UV−vis, and ELS detection using reversed (RediSep C_{18} Bulk 950) (Teledyne Isco, Lincoln, NE, USA) and normal phase flash columns filled with silica 60 (0.045−0.063 mm) (Molar Chemicals, Halásztelek, Hungary) and also RediSep Rf Gold normal (Teledyne Isco). Preparative thin layer chromatography (TLC) was performed using silica plates (20 × 20 cm silica gel 60 F254, Merck 105554). High-resolution MS (HRMS) analyses were performed on a Thermo Velos Pro Orbitrap Elite (Thermo Fisher Scientific, Bremen, Germany) system. The ionization method was ESI, operating in the positive (or in the negative) ion mode. The (de)protonated molecular ion peaks were fragmented by the collision-induced dissociation method (CID) at a normalized collision energy of 35%. For the CID experiments, helium was used as collision gas. All samples were dissolved in methanol prior to the MS measurements. Data acquisition and analysis were accomplished with Xcalibur software version 4.0 (Thermo Fisher Scientific, Bremen, Germany). NMR data were acquired on a Bruker Avance III HD 800 MHz spectrometer equipped with a liquid helium cooled TCI cryoprobe. $CDCl_3$ was used as solvent in all cases. Chemical shifts are reported in the delta scale relative to a tetramethylsilane internal standard (0.00 ppm, 1H) and to the residual solvent signal (77.0 ppm, 13C). Standard one- and two-dimensional NMR spectra were recorded in all cases using the pulse sequences available in the TopSpin 3.5 sequence library. Data analysis and interpretation were performed with the ACD/Laboratories 2017.1.3 NMR Workbook Suite package.

Mushroom Material. Fruiting bodies of *Pholiota populnea* were collected in autumn 2017 in the vicinity of Szeged, Hungary. Fungal identification was made by Attila Sándor (Mushroom Society of Szeged). A voucher specimen (No. H019) has been deposited at the Department of Pharmacognosy, University of Szeged, Hungary.

Extraction and Isolation. The fresh mushroom material (4.2 kg) was crushed in a blender and then percolated with MeOH (20 L) at room temperature. After concentration, the dry MeOH extract (151 g) was dissolved in 50% aqueous MeOH (600 mL) and solvent−solvent partition was performed with *n*-hexane (5 × 500 mL), $CHCl_3$ (5 × 500 mL), and then EtOAc (5 × 500 mL). The *n*-hexane-soluble phase (24 g) was subjected to flash chromatography (NP-FC) on silica gel (80 g) using a gradient system of *n*-hexane−acetone (linear from 0% to 100% acetone, t = 55 min) and eluted with MeOH (100%, t = 5 min) at the end of this process. Fractions with similar compositions were combined according to TLC monitoring (H1−H26). Fractions H20 (130 mg), H21 (400 mg), and H22 (200 mg) were further separated by NP-FC (12 g of sorbent) applying an *n*-hexane−acetone solvent system (linear gradient from 0% to 30% acetone, t = 50 min) and then using *n*-hexane−acetone (linear gradient from 0% to 35% acetone, t = 40 min), which led to the isolation of compound **5** (10 mg) and obtaining other 13 fractions (D1−D13). Purification of D9 and D10 fractions was performed by preparative TLC using an *n*-hexane−acetone (45:55) solvent system to give compound **4** (13 mg). Fractions H23 and H24 (1.7 g) were subjected to NP-FC (20 g sorbent) using a solvent system of *n*-hexane−acetone (linear gradient from 0% to 80% acetone, t = 50 min), which resulted in 22 fractions (B1−B22). The combined fractions B16 (94 mg) and B17 (294 mg) were purified by NP-FC (12 g of sorbent) using a mixture of *n*-hexane−acetone (linear gradient from 0% to 50% acetone, t = 55 min) to obtain compound **1** (18 mg) and compound **3** (12 mg), respectively. Fractions B10 (95 mg) and B11 (300 mg) were first separated by FC on an RP_{18} column (20 g) using H_2O−MeOH (linear gradient from 60% to 90% MeOH, t = 50 min), then by preparative TLC using $CHCl_3$−MeOH (95:5) to isolate compound **2**. Finally, compound **6** (130 mg) was isolated from fractions H10−H12 (2 g) using *n*-hexane−acetone (40 g of sorbent, linear gradient from 100:0 to 75:25, t = 45 min). The presence of 3β-hydroxyergosta-7,22-diene (**7**) was detected in the *n*-hexane fraction using an authentic standard.

*Pholiol A (**1**):* amorphous solid; $[\alpha]_D$ +10 (c 0.1, $CHCl_3$); HRESIMS m/z 673.39752 $[M - H]^-$ (Δ 2.7 ppm; $C_{38}H_{57}O_{10}$); ^1H and ^{13}C NMR data, see Tables 1 and 2; HRESI-MSMS (CID = 35%; rel int %) m/z 611(100), 571(63), 529(44), 469(4).

*Pholiol B (**2**):* amorphous solid; $[\alpha]_D$ +80 (c 0.1, $CHCl_3$); HRESIMS m/z 689.42289 $[M + H]^+$ (Δ −4.4 ppm, $C_{39}H_{61}O_{10}$); ^1H and ^{13}C NMR data, see Tables 1 and 2; HRESI-MSMS (CID = 35%; rel int %) m/z 671(8), 531(100), 513(30), 471(55), 453(56), 435(8), 417(4), 377(1).

*Pholiol C (**3**):* amorphous solid; $[\alpha]_D$ +16 (c 0.1, $CHCl_3$); HRESIMS m/z 675.41283 $[M - H]^-$ (Δ 2.2 ppm, $C_{38}H_{59}O_{10}$).; ^1H and ^{13}C NMR data, see Tables 1 and 2; HRESI-MSMS (CID = 35%; rel int %) m/z 613(100), 573(92), 555(6), 531(31).

*Pholiol D (**4**):* white powder; $[\alpha]_D$ −90 (c 0.1, $CHCl_3$); HRESIMS m/z 1403.85130 $[2M + Na]^+$ (Δ −4.6 ppm, $C_{78}H_{124}O_{20}Na$); ^1H and ^{13}C NMR data, see Tables 1 and 2; HRESI-MS^3 (1408/713; CID = 35%, 45%; rel int %) m/z 653(12), 639(6), 537(100), 477(41), 437(3).

*(3S,6E,10E,14E,18E,22S)-2,3,22,23-Tetrahydroxy-2,6,10,15,19,23-hexamethyl-6,10,14,18-tetracosatetraene (**5**):* amorphous solid; $[\alpha]_D$ −2.3 (c 0.16, $CHCl_3$) and −15.75 (c 0.16, MeOH); ^1H and ^{13}C NMR data, Table S1; HRESIMS m/z 479.40900 $[M + H]^+$ (Δ −1.0 ppm; $C_{30}H_{55}O_5$); HRESI-MSMS (CID = 35%; rel int %) m/z 461(100), 443(31).

Cell Culture. The human colon adenocarcinoma cell lines, the Colo 205 (ATCC-CCL-222) doxorubicin-sensitive parent and Colo 320/MDR-LRP (ATCC-CCL-220.1) resistant to anticancer agents expressing ABCB1, were purchased from LGC Promochem (Teddington, UK). The cells were cultured in RPMI-1640 medium supplemented with 10% heat-inactivated fetal bovine serum (FBS), 2 mM L-glutamine, 1 mM Na-pyruvate, 100 mM Hepes, nystatin, and a penicillin−streptomycin mixture in concentrations of 100 U/L and 10 mg/L, respectively. The MRC-5 (ATCC CCL-171) human embryonic lung fibroblast cell line (LGC Promochem) was cultured in EMEM medium, supplemented with 1% nonessential amino acid mixture, 10% heat-inactivated FBS, 2 mM L-glutamine, 1 mM Na-pyruvate, nystatin, and a penicillin−streptomycin mixture in concentrations of 100 U/L and 10 mg/L, respectively. The cell lines were incubated in a humidified atmosphere (5% CO_2, 95% air) at 37 °C.

Assay for Cytotoxic Effect. The effects of increasing concentrations of the compounds on cell growth were tested in 96-well flat-bottomed microtiter plates. The 2-fold serial dilutions of the tested compounds were made starting with 100 μM. Then, 10^4 human colonic adenocarcinoma cells in 100 μL of the medium (RPMI-1640) were added to each well, except for the medium control wells. The adherent human embryonic lung fibroblast cell line (10^4/well) was seeded in EMEM medium in 96-well flat-bottomed microtiter plates for 4 h before the assay. The serial dilutions of the compounds were made in a separate plate starting with 100 μM and then transferred to the plates containing the adherent corresponding cell line. Culture plates were incubated at 37 °C for 24 h; at the end of the incubation period, 20 μL of MTT (thiazolyl blue tetrazolium bromide) solution (from a 5 mg/mL stock solution) was added to each well. After incubation at 37 °C for 4 h, 100 μL of sodium dodecyl sulfate (SDS) solution (10% SDS in 0.01 M HCl) was added to each well, and the plates were further incubated at 37 °C overnight. Cell growth was determined by measuring the optical density (OD) at 540 nm (ref 630 nm) with a Multiscan EX ELISA reader (Thermo Labsystems, Cheshire, WA, USA). Inhibition of cell growth was expressed as IC_{50}

https://doi.org/10.1021/acs.jnatprod.1c01024
J. Nat. Prod. 2022, 85, 910−916

values, defined as the inhibitory dose that reduces the growth of the cells exposed to the tested compounds by 50%. IC_{50} values and the SD of triplicate experiments were calculated by using GraphPad Prism software version 5.00 for Windows with nonlinear regression curve fit (GraphPad Software, San Diego, CA, USA; www.graphpad.com).

Rhodamine 123 Accumulation Assay. The cell numbers of the human colon adenocarcinoma cell lines were adjusted to 2×10^6 cells/mL, resuspended in serum-free RPMI 1640 medium, and distributed in 0.5 mL aliquots into Eppendorf centrifuge tubes. The tested compounds were added at 2 or 20 μM concentrations, and the samples were incubated for 10 min at room temperature. Tariquidar was applied as positive control at 0.2 μM. DMSO at 2% v/v was used as solvent control. Next, 10 μL (5.2 μM final concentration) of the fluorochrome and ABCB1 substrate rhodamine 123 (Sigma) were added to the samples, and the cells were incubated for a further 20 min at 37 °C, washed twice, and resuspended in 1 mL of PBS for analysis. The fluorescence of the cell population was measured with a PartecCyFlow flow cytometer (Partec, Münster, Germany). The FAR was calculated as the quotient between FL-1 of the treated/untreated resistant Colo 320 cell line over the treated/untreated sensitive Colo 205 cell line according to the following equation:

$$\mathrm{FAR} = \frac{\mathrm{Colo320}_{\mathrm{treated}}/\mathrm{Colo320}_{\mathrm{control}}}{\mathrm{Colo205}_{\mathrm{treated}}/\mathrm{Colo205}_{\mathrm{control}}}$$

Checkerboard Combination Assay. A checkerboard microplate method was applied to study the effect of drug interactions between the compounds (**2**, **4**–**6**) and the chemotherapeutic drug doxorubicin. The assay was carried out on the Colo 320 colon adenocarcinoma cell line. The final concentration of the compounds and doxorubicin used in the combination experiment was chosen in accordance with their cytotoxicity toward this cell line. The dilutions of doxorubicin were made in a horizontal direction in 100 μL, and the dilutions of the compounds vertically in the microtiter plate in a 50 μL volume. Then, 6×10^3 of Colo 320 cells in 50 μL of the medium were added to each well, except for the medium control wells. The plates were incubated for 72 h at 37 °C in a 5% CO_2 atmosphere. The cell growth rate was determined after MTT staining. At the end of the incubation period, 20 μL of MTT solution (from a stock solution of 5 mg/mL) was added to each well. After incubation at 37 °C for 4 h, 100 μL of SDS solution (10% in 0.01 M HCl) was added to each well, and the plates were further incubated at 37 °C overnight. OD was measured at 540 nm (ref 630 nm) with a Multiscan EX ELISA reader. CI values at 50% of the growth inhibition dose were determined using CompuSyn software (ComboSyn, Inc., Paramus, NJ, USA) to plot four to five data points at each ratio. CI values were calculated by means of the median-effect equation, according to the Chou–Talalay method, where CI < 1, CI = 1, and CI > 1 represent synergism, additive effect (or no interaction), and antagonism, respectively.[17,18]

Bacterial Strains and Determination of Antibacterial Activity. See ref 8.

■ ASSOCIATED CONTENT

Supporting Information

The Supporting Information is available free of charge at https://pubs.acs.org/doi/10.1021/acs.jnatprod.1c01024.

1D and 2D NMR and HRESIMS spectra of compounds **1**–**5** (PDF)

■ AUTHOR INFORMATION

Corresponding Authors

Judit Hohmann − *Department of Pharmacognosy, Interdisciplinary Excellence Centre, University of Szeged, 6720 Szeged, Hungary; Interdisciplinary Centre for Natural Products, University of Szeged, H-6720 Szeged, Hungary;* orcid.org/0000-0002-2887-6392; Phone: +36-62-546453; Email: hohmann.judit@szte.hu

Attila Ványolós − *Department of Pharmacognosy, Semmelweis University, H-1085 Budapest, Hungary*; Phone: +36 1 4591500/55303; Email: vanyolos@pharmacognosy.hu

Authors

Morteza Yazdani − *Department of Pharmacognosy, Interdisciplinary Excellence Centre, University of Szeged, 6720 Szeged, Hungary;* orcid.org/0000-0001-6569-5681

Zoltán Béni − *Spectroscopic Research Department, Gedeon Richter Plc., H-1103 Budapest, Hungary*

Miklós Dékány − *Spectroscopic Research Department, Gedeon Richter Plc., H-1103 Budapest, Hungary*

Nikoletta Szemerédi − *Department of Medical Microbiology, Albert Szent-Györgyi Health Center and Faculty of Medicine, University of Szeged, H-6725 Szeged, Hungary*

Gabriella Spengler − *Department of Medical Microbiology, Albert Szent-Györgyi Health Center and Faculty of Medicine, University of Szeged, H-6725 Szeged, Hungary*

Complete contact information is available at: https://pubs.acs.org/10.1021/acs.jnatprod.1c01024

Notes

The authors declare no competing financial interest.

■ ACKNOWLEDGMENTS

Financial support for this research was provided by the Economic Development and Innovation Operative Program GINOP-2.3.2-15-2016-00012 and the National Research, Development and Innovation Office, Hungary (NKFIH; K135845). The authors thank Attila Sándor for his help in the collection and identification of mushroom material.

■ REFERENCES

(1) Sung, H.; Ferlay, J.; Siegel, R. L.; Laversanne, M.; Soerjomataram, I.; Jemal, A.; Bray, F. *CA Cancer J. Clin.* **2021**, *71*, 1–41.

(2) Marc, M. A.; Kincses, A.; Rácz, B.; Nasim, M. J.; Sarfraz, M.; Lázaro-Milla, C.; Domínguez-Álvarez, E.; Jacob, C.; Spengler, G.; Almendros, P. *Pharmaceuticals* **2020**, *13*, 453.

(3) Zhou, B.; Xiao, X.; Xu, L.; Zhu, L.; Tan, L.; Tang, H.; Zhang, Y.; Xie, Q.; Yao, S. *Talanta* **2012**, *88*, 345–351.

(4) Bao, Y.; Zhang, S.; Chen, Z.; Chen, A. T.; Ma, J.; Deng, G.; Xu, W.; Zhou, J.; Yu, Z. Q.; Yao, G.; Chen, J. *Mol. Pharmaceutics* **2020**, *17*, 1343–1351.

(5) Wang, K.; Zhu, X.; Yin, Y. *Front. Pharmacol.* **2020**, *11*, 835.

(6) Silva, V. A. O.; Rosa, M. N.; Miranda-Gonçalves, V.; Costa, A. M.; Tansini, A.; Evangelista, A. F.; Martinho, O.; Carloni, A. C.; Jones, C.; Lima, J. P.; Pianowski, L. F.; Reis, R. M. *Invest. New Drugs* **2019**, *37*, 223–237.

(7) Ali, S. A.; Zaitone, S. A.; Moustafa, Y. M. *Can. J. Physiol. Pharmacol.* **2015**, *93*, 695–708.

(8) Béni, Z.; Dékány, M.; Sárközy, A.; Kincses, A.; Spengler, G.; Papp, V.; Hohmann, J.; Ványolós, A. *Molecules* **2021**, *26*, 1657.

(9) Becker, U.; Anke, T.; Sterner, O. *Nat. Prod. Lett.* **1994**, *5*, 171–174.

(10) Mleczek, M.; Gąsecka, M.; Budka, A.; Siwulski, M.; Mleczek, P.; Magdziak, Z.; Budzyńska, S.; Niedzielski, P. *Environ. Sci. Pollut. Res. Int.* **2021**, *28*, 4430–4442.

(11) Takahashi, A.; Kusano, G.; Ohta, T.; Ohizumi, Y.; Nozoe, S. *Chem. Pharm. Bull.* **1989**, *37*, 3247–3250.

(12) Kim, K. H.; Moon, E.; Choi, S. U.; Kim, S. Y.; Lee, K. R. *J. Nat. Prod.* **2013**, *76*, 845–851.

(13) Nishiyama, Y.; Moriyasu, M.; Ichimaru, M.; Tachibana, Y.; Kato, A.; Mathenge, S. G.; Nganga, J. N.; Juma, F. D. *Phytochemistry* **1996**, *42*, 803–807.

(14) Nishiyama, Y.; Moriyasu, M.; Ichimaru, M.; Kato, A.; Mathenge, S. G.; Nganga, J. N.; Juma, F. D. *Phytochemistry* **1999**, *52*, 1593−1596.
(15) Alexandre, T. R.; Lima, M. L.; Galuppo, M. K.; Mesquita, J. T.; do Nascimento, M. A.; dos Santos, A. L.; Sartorelli, P.; Pimenta, D. C.; Tempone, A. G. *J. Venom. Anim. Toxins Incl. Trop. Dis.* **2017**, *23*, 30.
(16) Spengler, G.; Gajdács, M.; Marc, M. A.; Domínguez-Álvarez, E.; Sanmartín, C. *Molecules* **2019**, *24*, 336.
(17) Chou, T. C. *Pharmacol Rev.* **2006**, *58*, 621−681.
(18) Chou, T. C. *Cancer Res.* **2010**, *70*, 440−446.

https://doi.org/10.1021/acs.jnatprod.1c01024
J. Nat. Prod. 2022, 85, 910−916

II.

Phytochemistry 205 (2023) 113480

Contents lists available at ScienceDirect

Phytochemistry

journal homepage: www.elsevier.com/locate/phytochem

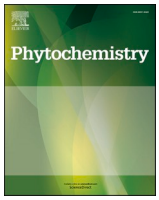

Pholiols E–K, lanostane-type triterpenes from *Pholiota populnea* with anti-inflammatory properties

Morteza Yazdani [a], Anita Barta [a], Róbert Berkecz [b], Orinamhe Godwin Agbadua [a], Attila Ványolós [c], Judit Hohmann [a,d,e,*]

[a] Institute of Pharmacognosy, University of Szeged, Eötvös u. 6, H-6720, Szeged, Hungary
[b] Institute of Pharmaceutical Analysis, University of Szeged, Somogyi u. 4, 6720, Szeged, Hungary
[c] Department of Pharmacognosy, Semmelweis University, Üllői u. 26, H-1085, Budapest, Hungary
[d] Interdisciplinary Centre for Natural Products, University of Szeged, Eötvös u. 6, H-6720, Szeged, Hungary
[e] ELKH-USZ Biologically Active Natural Products Research Group, University of Szeged, Eötvös u. 6, H-6720, Szeged, Hungary

ARTICLE INFO

Keywords:
Pholiota populnea
Strophariaceae
Anti-inflammatory activity
Lanostane triterpenes
Pholiols e–k

ABSTRACT

Investigation of the chloroform and ethyl acetate extracts of the edible mushroom *Pholiota populnea* led to the isolation of eight triterpenes, the undescribed natural products pholiols E–K and the known (+)-clavaric acid. HRESIMS and 1D and 2D NMR spectroscopy were employed to determine the structures of the undescribed compounds. The NOESY spectra were used to assign the relative configurations of triterpenes. The isolated compounds were screened for their anti-inflammatory activity on cyclooxygenase (COX-1 and COX-2), and lipoxygenase (5-LOX and 15-LOX) inhibitory assays. Dose–response investigations revealed that lanostane derivatives exhibited moderate 5-LOX and COX-2 inhibitory activities, with pholiol F (IC_{50} 194.5 μM against 5-LOX and 439.8 μM against COX-2) the most active among the isolated compounds. Our findings indicated that *P. populnea* is an abundant source of new bioactive lanostane-type triterpenes.

1. Introduction

The nutritional, medicinal, and bioremediation significance of mushrooms has recently increased because they are an abundant source of nutrients and bioactive compounds, including polysaccharides, proteins, fats, phenolics, alkaloids, terpenoids, nucleosides, lectins, minerals, and vitamins. Triterpenoids and steroids frequently occur among the fungal metabolites that can be classified into nine primary groups based on their carbon skeletons: squalene, lanostane, ergostane, fernane, friedelane, lupane, malabaricane, eburicane, and cucurbitane (Öztürk et al., 2015). The most frequently occurring triterpenes are lanostane and ergostane; other triterpenoids are relatively uncommon mushroom metabolites. Generally, the compounds are substituted with hydroxy, keto, aldehyde, and carboxyl groups or have ether and acetonide functionalities. Esterification is also a characteristic of some fungal triterpenes; esterifying acids are simple organic or fatty acids. Some compounds have special structures, including lactones, seco-ring-A, or nor-triterpenoids. Several compounds were also found to have potent bioactivities, such as cytotoxic, anti-invasive, anti-inflammatory, antimycobacterial, anticandidal, antimalarial, antiviral, and anticholinesterase, and effects on adipocyte differentiation (Öztürk et al., 2015).

In the literature, numerous examples can be found where fungal triterpenes are efficient in anti-inflammatory test models. Lanostane triterpenes of *Macrolepiota procera*, called lepiotaprocerins, were found to inhibit nitric oxide (NO) production (Chen et al., 2018). *Ganoderma lucidum*, which is extensively used in traditional Chinese medicine, was investigated for its protective effect on lipopolysaccharide-induced inflammatory responses and acute liver injury. Triterpenes were also found to play a crucial role in the inhibition of inflammatory diseases by blocking nuclear factor κ-activated B cell (NF-κB) and mitogen-activated protein kinase (MAPK) signaling pathways (Hu et al., 2020). The edible cultivated mushroom *Wolfiporia cocos* is also abundant in lanostane triterpenes; its constituent, poricoic acid GM, was also found to inhibit NO production (IC_{50} 9.73 μM), inducible nitric oxide synthase (iNOS), and cyclooxygenase-2 (COX-2) protein expression in LPS-induced RAW264.7 murine macrophages (Bao et al., 2019). Lanostane triterpenoids and ergosterols isolated from the fruiting bodies of *Pyropolyporus fomentarius* also exhibited inhibitory activities against NO production in the same test model (Zhang et al., 2021). Triterpenes of *Hypholoma*

* Corresponding author. Institute of Pharmacognosy, University of Szeged, Eötvös u. 6, H-6720, Szeged, Hungary.
E-mail address: hohmann.judit@szte.hu (J. Hohmann).

https://doi.org/10.1016/j.phytochem.2022.113480
Received 25 July 2022; Received in revised form 30 September 2022; Accepted 16 October 2022
Available online 22 October 2022

lateritium exerted a significant inhibitory effect on COX-2 and were able to promote the Nrf2 pathway. Fasciculol C, the hexahydroxylated lanostane, synthesized the highest level of Nrf2 (Ványolós et al., 2020).

The present study focused on the isolation, structural determination, and biological activity evaluation of the compounds of *Pholiota populnea* (Pers.) Kuyper & Tjall.-Beuk. [syn. *Pholiota destruens* (Brond.) Quel., *Hemipholiota populnea* (Pers.) Kühner ex Bon] (Strophariaceae) as a continuation of our study on bioactive fungal metabolites. This mushroom is not poisonous and is robust with a large cap and white to buff scales. In our previous study, four undescribed lanostane diesters, called pholiols A–D were reported, together with an acyclic triterpene tetraol, ergosterol, and 3β-hydroxyergosta-7,22-diene from the *n*-hexane extract of *P. populnea* (Yazdani et al., 2022). These isolates were investigated for their cytotoxic activity against human colon adenocarcinoma cells (Colo205 and Colo320). The combination with doxorubicin and the efflux pump inhibitory activity of the compounds on drug-resistant Colo 320 cells was also assayed, and the P-glycoprotein efflux pump modulatory effects and synergism of triterpenes with doxorubicin were discovered.

Investigation of the chloroform and ethyl acetate extracts of *P. populnea* led to the isolation of seven undescribed triterpenes, namely, pholiols E–K (**1–7**), and the known (+)-clavaric acid (**8**) (Fig. 1). On cyclooxygenase (COX-1, COX-2) and lipoxygenase (5-LOX and 15-LOX) assays, the anti-inflammatory activity of the isolated compounds (**1–8**) and the previously isolated pholiol C (**9**) (Yazdani et al., 2022) was evaluated.

2. Results and discussion

2.1. Structure elucidation of triterpenes (1–8)

Compound **1** was isolated as a white amorphous powder with an optical rotation of $[\alpha]_D^{25}$ +49 (*c* 0.1, MeOH). Its protonated molecular ion at *m/z* 617.4063 $[M+H]^+$ (calcd for $C_{36}H_{57}O_8$ 617.4048) in the HRESIMS spectrum offered the molecular formula $C_{36}H_{56}O_8$. The ^{1}H NMR spectrum exhibited the presence of a 3-hydroxy-3-methylglutarate [δ_H

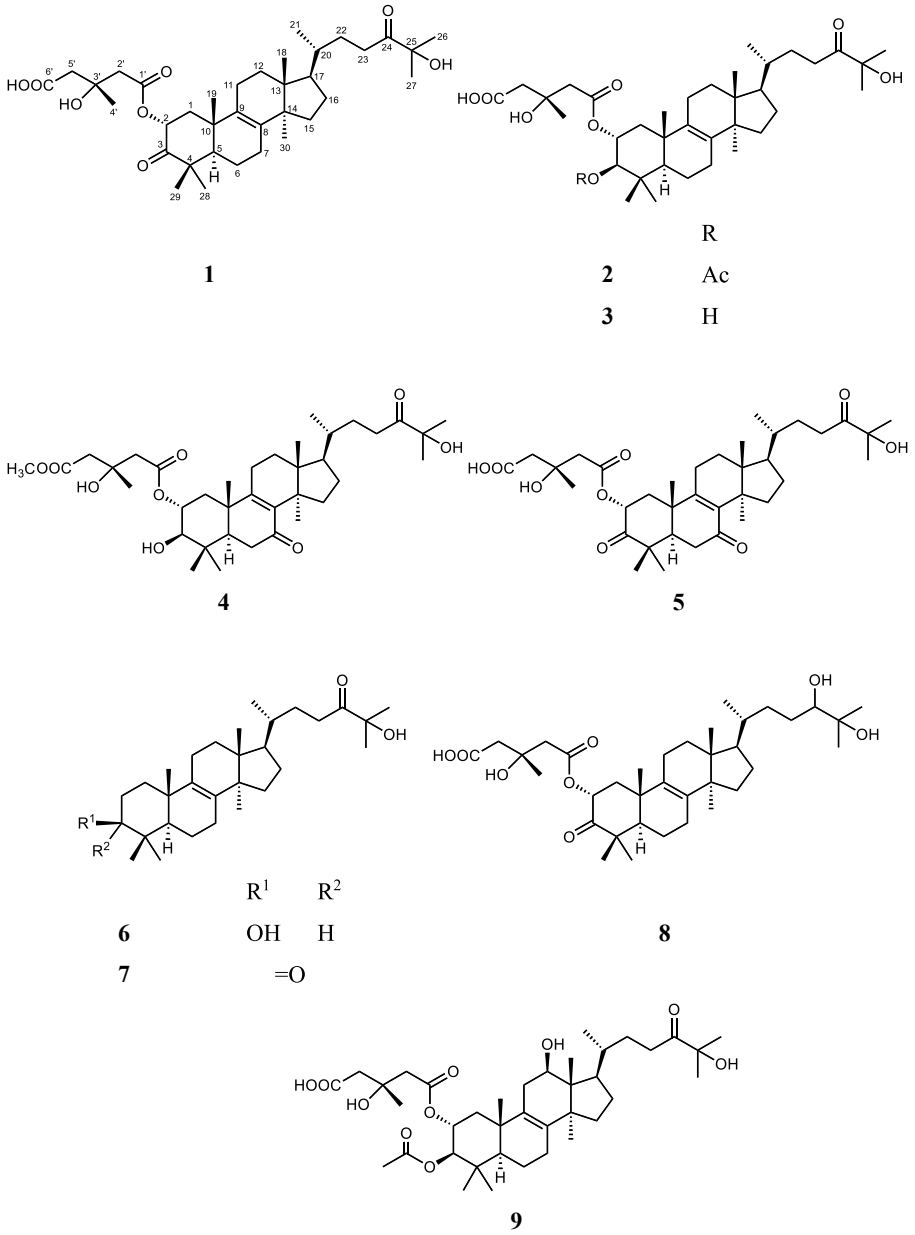

Fig. 1. Compounds **1–9** isolated from *Pholiota populnea*.

2.80 m (2H), 2.75 m (2H), 1.41 s (CH_3); δ_C 2 × 171.63, 2 × 46.56, 45.83, 70.90, 27.56] ester group in the molecule characteristic to members of pholiol series (Yazdani et al., 2022) (Tables 1 and 2). Furthermore, the ^{1}H NMR spectrum demonstrated resonances of seven tertiary (δ_H 1.40, 2 × 1.30, 1.11, 1.18, 0.93, and 0.78, each 3H, s) and one secondary (δ_H 0.94, 3H, d, J = 6.2 Hz) methyl groups as well as one oxymethine (δ_H 5.67, dd, J = 13.62 and 5.6 Hz). From the ^{13}C J-MOD spectrum, two keto groups (δ_C 210.92 and 217.79) and an oxygen-substituted non-protonated carbon (δ_C 77.90) could be identified. The presence of a tetrasubstituted olefin bond was obvious from the nonprotonated sp^2 carbon signals at δ_C 136.90 and 134.69. The 1D NMR data proposed that compound **1** is a lanostanol-en-dione monoester. Regarding its HMBC correlations with δ_H 2.36 (H-1a), 1.66 (H-1b), 5.67 (H-2), 1.11 (H_3-28), and 1.18 (H_3-29), the keto group at δ_C 210.92 was placed at C-3. The other keto group (δ_C 217.79) was concluded to be at C-24 based on its long-range correlations with δ_H 1.30 (H_3-26, H_3-27) and 2.67 (H_2-23). The HMBC correlations of C-25 (δ_C 77.90) with protons at δ_H 1.30 (H_3-26 and H_3-27) depicted the hydroxy group at C-25, whereas correlations between δ_C 171.63 (C-1′) and δ_H 5.67 (H-2) as well as 2.80 and 2.75 (H_2-2') were indicative of the position of the ester group at C-2. Based on the HMBC cross-peaks of signals at δ_C 136.90 (C-8) with δ_H 0.93 (H_3-30), 2.18 (H_2-7), and 1.73 (H-6) as well as δ_C 134.69 (C-9) with δ_H 1.40 (H_3-19) and 2.18 (H_2-7), the location of the olefin group at C-8–C-9 was determined. The relative configuration of compound **1** was examined using diagnostic Overhauser effects detected in a NOESY spectrum. The NOESY correlations of H-2 (δ_H 5.67) with H_3-19 (δ_H 1.40), H_3-29 (δ_H 1.18), and H-1a (δ_H 2.36) pointed these protons in the β orientation and the ester group in the α orientation. The NOEs between H_3-18/H-20 and H-17/H_3-30 were in line with those of lanostane triterpenes (Aichour et al., 2014). The above findings were consistent with the proposed structure of compound **1** [2α-(3-hydroxy-3-methylglutaroyloxy)-25-hydroxylanosta-8-en-3,24-dione], which was called pholiol E (**1**) (Fig. 1).

Compound **2** was obtained as a white amorphous powder with $\alpha]_D^{25}$ +5 (c 0.1, $CHCl_3$). Its molecular formula was deduced to be $C_{38}H_{60}O_9$ from the protonated molecular ion at m/z 661.4320 $[M+H]^+$ (calcd for $C_{38}H_{61}O_9$, 661.4310) detected in the HRESIMS spectrum. A comprehensive analysis of ^{1}H and ^{13}C J-MOD as well as 2D data demonstrated the presence of the same parent system and 3-hydroxy-3-methylglutarate moiety as in compound **1**, except the C-3 keto group, which was replaced by an acetoxy group (Tables 1 and 2). The acetoxy group is attached at C-3, as demonstrated by the sequences of the correlated protons in the ^{1}H–^{1}H–COSY spectrum: CH_2–CH(OR)–CH(OR)–(δ_H 2.11 m, 1.38 m, 5.19 t (10.8 Hz), 4.79 d). The location of the ester functionalities was corroborated by the HMBC correlations observed between δ_C 171.14 (C-1′) and δ_H 5.19 (H-2), 2.62 and 2.51 (H-2') and δ_C 171.84 (AcCO) and δ_H 4.79 (H-3), and 2.10 (AcMe), showing 3-hydroxy-3-methylglutarate at C-2 and acetate at C-3. The coupling constant of H-2 and H-3 (J = 10.5 Hz) and NOESY correlations between H-3 (δ_H 4.79)/H-1b (δ_H 1.38), H-3/H_3-28 (δ_H 0.92), H-2 (δ_H 5.19)/H-1a (δ_H 2.11), and H-2/H_3-29 (δ_H 0.95) confirmed the opposite orientation of the ester groups. The Overhauser effect of H-2 with H_3-19 (δ_H 1.13) indicated the H-2β and H-3α positions. Thus, the structure of this compound was elucidated as 2α-(3-hydroxy-3-methylglutaroyloxy)-3-acetoxy-25-hydroxylanosta-8-en-24-one (**2**), called pholiol F.

Table 1
^{1}H NMR data of compounds **1**–**8** (500 MHz, δ ppm, J = Hz).

H	1[a]	2[b]	3[a]	4[a]	5[a]	6[a]	7[b]	8[a]
1	2.36 dd (12.3, 5.6), 1.66 m	2.11 m, 1.38 m	2.05 m, 1.18 m	2.20 dd (12.3, 4.3), 1.45 m	2.50 m, 1.93 t (13.1)	1.76 m, 1.22 m	1.98 m, 1.61 m	2.36 dd (12.3, 5.6), 1.66 m
2	5.67 dd (13.6, 5.6)	5.19 dt (3.4, 10.5)	4.92 dt (3.9, 10.6)	5.07 dt (4.3, 11.5)	5.72 dd (13.5, 5.8)	1.63 m (2H)	2.57 m, 2.41 ddd (15.8, 6.7, 3.5)	5.66 dd (13.4, 5.6)
3	–	4.79 d (10.5)	3.20 d (10.1)	3.24 d (10.1)	–	3.17 dd (10.1, 6.3)	–	–
5	1.53 m	1.51 m	1.53 m	1.77 m	2.10 dd (14.6, 3.2)	1.06 m	1.60 m	1.53 m
6	1.80 m, 1.73 m	1.69 m, 1.56 m	1.74 m, 1.57 m	2.55 dd (16.3, 14.5), 2.36 m	2.73 m, 2.32 dd (16.6, 3.2)	1.71 m, 1.54 m	1.61 m (2H)	1.80 m, 1.72 m
7	2.18 m (2H)	2.09 m (2H)	2.10 m (2H)	–	–	2.07 m (2H)	2.08 m (2H)	2.17 m (2H)
11	2.16 m, 2.09 m	2.00 m (2H)	2.04 m (2H)	2.38 m (2H)	2.47 m (2H)	2.06 m (2H)	2.04 m (2H)	2.16 m, 2.10 m
12	1.79 m (2H)	1.73 m (2H)	1.74 m (2H)	1.84 m (2H)	1.87 m (2H)	1.78 m, 1.72 m	1.75 m, 1.70 m	1.81 m (2H)
15	1.78 m, 1.23 m	1.61 m, 1.21 m	1.65 m, 1.22 m	2.01 m, 1.72 m	2.03 m, 1.76 m	1.67 m, 1.21 m	1.62 m, 1.22 dd (13.7, 2.5)	1.69 m, 1.25 m
16	2.01 m, 1.46 m	1.97 m, 1.39 m	1.98 m, 1.41 m	2.00 m, 1.42 m	2.02 m, 1.45 m	1.98 m, 1.42 m	1.97 m, 1.38 m	2.01 m, 1.43 m
17	1.56 m	1.30 m	1.53 m	1.47 m	1.49 m	1.53 m	1.50 m	1.57 m
18	0.78 s	0.70 s	0.74 s	0.71 s	0.74 s	0.74 s	0.72 s	0.79 s
19	1.40 s	1.13 s	1.12 s	1.32 s	1.57 s	1.01 s	1.12 s	1.40 s
20	1.45 m	1.40 m	1.42 m	1.42 m	1.44 m	1.43 m	1.40 m	1.46 m
21	0.94 d (6.2)	0.89 d (6.4)	0.92 d (6.4)	0.95 d (6.1)	0.96 d (6.2)	0.93 d (6.2)	0.91 d (6.4)	0.96 d (6.4)
22	1.70 m, 1.27 m	1.82 m, 1.30 m	1.76 m, 1.21 m	1.77 m, 1.23 m	1.78 m, 1.30 m	1.77 m, 1.22 m	1.81 m, 1.31 m	1.82 m, 1.01 m
23	2.67 m (2H)	2.54 m, 2.50 m	2.66 m (2H)	2.66 m (2H)	2.69 m (2H)	2.65 m (2H)	2.55 m, 2.48 m	1.74 m, 1.14 m
24	–	–	–	–	–	–	–	3.17 d (9.9)
26	1.30 s	1.39 s	1.29 s	1.29 s	1.29 s	1.29 s	1.39 s	1.16 s
27	1.30 s	1.39 s	1.29 s	1.29 s	1.29 s	1.29 s	1.38 s	1.16 s
28	1.11 s	0.92 s	1.06 s	1.05 s	1.09 s	0.98 s	1.10 s	1.10 s
29	1.18 s	0.95 s	0.89 s	0.96 s	1.24 s	0.81 s	1.07 s	1.18 s
30	0.93 s	0.89 s	0.93 s	0.95 s	0.94 s	0.92 s	0.90 s	0.93 s
2′	2.80 m, 2.75 m	2.62 m, 2.51 m	2.51 m, 2.33 m	2.71 m (2H)	2.70 m, 2.65 m			2.75 m, 2.71 m
4′	1.41 s	1.39 s	1.33 s	1.41 s	1.37 s			1.41 s
5′	2.69 m (2H)	2.62 m, 2.51 m	2.66 m, 2.50 m	2.71 s (2H)	2.70 m, 2.65 m			2.75 m, 2.71 m
7′	–			3.68 s				
OAc	–	2.10 s						

[a] Recorded in CD_3OD.
[b] Recorded in $CDCl_3$.

Table 2
^{13}C NMR data of compounds **1**–**8** in CD_3OD (125 MHz, δ ppm).

Atom	1[a]	2[b]	3[a]	4[a]	5[a]	6[a]	7[b]	8[a]
1	43.68	41.28	42.21	41.10	42.36	37.01	36.22	43.69
2	73.73	71.92	74.64	73.41	72.97	28.54	34.76	73.91
3	210.92	80.47	80.59	79.99	208.51	79.72	215.13	210.87
4	49.00	39.57	40.58	40.75	49.10	39.97	47.55	49.13
5	53.97	50.58	51.78	51.15	52.57	52.04	51.40	53.99
6	19.98	18.24	19.36	37.48	37.73	19.45	19.60	19.99
7	27.21	26.39	27.42	201.26	200.27	27.69	26.50	27.22
8	136.90	135.25	136.07	139.95	140.18	135.76	135.44	136.86
9	134.69	133.50	135.21	167.19	166.56	136.09	133.35	134.76
10	39.14	38.36	39.40	42.10	41.75	38.26	37.06	39.14
11	22.56	21.40	22.19	24.89	25.34	22.08	21.23	22.51
12	32.16	31.01	32.17	31.23	31.23	32.36	31.03	32.19
13	51.05	44.77	51.05	49.07	46.23	45.80	44.70	51.04
14	45.83	50.05	45.73	46.11	49.72	51.08	50.11	45.78
15	31.11	30.90	31.84	33.18	33.17	31.92	31.12	31.81
16	29.05	28.23	29.07	41.10	29.57	29.07	28.25	29.17
17	51.82	50.26	51.78	50.36	50.30	51.86	50.56	51.94
18	16.35	15.97	16.32	16.35	16.38	16.37	16.04	16.35
19	20.16	20.23	20.44	19.55	19.46	19.61	18.84	20.16
20	37.32	36.23	37.33	37.22	37.22	37.36	36.26	38.12
21	19.01	18.64	19.00	19.05	19.05	19.03	18.62	19.40
22	31.78	30.38	31.07	31.03	31.04	31.14	30.33	34.95
23	33.97	32.79	33.97	33.94	33.92	33.99	32.78	29.29
24	217.79	215.05	217.85	217.82	217.78	217.81	217.94	80.64
25	77.90	76.40	78.05	77.93	77.91	77.89	76.37	73.69
26	26.76	26.75	26.77	26.73	26.73	26.76	26.73	25.63
27	26.78	26.75	26.74	26.78	26.76	26.78	26.72	25.63
28	25.06	28.43	29.04	28.26	24.46	28.61	26.37	25.07
29	21.50	17.61	17.23	16.93	21.33	16.11	21.45	21.51
30	24.64	24.43	24.16	25.28	25.31	24.64	24.45	24.66
1′	171.63	171.14	180.34	172.52	171.55			171.68
2′	46.56	44.77	47.51	46.19	47.19			46.76
3′	70.90	n.d.	71.26	70.97	72.97			71.01
4′	27.56	26.7	27.98	27.86	27.68			27.59
5′	45.83	44.77	48.66	46.63	47.19			46.76
6′	171.63	171.14	172.6	173.22	172.80			171.68
7′	–	–	–	52.01	–	–	–	–
OAc-CH_3		21.13						
OAc-CO		171.84						

[a] Recorded in CD_3OD.
[b] Recorded in $CDCl_3$.

Compound **3**, called pholiol G, was isolated as a white amorphous solid with $[\alpha]_D^{25}$ +4 (*c* 0.1, MeOH). It gave the molecular formula $C_{36}H_{58}O_8$, which was determined *via* HRESIMS using the sodiated molecular ion peak at *m/z* 641.4017 $(M + Na)^+$ (calcd for $C_{36}H_{58}O_8Na$ 641.4029). In the comparison of the ^1H NMR spectra of **2** and **3**, the major differences were the remarkable paramagnetic shifts of H-3 (δ_H **2**: 4.79 d versus **3**: 3.20 d) and the absence of acetyl resonance (Table 1). To define the structure of **3**, a complete series of 2D NMR spectra was recorded and analyzed affording the structure 2*α*-(3-hydroxy-3-methylglutaroyloxy)-3*β*,25-dihydroxylanosta-8-en-24-one. Regarding the NOESY correlations between H-3/H_3-28, H-3/H-1b (δ_H 1.18 m), H-2/H-1a (δ_H 2.05 m), H-2/H_3-19, H-2/H_3-29, H-1$8_3$/H-20, and H-17/H_3-30, the stereochemistry of **3** was found to be the same as that of pholiol F (**2**). The fragmentation behaviour of **3** was investigated by direct-injection electrospray ionization quadrupole Orbitrap high-resolution mass spectrometry. The negative ion HRMS/MS spectrum with the proposed fragmentation pathway of **3** is shown in Fig. S56. Interestingly, mainly the 3-hydroxy-3-methylglutarate ester group of the precursor ion is involved in the fragmentation process and thus resulting in characteristic fragment ions.

Compound **4** was obtained as a white amorphous solid with optical rotation $[\alpha]_D^{25}$ +16.5 (*c* 0.5, MeOH). Its formula was assigned as $C_{37}H_{58}O_9$ by the protonated molecular ion at *m/z* 647.4166 $[M+H]^+$ (calcd for $C_{37}H_{59}O_9$, 647.4154) in HRESIMS. A detailed ^1H and ^{13}C J-MOD as well as 2D NMR spectroscopic analysis revealed that the difference between **3** and **4** was the replacement of the 7-methylene group in **3** for a keto group in **4** (δ_C 201.26). The position of the 7-keto group was established based on the HMBC correlations between C-7 and H_2-6 protons [δ_H 2.55 dd (16.3, 14.5 Hz), 2.36 m]. Furthermore, in the NMR spectra of **4**, an additional methoxy group could be observed [δ_H 3.68 s (3H), δ_C 52.01], which was assigned to the carboxymethyl ester of 3-hydroxy-3-methylglutarate moiety, as indicated by the HMBC correlation of OCH_3 group with C-6'. Therefore, compound **4** [lanosta-8-ene-3,25-diol-7,24-dione 2α-(methyl 3-hydroxy-3-methylglutarate)] was elucidated as depicted in Fig. 1 and named pholiol H.

Compound **5** with optical rotation $[\alpha]_D^{25}$ +11 (*c* 0.1, MeOH) had the molecular formula of $C_{36}H_{54}O_9$ as deduced from the prominent pseudomolecular ion peak in HRESIMS at *m/z* 631.3844 $[M+H]^+$ (calcd for $C_{36}H_{55}O_9$, 631.3841). The ^1H and ^{13}C NMR spectral data (Tables 1 and 2) depicted that **5** was also a lanostane-type triterpene, exhibiting a similar structure to that of pholiol E (**1**). A detailed comparison of these two compounds revealed an additional keto group at δ_C 200.27 in **5** instead of a methylene group, which is bonded at C-7 as displayed by the long-range correlation of C-7 with H-6. The tetrasubstituted $\Delta^{8,9}$ olefin was downfield shifted [δ_C **1**: 136.90 (C-8), 134.69 (C-9); **5**: 140.18 (C-8), 166.56 (C-9)] as a consequence of the emerging enone system (Yazdani et al., 2022). Diagnostic ^1H,^1H–COSY, HSQC, and HMBC correlations resulted in the assignment of all proton and carbon chemical shifts, and NOESY cross-peaks (Fig. 2) afforded the stereochemical assignment of compound **5** [2*α*-(3-hydroxy-3-methylglutaroyloxy)-25-hydroxylanosta-8-en-3,7,24-tri-one] named pholiol I.

The molecular formula of compound **6** was determined as $C_{30}H_{50}O_3$ by analyzing the prominent pseudomolecular ion peak at *m/z* 459.3833 $[M+H]^+$ (calcd for $C_{30}H_{51}O_3$ 459.3833) in HRESIMS. Compound **6** was

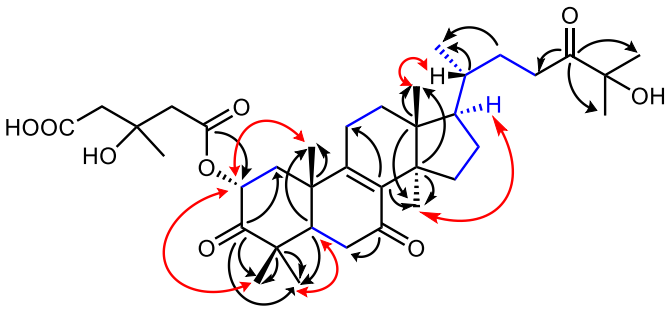

Fig. 2. Diagnostic $^{1}H,^{1}H$–COSY, HMBC and NOESY correlations of pholiol I (**5**).

obtained as a colorless amorphous solid with $[\alpha]_D^{25}$ +39 (*c* 0.1, MeOH). It exhibited close similarity to pholiol F (**2**), but the 3-hydroxy-3-methylglutarate ester moiety was absent in **6**. The 3-hydroxy, 8,9-olefin, 24-keto, and 25-hydroxy functionalities of lanostane triterpene were confirmed by the HMBC correlations of C-3 (δ_C 79.72) with H_3-28 (δ_H 0.98 s) and H_3-29 (δ_H 0.81 s); C-8 (δ_C 135.76) with H_3-30 (δ_H 0.92 s); C-9 (δ_C 136.09) with H_3-19 (δ_H 1.01 s) and H_2-7 (δ_H 2.07 m); C-24 (δ_C 217.81) with H_2-23 (δ_H 2.65 m); and C-25 (δ_C 77.89) with H_3-26 (δ_H 1.29 s) and H_3-27 (δ_H 1.29 s), respectively (Tables 1 and 2). Based on the Overhauser effects of H-3/H-5 and H-3/H_3-28 as well as the coupling constants of H-3 (10.1 and 6.3 Hz), the 3β orientation of the hydroxy group was determined [Nakamura et al., 2009]. Therefore, compound **6**, named pholiol J, was identified as 3β,25-dihydroxylanosta-8-en-24-one. This compound was first isolated from natural source, but previously synthesized without assignments of NMR chemical shifts (Yang et al., 2018). In their experiment, side-chain modified lanosterol derivatives were produced with the aim to develop compounds that reverse protein aggregation in cataracts. Lanosterol analogs with remarkable potency and efficacy in reversing several types of mutant crystalline aggregates were identified.

Compound **7**, named pholiol K, was isolated as a colorless amorphous solid with optical rotation $[\alpha]_D^{25}$ +29 (*c* 0.1, $CHCl_3$). Based on the HRESIMS pseudomolecular ion peak at *m/z* 457.3677 $[M+H]^+$ (calcd for $C_{30}H_{49}O_3$, 457.3676), the molecular formula of compound **7** was deduced to be $C_{30}H_{48}O_3$. The ^{13}C J-MOD spectrum of compound **7** demonstrated the existence of two keto groups (δ_C 215.13 and 217.94) in the molecule; one of them was placed at C-3 (δ_C 215.13) with regard to the HMBC correlations between C-3 and H_3-28 (δ_H 1.10 s), H_3-29 (δ_H 1.07 s), and H-2a (δ_H 2.57 m) whereas the other at C-24 (δ_C 217.94) based on the long-range correlations of C-24 and H_3-26 (δ_H 1.39 s), H_3-27 (δ_H 1.38 s), and H_2-23 (δ_H 2.55 m). The 25-hydroxy functionality was proposed by the carbon chemical shift value of $\delta_{C\text{-}25}$ 76.37. NOESY cross-peaks between H_3-18/H-20, H_3-28/H-5, and H-17/H_3-30 were consistent with the suggested structure of compound **7** [25-dihydroxylanosta-8-en-3,24-dione] (Fig. 1).

Compound **8** was identical in all of its spectral characteristics with (+)-clavaric acid. This compound was reported to be a specific inhibitor of human farnesyl protein transferase (FPTase) (IC_{50} 1.3 μM) (Lingham et al., 1998) and was first isolated from the fungus *Clavariadelphus truncatus* (Jayasuriya et al., 1998). The ^{1}H and ^{13}C NMR assignments of compound **8** were published in $CDCl_3$, but in our experiment, these data were determined in CD_3OD (Tables 1 and 2). The NOESY correlations between H-2/H_3-19, H-2/H_3-28, H_3-18/H-20, H-2/H-1a (δ_H 2.36), H-1a/H-11a (δ_H 2.16), and H-20/H-22a (δ_H 1.82) matched the relative stereostructure of (+)-clavaric acid.

2.2. Anti-inflammatory screening

The isolated compounds (**1**–**8**) and) pholiol C (**9**) were examined for their anti-inflammatory activity using COX-1, COX-2, 5-LOX, and 15-LOX assays, and Tables 3 and 4 present the results. The COX inhibitory activities of the compounds at 50 μM indicated a moderate-to-weak inhibition for the compounds. Dose–response investigations revealed that pholiols F (**2**) and (+)-clavaric acid (**8**) exhibited moderate anti-inflammatory activity on COX-2 with IC_{50} values of 439.8 and 766.7 μM, respectively. Furthermore, the other compounds had inhibition below 50% at the highest concentration tested (2.5 mM). Pholiols F (**2**), G (**3**), I (**5**), and C showed the best inhibitory activity against 5-LOX among the compounds (IC_{50} 194.5–519.7 μM). Pholiol F (**2**) with an IC_{50} value of 194.5 μM was the most active on 5-LOX test. However, all compounds were considered inactive against 15-LOX at the used concentrations.

Table 3
COX-1 and COX-2 inhibitory activities of the triterpenes of *P. populnea*.

Compound	COX-1			COX-2		
	Inhibitory (%)[a]	S.D.	IC_{50} (μM)	Inhibitory (%)	S.D.	IC_{50} (μM)
Pholiol E (**1**)	−10.42	9.43	–	7.00	4.59	–
Pholiol F (**2**)	20.32	0.19	–	35.74	10.67	439.8
Pholiol G (**3**)	−0.56	6.87	–	2.82	3.89	–
Pholiol H (**4**)	6.65	1.487	–	−2.50	4.99	–
Pholiol I (**5**)	4.89	17.26	–	−3.26	3.95	–
Pholiol J (**6**)	−16.16	13.84	–	−5.26	6.60	–
Pholiol K (**7**)	−37.13	3.20	–	−8.40	2.27	–
(+)-Clavaric acid (**8**)	20.96	9.99	–	37.27	8.54	766.7
Pholiol C (**9**)	17.7	0.64	–	3.28	36.76	–
Standard	50.94[b]	2.13	–	79.02	3.071	0.45[b]

[a] Relative percentage inhibition was assessed at 50 μM of the compounds and in triplicates. Dose–response investigations were conducted in duplicates with 2.5 mM as the highest concentration.
[b] Standards: SC560 for COX-1, Celecoxib for COX-2.

Table 4
5-LOX and 15-LOX inhibitory activities of the triterpenes of *P. populnea*.

Compound	5-LOX			15-LOX		
	Inhibitory (%)[a]	S.D.	IC_{50} (μM)	Inhibitory (%)	S.D.	IC_{50} (μM)
Pholiol E (**1**)	−35.25	3.05	–	−23.22	11.2	–
Pholiol F (**2**)	−7.91	16.28	194.5	−16.19	15.27	–
Pholiol G (**3**)	15.11	2.04	519.7	−77.38	24.05	–
Pholiol H (**4**)	−55.04	23.91	–	−94.87	11.21	–
Pholiol I (**5**)	0.72	4.07	480.5	−50.72	24.91	–
Pholiol J (**6**)	−102.2	19.33	–	−79.45	30.41	–
Pholiol K (**7**)	−302.5	8.65	–	−58.33	28.85	–
(+)-Clavaric acid (**8**)	−35.61	5.60	–	−39.6	22.47	–
Pholiol C (**9**)	17.27	9.16	370.1	−112.1	15.97	–
Standard	50.72	2.54	0.53[b]	103.5[b]	18.59	–

[a] Relative percentage inhibition was assessed at 100 μM of the compounds and in triplicates. Dose–response investigations were conducted in duplicates with 3 mM as the highest concentration.
[b] Standards: Zileuton for 5-LOX, NDGA for 15-LOX.

3. Conclusions

The present study showed a detailed mycochemical analysis of the chloroform and ethyl acetate extracts of the edible mushroom *P. populnea*. The combination of different chromatographic techniques and spectroscopic analysis resulted in the identification of eight lanostane triterpenoids (**1**–**8**), including the undescribed pholiols E–K (**1**–**7**). The evaluation of anti-inflammatory activity against cyclooxygenase (COX-1 and COX-2) and lipoxygenase (5-LOX and 15-LOX) enzymes revealed that pholiol F (**2**) and (+)-clavaric acid (**8**) bearing 2-(3-hydroxy-3-methylglutaryl) and only one keto group in their structure are the most effective COX-2 inhibitors, whereas the diester derivative pholiol F (**2**) possesses the best 5-LOX inhibitory activity. Pholiol F (**2**) with a dual 5-LOX/COX-2 inhibitory effect can be regarded as the most

interesting compound. It functions by blocking the formation of both prostaglandins and leukotrienes but does not influence lipoxin formation responsible for damaging the GI mucosa (Martel-Pelletier et al., 2003). In sum, our findings indicated that *P. populnea* is an excellent source of novel fungal metabolites.

4. Experimental

4.1. General

A Jasco P-2000 polarimeter was used to measure optical rotations (Jasco International, Co., Ltd., Hachioji, Tokyo, Japan). Molar Chemicals (Halásztelek, Hungary) and Sigma-Aldrich Kft. (Budapest, Hungary) supplied the chemicals used in this study. HPLC separations were conducted on a Shimadzu LC-10 A S HPLC instrument equipped with a UV–Vis detector (Shimadzu, Co., Ltd., KYOTO, Japan) over normal-phase (NP-HPLC, LiChrospher Si60, 5 μm, 250 × 4 mm) and reversed-phase (RP-HPLC, LiChrospher RP-18, 5 μm, 250 × 4 mm) columns. Furthermore, NP-HPLC was performed using a Zorbax-Sil column (250 × 9.4 mm, 5 μm; Agilent Technologies, Santa Clara, CA, USA) on a Waters HPLC instrument equipped with a PDA detector (Waters, Co., Ltd., Milford, USA). Flash chromatography (FC) was carried out on a CombiFlash Rf + Lumen instrument with integrated UV, UV–Vis, and ELS detection using reversed phase (RediSep C_{18} Bulk 950, Teledyne Isco, Lincoln, NE, USA) and normal phase (silica 60, 0.045–0.063 mm, Molar Chemicals, and RediSep Rf Gold, Teledyne Isco, Lincoln NE, USA) flash columns. Preparative thin-layer chromatography (TLC) was performed using silica plates (20 × 20 cm silica gel 60 F254, Merck 105,554). Sephadex LH-20 (25–100 μm, Sigma-Aldrich) was used for gel filtration. The direct-injection high-resolution mass spectrometry (HRMS) and high-resolution tandem mass spectrometry (HRMS/MS) measurements were performed by Waters Acquity I-Class UPLC™ (Milford, MA, UK) coupled to Thermo Scientific Q Exactive™ Plus Hybrid Quadrupole-Orbitrap™ (Waltham, MA, USA) mass spectrometer. The mass spectrometer was operated in heated electrospray ionization (ESI) mode with positive and negative ion detection. The instrument settings were as follows: capillary temperature 250 °C, S-Lens RF level 50, spray voltage 3.5 kV in positive and 2.5 kV in negative ionization mode. For HRMS/MS analysis, the collision energy was set to 30 eV, and 1 Da isolation window was applied. The eluent composition was 20/80/0.1 water/acetonitrile/formic acid (v/v/v) in positive ESI mode, while in negative ESI mode 20/80 water/acetonitrile was used (v/v). The flow rate was set to 0.4 mL/min. All samples were dissolved in methanol prior to the MS measurements. MassLynx 4.1 (Milford, MA, USA) software was used for UPLC and Xcalibur 4.3.73.11 software (Waltham, MA, USA) was used for spectra acquisition. NMR spectra were recorded in $CDCl_3$ or CD_3OD on a 500 MHz Bruker Avance DRX spectrometer (Bruker, Billerica, MA, USA) at 500 MHz (^{1}H) and 125 MHz (^{13}C). The signals of the deuterated solvents were taken as references. Two-dimensional NMR measurements were performed using the standard Bruker software. In the COSY, HSQC, and HMBC experiments, gradient-enhanced versions were used.

4.2. Mushroom material

Samples of *Pholiota populnea* (Pers.) Kuyper & Tjall.-Beuk. (Strophariaceae)were collected in the autumn of 2017 near Szeged, Hungary (46.400556, 20.190556), and identified by Attila Sándor (Mushroom Society of Szeged, Hungary). Fruiting bodies of *P. populnea* were stored at −20 °C until processing. A voucher specimen (No. H019) was deposited at the Department of Pharmacognosy, University of Szeged, Hungary.

4.3. Extraction and isolation

The fruiting bodies (4.2 kg) of *P. populnea* were ground in a blender and then percolated with MeOH (20 L) at room temperature. After evaporation of the solvent, the methanol extract (151 g) was dissolved in 50% aqueous MeOH and subjected to liquid–liquid partition using *n*-hexane (5 × 500 mL), chloroform (5 × 500 mL), and then ethyl acetate (5 × 500 mL). The ethyl acetate-soluble phase (16.7 g) was subjected to flash chromatography (NP-FC) on silica gel (80 g) using a gradient system of *n*-hexane–acetone (linear from 0% to 100% acetone, t = 60 min) and eluted with MeOH (100%, t = 5 min) at the end of this process, providing 17 combined fractions (E1–17). Fraction E7 (30 mg) was further separated by NP-HPLC (mobile phase: *n*-hexane–EtOAc–MeOH, 50:45:5), allowing the isolation of compound **6** (2.7 mg). Fraction E11 (4.2 g) was subjected to flash chromatography (NP-FC) on silica gel (40 g) using an *n*-hexane–acetone gradient system (linear from 0% to 100% acetone, t = 60 min) as a mobile phase, which also led to 14 fractions (EA 1–14). To further purify EA3 (370 mg), NP-HPLC was employed (mobile phase: cyclohexane–EtOAc 20:80) yielding fraction EA3-c (90 mg), which led to the isolation of **3** (2.4 mg), **5** (4.7 mg), **1** (25.8 mg), and **2** (3.7 mg) *via* RP-HPLC (mobile phase: H_2O–MeOH 20:80) separation. The chloroform-soluble phase (25.3 g) was subjected to NP-FC on silica gel (80 g) using a gradient system of *n*-hexane–EtOAc (linear from 40% to 100% EtOAc, t = 75 min) and eluted with MeOH (100%, t = 10 min) at the end of this process. Fractions with similar compositions were combined according to TLC monitoring (C1–C18). Compound **7** (2.1 mg) was produced by further purifying fraction C5 (390 mg) *via* NP-HPLC (mobile phase: *n*-hexane–EtOAc–MeOH 50:45:5). Fraction C7 (800 mg) was further separated using multiple steps of NP-FC, applying a gradient system of *n*-hexane–EtOAc (40 g of sorbent, linear elution from 45% to 100% EtOAc, t = 60 min) and cyclohexane–EtOAc (12 g of sorbent, linear from 0% to 100% EtOAc, t = 50 min), affording 14 (C7A a-n) and 12 (C7B a-l) combined fractions, respectively. Then, a final purification was conducted on C7Ae (17.5 mg) *via* preparative TLC using an *n*-hexane–EtOAc–MeOH (5:4:1) solvent system to produce compound **4** (2.5 mg). Finally, compound **8** (5.2 mg) was isolated from fraction C7Bb (5.9 mg) *via* RP-HPLC (mobile phase: H_2O–acetonitrile, 4:6).

4.3.1. Pholiol E (1)

White amorphous powder; $[\alpha]_D^{25}$ +49 (c 0.1, MeOH); ^{1}H and ^{13}C NMR data, see Tables 1 and 2; HRESIMS + m/z 617.4063 $[M+H]^+$ calcd for $C_{36}H_{57}O_8$ 617.4048; ESI– m/z 615.3926 $[M–H]^-$ (calcd for $C_{36}H_{55}O_8$ 615.3902).

4.3.2. Pholiol F (2)

White amorphous powder; $[\alpha]_D^{25}$ +5 (c 0.1, $CHCl_3$); ^{1}H and ^{13}C NMR data, see Tables 1 and 2; HRESIMS + m/z 661.4320 $[M+H]^+$ (calcd for $C_{38}H_{61}O_9$, 661.4310).

4.3.3. Pholiol G (3)

White amorphous solid; $[\alpha]_D^{25}$ +4 (c 0.1, MeOH); ^{1}H and ^{13}C NMR data, see Tables 1 and 2; HRESIMS + m/z 641.4017 $(M + Na)^+$ (calcd for $C_{36}H_{58}O_8Na$ 641.4029; HRESIMS– m/z 617.4089 $[M–H]^-$ (calcd for $C_{36}H_{57}O_8$, 617.4053).

4.3.4. Pholiol H (4)

White amorphous solid; $[\alpha]_D^{25}$ +16.5 (c 0.5, MeOH); ^{1}H and ^{13}C NMR data, see Tables 1 and 2; HRESIMS + m/z 647.4166 $[M+H]^+$ (calcd for $C_{37}H_{59}O_9$, 647.4154).

4.3.5. Pholiol I (5)

White amorphous powder; $[\alpha]_D^{25}$ +11 (*c* 0.1, MeOH); ^{1}H and ^{13}C NMR data, see Tables 1 and 2; HRESIMS + *m/z* 631.3844 $[M+H]^+$ (calcd for $C_{36}H_{55}O_9$, 631.3841).

4.3.6. Pholiol J (6)

Colorless amorphous solid; $[\alpha]_D^{25}$ +39 (c 0.1, MeOH); ^{1}H and ^{13}C NMR data, see Tables 1 and 2; HRESIMS + m/z 459.3833 $[M+H]^+$ (calcd for $C_{30}H_{51}O_3$ 459.3833)

4.3.7. Pholiol K (7)

Colorless amorphous solid; $[\alpha]_D^{25}$ +29 (c 0.1, $CHCl_3$), ^1H and ^{13}C NMR data, see Tables 1 and 2; HRESIMS + m/z 457.3677 $[M+H]^+$ (calcd for $C_{30}H_{49}O_3$, 457.3676).

4.3.7. (+)-Clavaric acid (8)

White amorphous powder; $[\alpha]_D$ +29 (*c* 0.1, MeOH); ^1H and ^{13}C NMR data, see Tables 1 and 2; HRESIMS– *m/z* 617.4086 $[M–H]^+$ (calcd for $C_{36}H_{57}O_8$, 617.4053).

4.4. Anti-inflammatory screening

4.4.1. Cyclooxygenase (COX) inhibitory activity

Based on the fluorometric method described in BioVision's COX-1 inhibitor screening kit leafkit (K548-100, BioVision, CA, USA) and COX-2 inhibitor screening kit leafkit (K547-100, BioVision, CA, USA), respectively, COX-1 and COX-2 inhibitory activities were assessed. The sample solutions were dissolved in DMSO and then in buffer to achieve suitable concentrations. In a 96-well white plate (655,101, F-bottom, Greiner Bio-One, Germany), 80-μL reaction mix (containing 76-μL assay buffer, 1-μL COX Probe, 2-μL COX cofactor, and 1-μL COX enzyme) was added to 10-μL sample solution, DMSO, and assay buffer to obtain test wells assigned for sample screen (S), negative control (N), and blank, respectively. Ten microliters of arachidonic/NaOH solution was added to each well using a multichannel pipette to start the reaction simultaneously, and the fluorescence of each well was measured kinetically at Ex/Em 550/610 nm, at 25 °C for 10 min, using a FluoStar Optima plate reader (BMG Labtech, Ortenberg, Germany). The COX inhibitory activity of SC560 and Celecoxib, standard inhibitors of COX-1 and COX-2, respectively, was also determined.

The change in fluorescence between two points, T_1 and T_2, were determined, and relative inhibition was computed as follows:

$$\text{Inhibition } \% = [(\text{change in N} - \text{change of S}) / \text{change in N}] \times 100$$

4.4.2. 5-Lipoxygenase (5-LOX) inhibitory activity

Based on the fluorometric method described in BioVision's 5-LOX inhibitor screening kit leafkit (K980-100, BioVision, CA, USA), measuring the decrease in fluorescence in the presence of potential 5-lipoxygenase inhibitors, 5-LOX inhibitory activity was tested. Briefly, to obtain a sample screen (S), the samples were dissolved in anhydrous DMSO, and 2-μL sample solutions were added to a 96-well white plate (655,101, F-bottom, Greiner Bio-One, Germany). Two microlitres each of assay buffer, anhydrous DMSO, and Zileuton solution, a standard inhibitor, were added to the corresponding wells to produce a blank, negative control (N), and positive control. Assay buffer (38 μL) was added to all wells and, subsequently, 40-μL reaction mix (containing 34-μL LOX assay buffer, 2-μL LOX probe, and 4-μL LOX enzyme). The reaction was started simultaneously after 10 min using a multichannel pipette to add 20-μL diluted substrate solution to each well, and the fluorescence of each well was determined kinetically at Ex/Em 485/520 nm, at 25 °C for 20 min, using a FluoStar Optima plate reader (BMG Labtech, Ortenberg, Germany).

The change in fluorescence between two points, T_1 (3 min) and T_2 (10 min), was determined, and relative inhibition was computed as follows:

$$\text{Inhibition } \% = [(\text{change in N} - \text{change in S}) / \text{change of N}] \times 100$$

4.4.3. 15-Lipoxygenase (15-LOX) inhibitory activity

15-LOX inhibitory activities of the compounds were assessed using Cayman's lipoxygenase inhibitor screening assay kit (760,700, Cayman Chemical, MI, USA), detecting and measuring the hydroperoxides produced in the lipoxygenation reaction using a lipoxygenase enzyme. Briefly, in a 96-well white plate (655,101, F-bottom, Greiner Bio-One, Germany), blank wells contained 100-μL assay buffer; negative-control wells contained 90-μL lipoxygenase standard solution and 10-μL assay buffer; standard inhibitor wells contained 90-μL lipoxygenase standard solution and 10-μL nordihydroguaiaretic acid (NDGA) solution, and sample wells contained 90-μL lipoxygenase standard solution and 10-μL sample solution prepared by dissolving in methanol and then assay buffer until suitable concentrations were achieved. After incubation for 10 min, 10-μL arachidonic/NaOH solution was added to all wells using a multichannel pipette to start the reaction simultaneously, and the plate was placed on a shaker. After 5 min, the reaction was stopped by adding 100 μL of chromogen to all wells, and the absorbance was read at 485 nm. The inhibition % was computed as

$$\text{inhibition } \% = [(\text{absorbance of control} - \text{absorbance of sample}) / \text{absorbance of control}] \times 100$$

The dose-effect investigations on the most active compounds were employed to measure the concentration, inhibiting 50% of COX-1, COX-2, 5-LOX, and 15-LOX enzyme activity. The sigmoidal dose–response model was obtained using GraphPad Prism 8.0 (La Jolla, CA, USA), and these were employed to determine the IC_{50} values of the compounds.

Declaration of competing interest

The authors declare that they have no known competing financial interests or personal relationships that could have appeared to influence the work reported in this paper.

Data availability

No data was used for the research described in the article.

Acknowledgments

This study was supported by National Research, Development and Innovation Office, Hungary (NKFIH; K135845). The authors are grateful to Attila Sándor for his help in the collection and identification of mushroom material.

Appendix A. Supplementary data

Supplementary data to this article can be found online at https://doi.org/10.1016/j.phytochem.2022.113480.

References

Aichour, S., Haba, H., Benkhaled, M., Harakat, D., Lavaud, C., 2014. Terpenoids and other constituents from *Euphorbia bupleuroides*. Phytochem. Lett. 10, 198–203.

Bao, T.R.G., Long, G.Q., Wang, Y., Wang, Q., Liu, X.L., Hu, G.S., Gao, X.X., Wang, A.H., Jia, J.M., 2019. New lanostane-type triterpenes with anti-inflammatory Activity from the epidermis of *Wolfiporia cocos*. Molecules 24, 1888.

Chen, H.-P., Zhao, Z.-Z., Li, Z.-H., Huang, Y., Zhang, S.-B., Tang, Y., Yao, J.-N., Chen, L., Isaka, M., Feng, T., Liu, J.-K., 2018. Anti-proliferative and anti-inflammatory lanostane triterpenoids from the Polish edible mushroom *Macrolepiota procera*. J. Agric. Food Chem. 66, 3146–3154.

Hu, Z., Du, R., Xiu, L., Bian, Z., Ma, C., Sato, N., Hattori, M., Zhang, H., Liang, Y., Yu, S., Wang, X., 2020. Protective effect of triterpenes of *Ganoderma lucidum* on

lipopolysaccharide-induced inflammatory responses and acute liver injury. Cytokine 127, 154917.
Jayasuriya, H., Silverman, K.C., Zink, D.L., Jenkins, R.G., Sanchez, M., Pelaez, F., Vilella, D., Lingham, R.B., Singh, S.B., 1998. Clavaric acid: a triterpenoid inhibitor of farnesyl-protein transferase from. Clavariadelphus truncates. J. Nat. Prod. 61, 1568–1570.
Lingham, R.B., Silverman, K.C., Jayasuriya, H., Kim, B.M., Amo, S.E., Wilson, F.R., Rew, D.J., Schaber, M.D., Bergstrom, J.D., Koblan, K.S., Graham, S.L., Kohl, N.E., Gibbs, J.B., Singh, S.B., 1998. Clavaric acid and steroidal analogues as RAS- and FPP-directed inhibitors of human farnesyl-protein transferase. J. Med. Chem. 41, 4492–4501.
Martel-Pelletier, J., Lajeunesse, D., Reboul, P., Pelletier, J.-P., 2003. Therapeutic role of dual inhibitors of 5-LOX and COX, selective and non-selective non-steroidal anti-inflammatory drugs. Ann. Rheum. Dis. 62, 501–509. https://doi.org/10.1136/ard.62.6.501.
Nakamura, S., Iwami, J., Matsuda, H., Mizuno, S., Yoshikawa, M., 2009. Absolute stereostructures of inoterpenes A–F from sclerotia of *Inonotus obliquus*. Tetrahedron 65, 2443–2450.
Öztürk, M., Tel-Çayan, G., Muhammad, A., Terzioğlu, P., Duru, M.E., 2015. Mushrooms: a source of exciting bioactive compounds. Stud. Nat. Prod. Chem. Chapter 10 (45), 363–456.
Ványolós, A., Muszyńska, B., Chuluunbaatar, B., Gdula-Argasińska, J., Kała, K., Hohmann, J., 2020. Extracts and steroids from the edible mushroom *Hypholoma lateritium* exhibit anti-inflammatory properties by inhibition of COX-2 and activation of Nrf2. Chem. Biodivers. 17, e2000391.
Yang, X., Chen, X.J., Yang, Z., Xi, Y.-B., Wang, L., Wu, Y., Yan, Y.-B., Rao, Y., 2018. Synthesis, evaluation, and structure-activity relationship study of lanosterol derivatives to reverse mutant-crystallin-induced protein aggregation. J. Med. Chem. 61, 8693–8706. https://doi.org/10.1021/acs.jmedchem.8b00705.
Yazdani, M., Béni, Z., Dékány, M., Szemerédi, N., Spengler, G., Hohmann, J., Ványolós, A., 2022. Triterpenes from *Pholiota populnea* as cytotoxic agents and chemosensitizers to overcome multidrug resistance of cancer cells. J. Nat. Prod. 85, 910–916.
Zhang, F.-L., Shi, C., Sun, L.-T., Yang, H.-X., He, J., Li, Z.-H., Feng, T., Liu, J.-K., 2021. Chemical constituents and their biological activities from the mushroom *Pyropolyporus fomentarius*. Phytochemistry 183, 112625.

III.

pharmaceuticals

MDPI

Article

Isolation of the Lanostane Triterpenes Pholiols L–S from *Pholiota populnea* and Evaluation of Their Antiproliferative and Cytotoxic Activities

Morteza Yazdani [1], Anita Barta [1], Anasztázia Hetényi [2], Róbert Berkecz [3], Gabriella Spengler [4], Attila Ványolós [5] and Judit Hohmann [1,6,7,*]

1 Institute of Pharmacognosy, University of Szeged, 6720 Szeged, Hungary
2 Department of Medical Chemistry, University of Szeged, 6720 Szeged, Hungary
3 Institute of Pharmaceutical Analysis, University of Szeged, 6720 Szeged, Hungary
4 Department of Medical Microbiology, Albert Szent-Györgyi Health Center and Albert Szent-Györgyi Medical School, University of Szeged, 6725 Szeged, Hungary
5 Department of Pharmacognosy, Semmelweis University, 1085 Budapest, Hungary
6 Interdisciplinary Centre for Natural Products, University of Szeged, 6720 Szeged, Hungary
7 ELKH-USZ Biologically Active Natural Products Research Group, University of Szeged, 6720 Szeged, Hungary
* Correspondence: hohmann.judit@szte.hu; Tel.: +36–62–546453

Abstract: Pholiols L-S (**1**–**8**), eight undescribed triterpenes were isolated from the sporocarps of the mushroom *Pholiota populnea*. Various chromatographic techniques, such as open column chromatography, flash chromatography, gel filtration, preparative thin layer chromatography, and HPLC, were applied to purify the compounds. The structure elucidation was carried out by spectroscopic analysis, including 1D (^{1}H NMR and ^{13}C JMOD) and 2D NMR (^{1}H-^{1}H COSY, HSQC, HMBC and NOESY) and HRESIMS experiments. The isolated compounds had lanostane (**1**–**7**) or trinorlanostane (**8**) skeletons; all of them were substituted with 3-hydroxy-3-methylglutaroyl group or its 6-methyl ester. Five compounds (**1**, **2**, **4**, **6**, and **8**) were investigated for their antiproliferative and cytotoxic activity in vitro by MTT assay on breast cancer (MCF-7), human colon adenocarcinoma (sensitive Colo 205, and resistant Colo 320), non-small cell lung cancer (A549), and human embryonic lung fibroblast (MRC-5) cell lines. Pholiols M (**2**) and O (**4**) showed antiproliferative activity against the MCF-7 cell line with IC_{50} of 2.48 and 9.95 μM, respectively. These compounds displayed tumor cell selectivity on MCF-7 cells with SI values of >40 (**2**) and 4.3 (**4**), but they did not show a cytotoxic effect, proving their action exclusively on tumor cell proliferation. Pholiols L (**1**) and Q (**8**) were found to have selective cytotoxicity on drug resistant cells in comparison to their effects on Colo320 and Colo205 cells [relative resistance values 0.84 (**1**) and 0.62 (**8**)].

Keywords: *Pholiota populnea*; strophariaceae; antiproliferative activity; cytotoxic activity; lanostane; pholiol

Citation: Yazdani, M.; Barta, A.; Hetényi, A.; Berkecz, R.; Spengler, G.; Ványolós, A.; Hohmann, J. Isolation of the Lanostane Triterpenes Pholiols L–S from *Pholiota populnea* and Evaluation of Their Antiproliferative and Cytotoxic Activities. *Pharmaceuticals* **2023**, *16*, 104. https://doi.org/10.3390/ph16010104

Academic Editors: Kuei-Hung Lai and Bo-Rong Peng

Received: 22 December 2022
Revised: 5 January 2023
Accepted: 6 January 2023
Published: 10 January 2023

1. Introduction

For many decades, mushrooms have been utilized because of their beneficial nutritional and medicinal values, including immunomodulatory and antitumor activities. Fungal metabolites can have a protective effect by stimulating the immune response and activating immune cells, macrophages, T cells, and natural killer cells. Furthermore, bioactive compounds of mushrooms have shown cytotoxicity, antiproliferative activity, apoptosis-inducing properties, and have been shown to act as cancer cell metastases inhibitory agents. Certain dietary mushrooms (e.g., *Agaricus bisporus*) were reported to contain anti-carcinogenic metabolites which alter the aromatase enzyme activity. The active ingredients responsible for the immunomodulatory and antitumor activities of mushrooms include

polysaccharides, polysaccharide-protein complexes, lectins, amino acids, polyphenols, sterols, and other terpenoids [1–3].

Polysaccharides from *Pholiota adiposa*, especially SPAP2-1, showed strong interference of the cell cycle of HeLa cells and induced apoptosis [4]. A protein purified from the edible fungus *Pholiota nameko* (PNAP) shows promise for the treatment of breast cancer, as it induced apoptosis of human breast adenocarcinoma MCF-7 cells in vivo and modulated cytokine secretion in mice bearing MCF-7 xenografts [5]. The glucan polysaccharides schizophyllan, derived from *Schizophyllum commune*, and lentinan, produced by *Lentinula edodes*, were investigated in clinical trials, and a better overall survival of patients with head and neck cancer and gastric and colorectal carcinomas, respectively, were found [6].

Ganoderma lucidum polysaccharides and triterpenoids were found to be potent inhibitors of tumor growth in vitro and in vivo [7]. Moreover, extracts of *G. lucidum* and *G. tsugae* were able to inhibit the growth of colorectal cancer cells in vitro [8]. Ergosterol, the main sterol of mushroom species, is able to induce apoptosis in leukemia cells and inhibits tumor-induced angiogenesis [9]. *Hypholoma lateritium* (Strophariaceae) was reported to contain lanostane-type triterpenoids, sublateriols A–C, and fasciculol A–C, some of them exhibited cytotoxicity against human cancer cell lines (A549, SK-OV-3, SK-MEL-2, and HCT-15) in vitro [10].

In our previous study, *Pholiota populnea* was investigated for antitumor compounds, and lanostane diesters, named pholiols A–D, ergosterol, 3β-hydroxyergosta-7,22-diene, and a polyhydroxy-squalene derivative were isolated. Ergosterol was found to show cytotoxic activity against sensitive (Colo 205) and resistant colon adenocarcinoma cells (Colo 320) with IC_{50} values of 4.9 and 6.5 μM, respectively. The *p*-glycoprotein (ABCB1) efflux pump inhibitory activity of the compounds was also tested against resistant Colo 320 cells and inhibitory activity was found for pholiols A and B and the squalene derivative. In addition, the drug interactions of triterpenes with doxorubicin were also studied by the checkerboard method on Colo 320 cells, and it was observed that pholiols B and D interacted in a synergistic manner, while the acyclic triterpene acted in a very strong synergistic manner [11]. Further mycochemical investigations led to the isolation of pholiols E-K and (+)-clavaric acid, some of the triterpenes exerted moderate COX-2 and 5-LOX inhibitory activities. Pholiol F (IC_{50} 194.5 μM against 5-LOX, and 439.8 μM against COX-2) was found to be the most effective among the investigated compounds [12].

In continuation of our study on *P. populnea*, we herein report the isolation of eight undescribed triterpenes, namely, pholiols L–S (**1**–**8**) from the chloroform and ethyl acetate extracts of the mushroom, and investigation of the cytotoxic and antiproliferative activity of the compounds.

2. Results and Discussion

2.1. Structure Determination of Compounds 1−8

Eight triterpenes (**1**–**8**) were isolated from the chloroform- and ethyl acetate–soluble phase of the MeOH extract obtained from *P. populnea* by a combination of different chromatographic methods, such as open column chromatography (OCC), flash chromatography (FC), gel filtration (GF), preparative thin layer chromatography (TLC), and high-performance liquid chromatography (HPLC). The structure elucidation was carried out by spectroscopic analysis, including 1D and 2D NMR [^{1}H-^{1}H Correlation Spectroscopy (^{1}H-^{1}H COSY), Heteronuclear Single Quantum Coherence (HSQC), Heteronuclear Multiple Bond Correlation (HMBC), and Nuclear Overhauser Effect Spectroscopy (NOESY)] and HRESIMS experiments. The NMR and MS data showed that all compounds were lanostane (**1**–**7**) or trinorlanostane esters (**8**) (Figure 1).

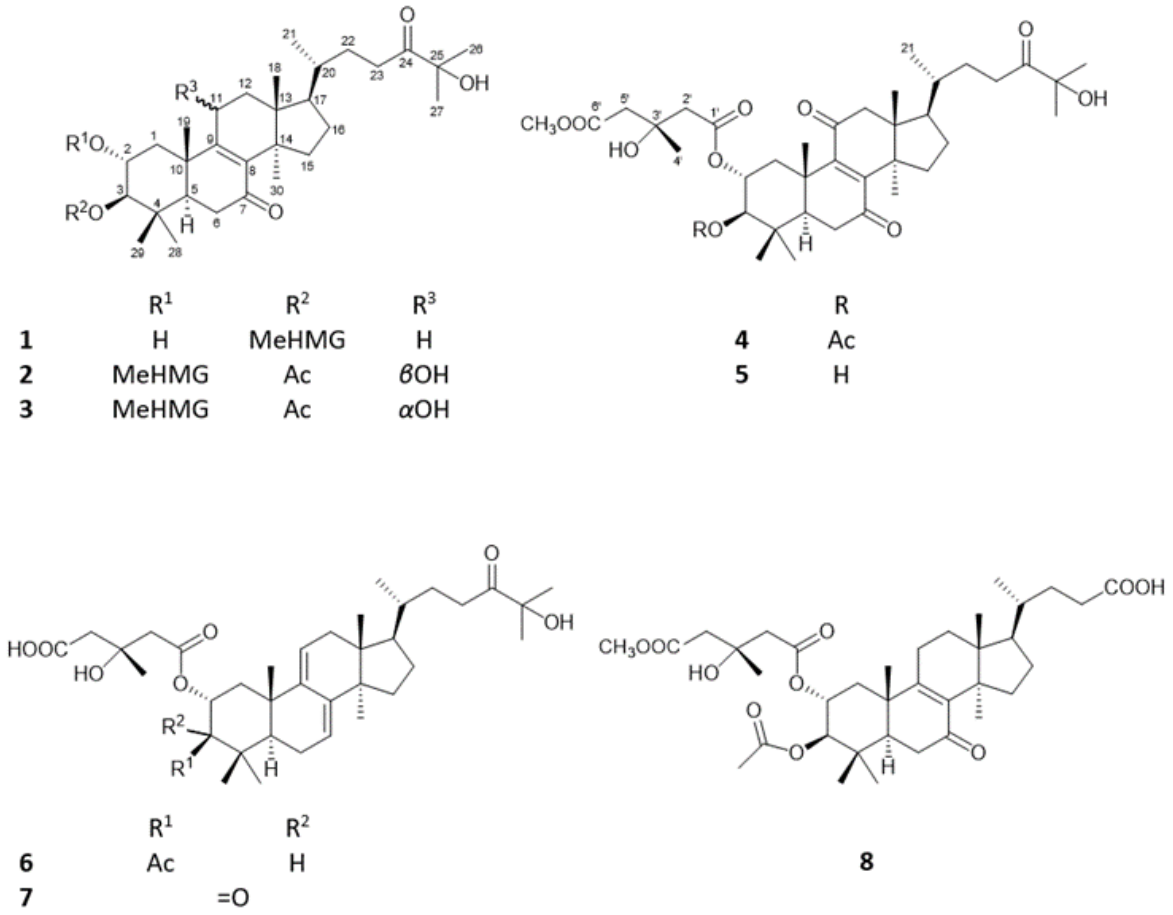

Figure 1. Pholiols L-S (**1**–**8**) isolated from *Pholiota populnea.* MeHMG = 3-hydroxy-3-methyl-glutaryl 6-methyl ester.

Compound **1**, named pholiol L, was obtained as a colorless amorphous solid with $[\alpha]^{23}_{D}$ −11.6 (*c* 0.1, $CHCl_3$). Its HRESIMS spectrum exhibited a protonated molecular ion at *m*/*z* 647.4147 $[M + H]^+$ (calcd for $C_{37}H_{59}O_9^+$ 647.4154), indicating the molecular formula of $C_{37}H_{58}O_9$. The ^{1}H NMR and ^{13}C-JMOD spectra indicated a 3-hydroxy-3-methylglutaric acid 6-methyl ester (MeHMG) derivative [δ_H 2.75 m, 2.57 m (H_2-2′), 2.92 m, 2.27 m (H_2-5′), 1.42 s (H_3-4′), 3.72 s (OCH_3-7′); δ_C 171.41 (1′), 173.26 (C-6′), 46.33 (C-2′), 43.68 (C-5′), 70.37 (C-3′), 28.29 (C-4′), 52.05 (OCH_3-7′)], substituted with two keto groups (δ_C 198.29 and 215.01); the presence of two hydroxy groups was suggested by the carbon resonances of a methine group at δ_C 66.89 (C-2) and a quaternary carbon at δ_C 76.34 (C-25). A sequence of the correlated protons in the ^{1}H–^{1}H COSY spectrum –CH_2–CH(OR)–CH(OR)– (δ_H 2.21 dd (12.5, 3.8 Hz), 1.44 m, 3.92 dt (3.8, 11.1 Hz), 4.60 d (9.9 Hz) could be assigned to the C-1–C-3 part of the molecule, with regard to the HMBC correlations between H_2-1 and C-10; H_3-19 and C-10; H-3 and C-4; H_3-28 and H_3-29 and C-4; H-1a, H_3-28, H_3-29, and H_3-19 with C-5 (Figure 2). NMR data of compound **1** were very similar to those of the previously isolated pholiol H, with the major differences in chemical shifts of H-2, H-3 (**1**: $\delta_{H\text{-}2}$ 3.92 dt, $\delta_{H\text{-}3}$ 4.60 d versus pholiol H: $\delta_{H\text{-}2}$ 5.07 dt, $\delta_{H\text{-}3}$ 3.24 d), and C-2 and C-3 (**1**: $\delta_{C\text{-}2}$ 66.89, $\delta_{C\text{-}3}$ 84.53 versus pholiol H: $\delta_{C\text{-}2}$ 73.41, $\delta_{C\text{-}3}$ 79.99) [12] demonstrating the connection of the ester group at position C-3 and hydroxyl group at C-2 in **1**. The relative configuration of **1** was determined based on the Overhauser effects detected in the NOESY spectrum. The NOESY correlation of H-3 (δ_H 4.60) with H-1α (δ_H 1.44), H_3-28 (δ_H 0.91), and H-5 (δ_H 1.82) showed these protons in the α orientation, while correlations of H-2 (δ_H 3.92) with H-1β (δ_H 2.21), H_3-19 (δ_H 1.24), and H_3-29 (δ_H 0.96) indicated the β orientation of H-2 and the 19- and 29-methyl groups (Figure 2). The Overhauser effect between H_3-18 and H-20 was indicative

for their β position, similar to the previously isolated pholiol compounds [11,12]. All of the above evidence confirmed the structure of pholiol L (**1**), as depicted in Figure 1.

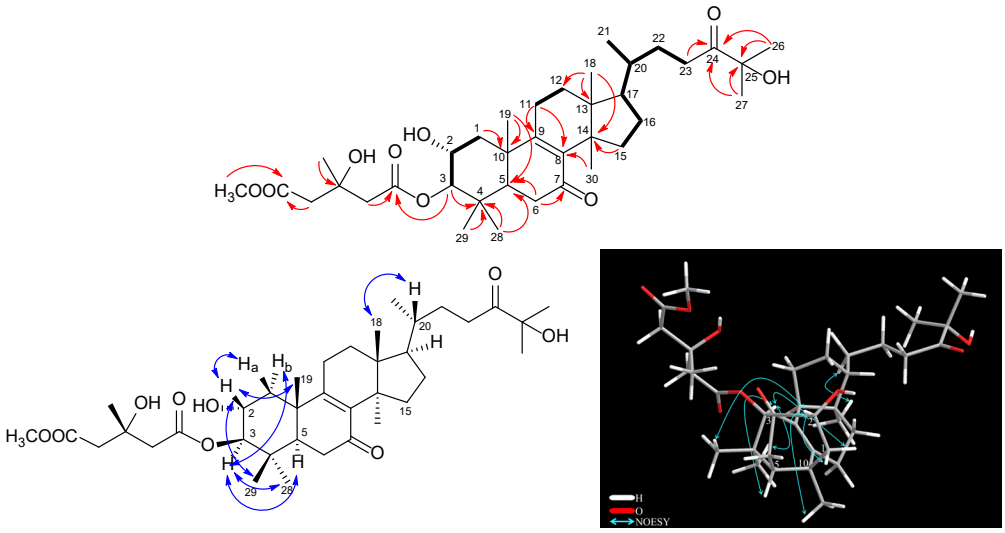

Figure 2. Key COSY (–), HMBC (→), and NOESY (H↔H) correlations of pholiol L (**1**).

Compound **2** (pholiol M) was obtained as a colorless amorphous solid with an optical rotation of $[\alpha]^{23}_{D}$ −10.9 (*c* 0.05, $CHCl_3$). Its molecular formula was assigned as $C_{39}H_{60}O_{11}$ by the deprotonated molecular ion at *m*/*z* 703.4078 $[M\text{-}H]^-$ (calcd for $C_{39}H_{59}O_{11}{}^-$ 703.4063) in HRESIMS. The ^{1}H NMR and ^{13}C-JMOD spectrum showed that compound **2** is a lanostane diester esterified with an acetic acid [δ_H 2.07 s (3H); δ_C 170.84 (CO), 21.07 (CH_3)], and a 3-hydroxy-3-methylglutaryl 6-methyl ester [δ_H 2.68 m, 2.54 m (H_2-2′), 2.70 m, 2.62 m (H_2-5′), 1.35 s (H_3-4′), 3.71 s (OCH_3-7′); δ_C 171.44 (1′), 172.28 (C-6′), 44.99 (C-2′), 45.04 (C-5′), 69.72 (C-3′), 27.70 (C-4′), 51.94 (OCH_3-7′)] (Tables 1 and 2). Similarly to pholiol L (**1**), compound **2** contained the 8,9-en-7-one moiety [δ_C 139.69 (C-8), 160.48 (C-9), 199.71 (C-7)] and C_8 aliphatic chain at C-17 substituted with a keto [δ_C 214.92 (C-24)] and a hydroxy group [δ_C 76.38 (C-25)]. The ^{1}H NMR and JMOD spectra exhibited an additional *O*-substituted methine at δ_H 4.57 br t (5.7 Hz), δ_C 67.31, which was placed at C-11 with regard to the ^{1}H-^{1}H COSY [δ_H 2.28 m, 1.88 m, 4.57 br t; –CH_2–CH(OH)–; C-12–C-11] and HMBC correlations of H-11 with C-8 and C-13; and H-12 with C-14. The assignment of C-11 (δ_C 67.31) and C-12 (δ_C 42.90) were in agreement with literature data [13]. The ^{1}H-^{1}H COSY spectrum defined the structural fragment with correlated protons –CH_2–CH(OR)–CH(OR)– (δ_H 2.87 dd, 1.70 t, 5.29 dt, and 4.83 d) (C-1–C-3). The positions of the ester groups were established via the HMBC experiment. The correlations of the carbonyl signals at δ_C 171.44 (1′) and 170.84 (AcCO) with the proton signals at δ_H 5.29 (H-2) and δ_H 4.83 (H-3) indicated the presence of the MeHMG and acetyl groups at C-2 and C-3, respectively. The relative configuration was determined with the use of a NOESY measurement. The Overhauser effects between H-5/H-3, H-3/H_3-28, H-3/H-1α, and H-1α/H-11 pointed these protons in the α position, while those between H-1β/H-2, H-2/H_3-19, H_3-19/H-1β, and H-2/H_3-29 indicated their β position. The above findings were consistent with the proposed structure of **1**, as depicted in Figure 1.

Table 1. ^{1}H NMR data of pholiols L–Q (**1**–**8**) [(500 MHz, δ ppm (*J* = Hz)].

No.	1 [a]	2 [a]	3 [a,c]	4 [b]	5 [b,c]	6 [b]	7 [b]	8 [a]
1 α	1.44 m	1.70 t (12.1)	2.18 t (11.6)	1.40 m	1.31 m	1.49 m	1.81 m	1.53 t (12.3)
1 β	2.21 dd (12.5, 3.8)	2.87 dd (12.1, 4.1)	2.26 dd (11.6, 4.3)	3.25 dd (13.0, 4.6)	3.23 dd (12.8, 4.6)	2.39 m	2.64 m	2.21 dd (12.5, 4.3)

Table 1. *Cont.*

No.	1 [a]	2 [a]	3 [a,c]	4 [b]	5 [b,c]	6 [b]	7 [b]	8 [a]
2	3.92 dt (3.8, 10.5)	5.29 dt (4.1, 10.9)	5.17 dt (4.3, 10.9)	5.24 dt (4.6, 11.0)	5.14 dt (4.6, 11.0)	5.24 dt (4.3, 10.6)	5.74 dd (13.9, 5.5)	5.19 dt (4.3, 10.9)
3	4.60 d (10.5)	4.83 d (10.9)	4.87 d (10.9)	4.81 d (11.0)	3.28 d (11.0)	4.75 d (10.6)	–	4.83 d (10.9)
5	1.82 m	1.81 m	2.01 m	1.83 dd (14.9, 2.3)	1.75 dd (14.9, 2.2)	1.30 m	1.51 m	1.85 m
6 α	2.42 m (2H)	2.44 m	2.48 m (2H)	2.46 dd (15.7, 2.3)	2.50 dd (15.4, 2.2)	2.14 m (2H)	2.14 m	2.43 m (2H)
6 β		2.54 m		2.66 m	2.71 m		2.34 m	
7	–	–	–	–	–	5.53 t (3.9)	5.59 d (6.7)	–
11 α	2.32 m (2H)	4.57 br t (5.7)		–	–	5.39 d (6.1)	5.49 d (6.1)	2.29 m (2H)
11 β			4.49 m					
12 α	1.79 m (2H)	2.28 m	2.46 m	2.87 d (16.1)	2.90 d (16.2)	2.25 d (17.5)	2.30 d (17.9)	1.78 m (2H)
12 β		1.88 m	1.84 m	2.58 d (16.1)	2.62 d (16.2)	2.14 dd (17.5, 6.1)	2.18 dd (17.9, 6.1)	
15	2.07 m, 1.74 m	2.08 m, 1.83 m	2.08 m, 1,65 m	2.13 m, 1.82 m	2.17 m, 1.82 m	1.66 m, 1.43 m	1.70 m, 1.47 m	2.07 m, 1.73 m
16	2.00 m, 1.37 m	2.04 m, 1.45 m	2.00 m, 1.33 m	2.04 m, 1.46 m	2.08 m, 1.49 m	2.03 m, 1.42 m	2.06 m, 1.45 m	2.00 m, 1.38 m
17	1.42 m	1.43 m	1.55 m	1.76 m	1.80 m	1.63 m	1.66 m	1.43 m
18	0.66 s	0.89 s	0.65 s	0.84 s	0.88 s	0.61 s	0.67 s	0.65 s
19	1.24 s	1.50 s	1.34 s	1.44 s	1.47 s	1.14 s	1.40 s	1.30 s
20	1.40 m	1.43 m	1.36 m	1.44 m	1.49 m	1.44 m	1.45 m	1.43 m
21	0.91 d (6.2)	0.94 d (6.2)	0.91 d (6.3)	0.92 d (7.1)	0.97 d (6.6)	0.93 d (6.6)	0.95 d (6.7)	0.92 d (6.7)
22	1.83 m, 1.31 m	1.83 m, 1.31 m	1,82 m, 1.30 m	1.80 m, 1.25 m	1.82 m, 1.33 m	1.77 m, 1.23 m	1.79 m, 1.26 m	1.85 m, 1.35 m
23	2.52 m (2H)	2.53 m (2H)	2.55 m, 2.49 m	2.68 m (2H)	2.72 m (2H)	2.67 m (2H)	2.67 m (2H)	2.40 m, 2.27 m
26	1.38 s	1.38 s	1.38 s	1.29 s	1.34 s	1.29 s	1.31 s	
27	1.38 s	1.38 s	1.39 s	1.29 s	1.34 s	1.29 s	1.31 s	
28	0.91 s	0.90 s	0.92 s	0.93 s	1.11 s	0.91 s	1.11 s	0.90 s
29	0.96 s	1.03 s	1.01 s	1.04 s	1.00 s	1.03 s	1.26 s	1.00 s
30	0.92 s	0.86 s	1.12 s	0.84 s	1.25 s	0.93 s	0.94 s	0.91 s
2′	2.75 m, 2.57 m	2.68 m, 2.54 m	2.63 m, 2.53 m	2.63 m (2H)	2.78 m, 2.73 m	2.66 m, 2.54 m	2.81 m, 2.74 m	2.67 m, 2.52 m
4′	1.42 s	1.35 s	1.35 s	1.35 s	1.44 s	1.33 s	1.44 s	1.33 s
5′	2.92 m, 2.27 m	2.70 m, 2.62 m	2.68 m, 2.62 m	2.68 m (2H)	2.76 m (2H)	2.54 m, 2.39 m	2.81 m, 2.74 m	2.70 m, 2.61 m
7′	3.72 s	3.71 s	3.71 s	3.67 s	3.73 s	–	–	–
OAc	–	2.07 s		2.06 s		2.06 s	–	2.06 s

[a] measured in $CDCl_3$; [b] in CD_3OD; Signal of H-12 in the ^1H NMR spectrum measured in CD_3OD was 4.48 dd (J = 9.1, 5.5 Hz); [c] measured at 600 MHz.

Table 2. ^{13}C NMR data of pholiols L–Q (**1**–**8**) (125 MHz, δ ppm).

Position	1 [a]	2 [a]	3 [a,c]	4 [b]	5 [b,c]	6 [b]	7 [b]	8 [a]
1	42.78	39.49	39.90	40.51	40.38	42.53	43.71	40.36
2	66.89	69.89	70.36	70.63	73.22	71.13	73.41	70.10
3	84.53	79.44	79.06	80.56	79.83	81.69	210.63	79.18
4	38.98	39.59	39.47	40.23	40.62	40.31	49.01	39.45
5	49.77	50.29	49.75	50.93	51.36	50.41	53.05	49.50
6	36.56	36.57	36.80	37.14	37.39	23.91	24.59	36.44
7	198.29	199.71	199.18	202.76	203.47	121.19	123.19	198.02
8	139.13	139.69	141.71	152.20	152.11	143.87	144.02	139.33
9	164.11	160.48	159.15	151.87	152.11	146.28	145.50	163.27
10	40.68	40.85	40.62	41.54	41.68	39.75	39.50	40.67
11	23.99	67.31	65.55	203.60	203.95	118.31	118.71	23.98
12	30.28	42.90	44.60	52.54	52.52	38.96	38.94	30.10
13	45.13	43.57	44.60	48.58	48.88	44.96	44.82	45.10
14	47.98	49.14	48.26	50.38	50.35	51.54	51.60	47.98
15	32.06	32.15	32.78	33.32	33.30	32.56	32.57	32.02
16	28.82	28.88	27.75	28.13	28.15	28.74	28.75	28.73
17	49.11	48.43	49.93	50.32	50.29	52.29	52.31	48.94
18	15.95	17.45	16.98	17.32	17.22	16.31	16.34	15.95
19	19.89	21.18	21.18	19.07	18.93	23.89	23.20	19.56
20	36.10	36.14	35.96	37.01	37.01	37.13	37.13	36.01
21	18.70	18.76	18.52	18.81	18.80	18.82	18.81	18.51
22	30.19	30.19	30.08	30.84	30.77	31.05	31.04	31.11
23	32.73	32.75	32.69	33.84	33.79	33.97	33.98	31.05
24	215.01	214.92	214.82	217.59	217.92	217.78	217.74	178.71
25	76.34	76.38	76.16	77.89	77.97	77.90	77.90	–
26	26.73	26.75	26.73	26.75	26.73	26.78	26.78	–
27	26.71	26.72	26.73	26.78	26.76	26.75	26.75	–
28	27.99	28.11	27.86	28.43	28.60	28.97	25.32	27.83
29	17.50	17.52	17.36	17.71	17.09	18.25	22.22	17.42
30	25.19	25.28	25.44	26.02	25.98	26.08	26.10	25.16
1′	171.41	171.44	171.66	171.94	172.54	172.17	171.66	171.41
2′	46.33	44.99	45.06	46.32	46.59	47.22	46.76	45.10
3′	70.37	69.72	69.81	70.60	70.94	70.76	71.15	69.70
4′	28.29	27.70	27.75	27.97	27.89	27.80	27.61	27.65
5′	43.68	45.04	45.15	45.96	45.97	47.70	46.79	44.88
6′	173.26	172.28	172.12	173.13	173.44	171.74	171.66	172.24
7′	52.05	51.94	52.00	51.93	51.99			
AcCO		170.84	170.68	172.52	–	172.64		170.75
$AcCH_3$		21.07	21.08	20.96.	–	21.05		21.04

[a] measured in $CDCl_3$; [b] in CD_3OD; [c] measured at 150 MHz.

Compound **3**, named pholiol *n*, was isolated as a white amorphous powder with an optical rotation of $[\alpha]^{23}_{D}$ −8.9 (*c* 0.05, $CHCl_3$). Its molecular composition was determined as $C_{39}H_{60}O_{11}$ based on the sodiated molecular ion peak at *m*/*z* 727.4041 $[M + Na]^+$ (calcd for $C_{39}H_{60}O_{11}Na^+$ 727.4028) detected in the HRESIMS spectrum. Careful evaluation of the 1D and 2D NMR spectra of **3** resulted in the elucidation of the same planar structure as that of compound **2**. The main differences were found in the chemical shift values of carbons C-11–C-12 [δ_C 65.55 (C-11), 44.40 (C-12) for **3**; δ_C 67.31 (C-11), 42.90 (C-12) for **2**], indicating that the orientation of 11-OH group may be different. This was confirmed by the NOESY correlations of **3**; the Overhauser effects between H_3-18 (δ_H 0.65 s) and H-12β (δ_H 2.46 m); H-12β and H-11 (δ_H 4.49 m); H-12α (δ_H 1.84 m) and H_3-30 (δ_H 1.12 s) proved the α position of the 11-hydroxy group. NOEs of H-2 with H_3-19 and H_3-28; and that of H-3 with H_3-29; H_3-18 with H-20 corroborated the stereostructure of compound **3**, as depicted in Figure 1.

Compound **4**, named pholiol O, was obtained as a colorless amorphous solid with an optical rotation of $[\alpha]^{27}_{D}$ +11.8 (*c* 0.05, $CHCl_3$). It gave the molecular formula $C_{39}H_{58}O_{11}$, determined from the HRESIMS by the sodiated molecular ion peak at *m*/*z* 725.3877 $(M + Na)^+$, (calcd for $C_{39}H_{58}O_{11}Na^+$ 725.3871). Analysis of ^{1}H NMR and ^{13}C-JMOD spectra of **4** indicated the presence of the same esterification pattern and aliphatic chain at C-17 as in compound **2** (Tables 1 and 2). The main differences were the remarkable difference in chemical shifts of C-8 (**2**: δ_C 139.69; **4**: δ_C 152.20), and C-9 (**2**: δ_C 160.48; **4**: δ_C 151.87), and the presence of an additional keto group (δ_C 203.60) at C-11 in compound **4**. The position of this keto group was established based on its HMBC correlations with H_2-12 [δ_H 2.87 d, 2.58 d (*J* = 16.1 Hz)]. NOESY correlations between H-3 and H-5, and H_3-28, H-1α; between H-2 and H-1β, and H_3-19; between H-12β and H_3-18; between H-12α and H-30; and between H-30 and H-20 allowed the stereochemical features identical with those of compounds **1** and **2** to be assigned for **4** (Figure 1).

Compound **5** (pholiol *p*) was obtained as a white amorphous solid with an optical rotation of $[\alpha]^{23}$ −1.6 (*c* 0.05, MeOH). Its molecular formula was deduced to be $C_{39}H_{56}O_{10}$ from HRESIMS sodium adduct ion peak at *m*/*z* 683.3767 $[M + Na]^+$ (calcd for $C_{37}H_{56}O_{10}Na^+$ 683.3766). Comprehensive analysis of ^{1}H NMR, ^{13}C JMOD and 2D NMR data of **4** and **5** indicated the presence of the same 2,3,25-trihydroxy-7,11,24-triketo-triterpene core and MeHMG esterification at C-2 as discussed at compound **4**, with the exception of the acetoxy group at C-3, which was replaced by a hydroxy group. This was clearly shown by the H-3 signal at δ_H 3.28 d (*J* = 11.0 Hz) for **5**, instead of H-3 at δ_H 3.28 d (*J* = 11.0 Hz) for **4** (Tables 1 and 2). NOESY correlations between H-2/H_3-19, H-3/H_3-28, H-11α/H_3-30, and H_3-28/H-6α permitted the same stereochemistry of **5** as that of **4**.

Compound **6**, pholiol Q, was isolated as a colorless amorphous solid with an optical rotation of $[\alpha]^{27}_{D}$ +5.0 (*c* 0.1, MeOH). Its molecular formula was determined to be $C_{38}H_{58}O_9$ based on the HRESIMS ion peak at *m*/*z* 657.4010 $[M–H]^-$ (calcd for $C_{38}H_{57}O_9^-$, 657.4008). Analysis of ^{1}H NMR and ^{13}C–JMOD as well as 2D NMR data demonstrated the presence of a 3-hydroxy-3-methyl glutarate and an acetate group in **6**, and the same side chain at C-17 as in pholiols L–N (**1**–**5**) (Tables 1 and 2). NMR signals of **6** at δ_H 5.53 t (H-7) and 5.39 d (H-11), and δ_C 121.19 (C-7), 143.87 (C-8), 146.28 (C-9), 118.31 (C-11) suggested two trisubstituted olefin groups which were placed at C-7–C-8, and C-9–C-11 considering the HMBC correlations of C-9 with H-7, H-12b, H-1b, H_3-19, and those of C-8 with H-11, H-6, and H_3-30. NOESY cross-peaks between H-2/H_3-29, H-2/H-1β, H-1β/H_3-19, H-3/H-1α, and H_3-30/H-17 afforded the same stereochemical assignment of compound **6** as that of **1**–**5**.

Compound **7**, pholiol R, was isolated as a white amorphous solid with an optical rotation of $[\alpha]^{22}_{D}$ +24.9 (*c* 0.05, MeOH). Its HRESIMS spectrum exhibited a molecular ion peak at *m*/*z* 613.3768 $[M–H]^-$ (calcd for $C_{36}H_{53}O_8^-$, 613.3746) indicating the molecular formula of $C_{36}H_{54}O_8$. ^{1}H and ^{13}C NMR assignments of **7**, prepared by analysis of the ^{1}H-^{1}H COSY, HSQC and HMBC spectra, showed that chemical shifts of **7** were very similar to that of **6** differing only in the resonances of ring A protons and carbons (Tables 1 and 2). In case of **7** a carbonyl group (δ_C 210.63) can be found at position C-3, as it was confirmed by the

HMBC correlation between C-3 and H_3-28 and H_3-29. Cross-peaks in the NOESY spectrum of **7** between H-2/H_3-29, H-2/H_3-19, H-20/H_3-18, H_3-30/H-17, H-5/H_3-28, H-5/H-6α, and H-6β/H-19 were in agreement with the stereostructure of **7**, as depicted in Figure 1.

Compound **8** (pholiol S) was a colorless amorphous solid and had an optical rotation of $[\alpha]^{23}_{D}$ −14.2 (*c* 0.1, $CHCl_3$). Its HRESIMS spectrum exhibited sodium adduct ion peak at 669.3623 $[M + H]^+$ (calcd for $C_{36}H_{54}O_{10}Na^+$ 669.3609), indicating the molecular formula of $C_{36}H_{54}O_{10}$. The ^{1}H NMR and ^{13}C JMOD spectra evidenced the presence of one acetate and one 3-hydroxy-3-methylglutaryl 6-methyl ester group in the molecule, and a 27 carbon atom containing basic skeleton (Tables 1 and 2). The chemical shifts of skeletal protons and carbons were very similar to those of pholiol B [11], with exception of the resonances of the C-17 side chain. The ^{1}H-^{1}H COSY spectrum of **8** indicated a structural fragment with correlated protons at δ_H 1.43 m, 0.92 d (3H), 1.85 m, 1.35 m, 2.40 m, 2.27 m [–CH(CH_3)–CH_2–CH_2–] which was assigned as C-20–C-23 part of **8**. This structural fragment was coupled with a carboxyl group (δ_C 178.71, C-24) with help of its HMBC correlations with H_2-22 (δ_H 1.85 m), and H_2-23 (δ_H 2.40 m, 2.27 m), and connected to C-17 as showed by the long-range correlation of C-17 (δ_C 48.94) with H_3-21 (δ_H 0.92 d). NOESY correlations between H-2/H_3-29, H-2/H_3-19, H-2/H-1β, H-3/H_3-28, H-3/H-1α, H_3-19/H-1β, and H_3-18/H-20 proved the stereochemistry of compound **8**, as shown in Figure 1.

2.2. Evaluation of the Antiproliferative and Cytotoxic Activity of the Isolated Compounds

The compounds isolated in good yield, such pholiols L, M, O, Q, and S (**1**, **2**, **4**, **6**, and **8**), were investigated for their antiproliferative activity in vitro by MTT assay in human colon adenocarcinoma cell lines, both sensitive (Colo 205) and resistant (Colo 320) ones, hormone-responsive breast cancer (MCF-7), human non-small cell lung cancer (A549), and human embryonic lung fibroblast cell line (MRC-5). The anticancer drug doxorubicin was used as a reference agent. The results, obtained as the concentration of the compound that produced half of the inhibition (IC_{50}), are shown in Table 3. The highest antiproliferative effects were observed for pholiols M (**2**) and O (**4**) against the MCF-7 cell line, with IC_{50} values of 2.48 and 9.95 μM, respectively. These compounds were also potent against Colo 205 cells, but to a lower extent [IC_{50} 23.91 (**2**), and 23.30 μM (**4**)], while pholiol L (**1**) was moderately active on the MRC-7 cell line (IC_{50} 21.74 μM). Structurally, compounds **2** and **4** are lanostane triterpenes with 2,3-diester-7-on-8 (9)-en functionalities, with a further 11-keto (**4**) or 12-hydroxy group (**2**). All other compounds exhibited weaker activity on the viability of the treated cancer cells, displaying IC_{50} values ranging from 28.07 to 89.84 μM. Compounds **1**, **2**, **4**, **6**, and **8** were tested for their antiproliferative activity in the non-cancerous human embryonic lung fibroblast cell line as well, and on the basis of these results, selectivity indexes (SI) were calculated. The SI values of pholiol M (**2**) > 40 and 4.18 indicated its strong and moderate tumor cell selectivity regarding the MCF-7 and Colo 205 cell lines, respectively, whereas SI values of 4.3 and 1.8 of pholiol O (**4**) indicated this compound to be moderately or slightly selective towards Colo 205 cells [14]. Compounds **1**, **6**, and **8** did not display selectivity to cancerous cell lines over normal cells.

The direct cytotoxic effects of the compounds were determined similarly by MTT assay on the Colo 205, Colo 320, MCF-7, A549, and MRC-5 cell lines, using a higher cell population and a shorter exposure than in the antiproliferative test. Under these conditions, the direct killing effect can be measured instead of the cell growth inhibitory activity. Significant difference between the antiproliferative and cytotoxic effects displayed selectivity for the growing cell population without directly killing the exposed cells. Such a result was exhibited by pholiols M (**2**) and O (**4**), for which, no cytotoxic effect could be detected on MCF-7 cells (IC_{50} > 100 μM), proving their action exclusively on tumor cell proliferation. Considering all other compounds and cell lines, moderate cytotoxic activities were measured with IC_{50} from 31.52 to over 100 μM (Table 4).

Table 3. Antiproliferative activity (IC_{50} μM) of pholiols L, M, O, Q, and S (**1**, **2**, **4**, **6**, and **8**) in human sensitive (Colo 205) and resistant (Colo 320) colon adenocarcinoma cells. and normal embryonal fibroblast (MRC-5) cell line.

Compd.	Colo 205		Colo 320		MCF-7		A549		MRC-5	
	Mean	SD	Mean	SD	Mean	SD	Mean	SD	Mean	SD
1	32.41	0.89	28.07	4.62	**21.74**	0.88	53.73	1.27	70.86	1.22
2	**23.91**	0.026	32.51	2.97	**2.48**	0.16	>100	–	>100	–
4	**23.39**	0.060	42.14	0.15	**9.95**	0.37	51.53	1.61	42.89	1.34
6	49.97	0.52	69.19	2.67	46.28	1.86	51.21	1.04	>100	–
8	59.87	0.55	68.54	4.40	35.33	3.03	89.84	0.75	>100	–
Dox	0.0617	0.0128	0.25	0.06	0.155	0.0027	1.04	0.097	0.52	0.018
DMSO	>2%	–	>2%	–	>2%	–	>2%	–	>2%	–

Dox = doxorubicin.

Table 4. Cytotoxic activity in human sensitive (Colo 205) and resistant (Colo 320) colon adenocarcinoma cells and relative resistance ratio of pholiols L, M, O, Q, and S (**1**, **2**, **4**, **6**, and **8**).

Compd.	IC_{50} (μM)				RR [a]	IC_{50} (μM)					
	Colo 205 (A)		Colo 320 (B)		(B/A)	MCF-7		A549		MRC-5	
	Mean	SD	Mean	SD		Mean	SD	Mean	SD	Mean	SD
1	40.33	1.64	33.92	1.84	**0.84**	43.69	0.03	93.61	1.94	66.08	1.36
2	35.93	0.44	67.22	3.86	1.87	>100	–	58.12	0.70	>100	–
4	31.52	0.91	91.52	4.96	2.90	>100	–	56.86	1.53	57.99	0.82
6	56.12	0.84	34.73	1.24	**0.62**	43.78	0.18	85.88	2.41	>100	–
8	57.50	0.96	57.52	2.36	1.0	42.99	0.61	83.65	6.06	55.27	0.41
Dox	3.32	0.083	11.96	0.88	3.60	5.73	1.02	10.22	0.07	3.60	0.35
DMSO	>2%	–	>2%	–		>2%	–	>2%	–	>2%	–

[a] RR (relative resistance ratio) = IC_{50} resistant/IC_{50} sensitive; Dox = doxorubicin

Comparison of the cytotoxic activities on drug-resistant (Colo 320) and sensitive (Colo 205) cells allowed for the detection of relative resistance (RR), which was calculated as the ratio of the IC_{50} value in the resistant and in sensitive cancer cell lines. Compounds with RR < 1 show selectivity against resistant cells, whereas RR $\leq$ 0.5 means that the compounds have a collateral sensitivity (CS) effect [15]. The calculated RR values of the tested compounds showed selectivity against the resistant Colo 320 cells of pholiols L (**1**) (RR 0.84) and Q (**8**) (RR 0.62) (Table 4).

3. Materials and Methods

3.1. General Experimental Procedures

The optical rotations were determined using a JASCO *p*-2000 polarimeter (JASCO International, Co., Ltd., Hachioji, Tokyo, Japan). High-resolution mass spectrometry (HRMS) was performed on a Thermo Velos Pro Orbitrap Elite (Thermo Fisher Scientific, Bremen, Germany) instrument, using electron spray ionization (ESI) method, operating in the positive or negative ion mode. The (de)protonated molecular ion peaks were fragmented by the collision-induced dissociation method (CID) at a normalized collision energy of 35%. Helium was used as a collision gas in the CID experiments. The data were acquired and processed with MassLynx software. NMR spectra were recorded in $CDCl_3$ or CD_3OD on a Bruker Avance DRX 500 spectrometer (Bruker, Billerica, MA, USA) at 500 MHz (^1H) and 125 MHz (^{13}C). The signals of the deuterated solvents were taken as references. Two-dimensional (2D) NMR measurements were carried out with standard Bruker software. In the COSY, HSQC, and HMBC experiments, gradient-enhanced versions were applied. Flash chromatography (FC) was performed on a CombiFlash Rf+ Lumen instrument with integrated UV, UV–Vis, and ELS detection using normal phase (silica 60, 0.045–0.063 mm, Molar Chemicals, and RediSep Rf Gold, Teledyne Isco, Lincoln NE, USA) flash column. Sephadex LH-20 (25–100 μm, Sigma-Aldrich, MO, USA) was employed for

gel filtration (GF). Reversed-phase HPLC (RP-HPLC) and normal-phase HPLC (NP-HPLC) separations were carried out on a Shimadzu LC-10 A S HPLC instrument equipped with a UV–Vis detector (Shimadzu, Co., Ltd., Kyoto, Japan) over reversed-phase (RP-HPLC, LiChrospher RP-18, 5 µm, 250 × 4 mm) and normal-phase (NP-HPLC, LiChrospher Si60, 5 µm, 250 × 4 mm) columns, respectively. Preparative thin-layer chromatography (Prep TLC) was conducted using silica plates (20 × 20 cm silica gel 60 F_{254}, Merck 105,554). Sigma-Aldrich Kft. (Budapest, Hungary) and Molar Chemicals (Halásztelek, Hungary) provided the chemicals used in this research.

3.2. Mushroom Material

Sporocarps of *Pholiota populnea* (Pers.) Kuyper & Tjall–Beuk. (*Strophariaceae*) were gathered in the autumn of 2017 near Szeged, Hungary (46.400556, 20.190556). The samples were identified by Attila Sándor (Mushroom Society of Szeged, Hungary) and stored at −20 °C until processing. A voucher specimen was deposited at the Institute of Pharmacognosy, University of Szeged, Szeged, Hungary (No. H019).

3.3. Extraction and Isolation

The fresh mushroom material (4.2 kg) was ground in a blender and then percolated with MeOH (20 L) at room temperature. After concentration, the dry residue (151 g) was dissolved in 600 mL of 50% aqueous MeOH and subjected to solvent–solvent partition with *n*-hexane (5 × 500 mL), $CHCl_3$ (5 × 500 mL), and then EtOAc (5 × 500 mL). The chloroform-soluble phase (7 g) was subjected to gel filtration (GF) on Sephadex LH-20, using dichloromethane–methanol (1:1) as a mobile phase, providing 10 fractions (F1-10). The combined fractions F5 (780 mg) and F6 (320 mg) were further separated by flash chromatography (NP-FC) on silica gel (12 g) using an *n*-hexane–acetone gradient system (linear from 0% to 100% acetone, t = 65 min), and at the end, MeOH for 8 min. Fractions with similar compositions were combined based on TLC monitoring (G1-21). Fraction G12 (161 mg) was separated by RP-HPLC with H_2O- MeCN (25:75) as mobile phase, which resulted in 5 fractions (K1-5). Purification of fraction K2 (54.6 mg) was conducted by NP-HPLC using a cyclohexane–ethyl acetate (25:75) solvent system to isolate compounds **1** (8.2 mg), **8** (8.3 mg), and to obtain 3 other subfractions (L1-3). Subfraction L1 (5.6 mg) was purified by NP-HPLC (mobile phase: cyclohexane–EtOAc, 15:50) to yield compound **2** (2 mg). Subfraction L3 (15 mg) was further purified by RP-HPLC, applying an isocratic system of H_2O-MeOH (28:72), which led to the isolation of compound **3** (1.1 mg) and compound **5** (1.2 mg). Compound **6** (7.9 mg) was obtained by further purification of fraction K4 (8.8 mg) via preparative Prep TLC, using *n*-hexane–acetone (1:1) as developing system. Fraction G11 (250 mg) was first separated by HPLC (mobile phase: H_2O-MeOH, 20:75) on a LiChrospher RP18 column, affording 3 subfractions (M1-3). RP-HPLC was applied for the final purification of M2 (10.3 mg) by using a H_2O–MeOH (20:80) solvent system to yield compound **4** (1.2 mg). In our previous work [12] on *P. populnea*, fraction EA3 (370 mg) was obtained from the ethyl acetate phase using multiple steps of chromatographic methods. Fraction EA3 (370 mg) was further separated by NP-HPLC using cyclohexane–EtOAc (2:8) as mobile phase, and 3 subfractions (EA3a-c) were yielded. Compound **7** (1.2 mg) was isolated from fraction EA3a (90 mg) by RP-HPLC, using a linear gradient system of H_2O–MeOH from 75% to 95% MeOH, and then an isocratic system of H_2O–MeOH (10:90).

3.4. Spectroscopic and Physical Characteristic of Compounds

Pholiol L (**1**) colorless amorphous solid; $[\alpha]^{23}_D$ −11.6 (*c* 0.1, $CHCl_3$); for ^1H and ^{13}C NMR spectroscopic data, see Tables 1 and 2; HRESIMS *m*/*z* 647.4147 $[M + H]^+$ (calcd for $C_{37}H_{59}O_9^+$ 647.4154).

Pholiol M (**2**) colorless amorphous solid; $[\alpha]^{23}_D$ −10.9 (*c* 0.05, $CHCl_3$); for ^1H and ^{13}C NMR spectroscopic data, see Tables 1 and 2; HRESIMS *m*/*z* 703.4078 $[M-H]^-$ (calcd for $C_{39}H_{59}O_{11}^-$ 703.4063).

Pholiol N (**3**) white amorphous powder; $[\alpha]^{23}_{D}$ −8.9 (*c* 0.05, $CHCl_3$); for ^{1}H and ^{13}C NMR spectroscopic data, see Tables 1 and 2; HRESIMS *m*/*z* 727.4041 $[M + Na]^+$ (calcd for $C_{39}H_{60}O_{11}Na^+$ 727.4028).

Pholiol O (**4**) colorless amorphous solid; $[\alpha]^{27}_{D}$ +11.8 (*c* 0.05, $CHCl_3$); for ^{1}H and ^{13}C NMR spectroscopic data, see Tables 1 and 2; HRESIMS *m*/*z* 725.3877 $(M + Na)^+$, (calcd for $C_{39}H_{58}O_{11}Na^+$ 725.3871) and 703.4063 $[M + H]^+$ (calcd for $C_{39}H_{59}O_{11}{}^+$ 703.4052).

Pholiol *p* (**5**) white amorphous powder; $[\alpha]^{23}$ −1.6 (*c* 0.05, MeOH); for ^{1}H and ^{13}C NMR spectroscopic data, see Tables 1 and 2; HRESIMS *m*/*z* 683.3767 $[M + Na]^+$ (calcd for $C_{37}H_{56}O_{10}Na^+$ 683.3766).

Pholiol Q (**6**) colorless amorphous solid; $[\alpha]^{27}_{D}$ +5.0 (*c* 0.1, MeOH); for ^{1}H and ^{13}C NMR spectroscopic data, see Tables 1 and 2; HRESIMS *m*/*z* 657.4010 $[M–H]^-$ (calcd for $C_{38}H_{57}O_9{}^-$, 657.4008).

Pholiol R (**7**) colorless white amorphous solid; $[\alpha]^{22}_{D}$ +24.9 (*c* 0.05, MeOH); for ^{1}H and ^{13}C NMR spectroscopic data, see Tables 1 and 2; HRESIMS *m*/*z* 613.3768 $[M–H]^-$ (calcd for $C_{36}H_{53}O_8{}^-$ 613.3746).

Pholiol S (**8**) colorless amorphous solid; $[\alpha]^{23}_{D}$ −14.2 (*c* 0.1, $CHCl_3$); for ^{1}H and ^{13}C NMR spectroscopic data, see Tables 1 and 2; HRESIMS *m*/*z* 669.3623 $[M + Na]^+$ (calcd for $C_{36}H_{54}O_{10}Na^+$ 669.3609).

3.5. Cytotoxic and Antiproliferative Assays

Cell Line Cultures: The human colon adenocarcinoma cell lines, Colo 205 (ATCC-CCL-222) doxorubicin-sensitive parent and Colo320/MDR-LRP (ATCC-CCL-220.1) doxorubicin resistant expressing ABCB1, were purchased from LGC Promochem (Teddington, UK). The cells were cultured in RPMI-1640 medium supplemented with 10% heat-inactivated fetal bovine serum (FBS), 2 mM L-glutamine, 1 mM Na-pyruvate, 100 mM HEPES. The MRC-5 (ATCC CCL-171) human embryonic lung fibroblast cell line and the hormone-responsive breast cancer cell line MCF-7 (ATCC HTB-22) were purchased from Sigma-Aldrich (Merck KGaA, Darmstadt, Germany). The MCF-7 and MRC-5 cells were cultured in Eagle's Minimal Essential Medium (EMEM) containing 4.5 g/L of glucose and supplemented with a non-essential amino acid mixture, a selection of vitamins, and 10% FBS. The cell lines were incubated at 37 °C, 5% CO_2, and 95% air atmosphere. The cells were detached with Trypsin-Versene (EDTA) solution for 5 min at 37 °C. The human non-small cell lung cancer cell line A549 was kindly provided by Brigitte Marian (Institute of Cancer Research, Department of Medicine I, Medical University of Vienna, Austria). A549 cells were grown in Eagle's Minimal Essential Medium (EMEM) supplemented with 10% heat-inactivated fetal bovine serum.

Antiproliferative Assays: The antiproliferative effect of the compounds was tested in decreasing serial dilutions of compounds (starting with 100 µM, then two-fold serial dilution) on human cell lines (Colo 205, Colo 320, MCF-7, A549, and MRC-5) in 96-well flat-bottomed microtiter plates. Firstly, the compounds were diluted in 100 µL of the medium, and then, 6×10^3 cells (Colo 205, Colo 320) in 100 µL of RPMI medium were added to each well, excluding the medium control wells. The adherent MCF-7, A549, and MRC-5 cells (6×10^3 cells/well) were seeded in EMEM medium for at least 4 h before the assay. The two-fold serial dilutions of the compounds were made in a separate plate (100–0.19 µM) and then transferred to the plates containing the adherent-corresponding cell line. Culture plates were incubated at 37 °C for 72 h, and at the end of the incubation period, 20 µL of MTT (thiazolyl blue tetrazolium bromide) solution (from a 5 mg/mL stock solution) was added to each well and incubated for an additional 4 h. Then, 100 µL of sodium dodecyl sulfate (SDS) solution (10% SDS in 0.01 M HCl) was added to each well, and the plates were further incubated at 37 °C overnight in a CO_2 incubator. Cell growth was determined by measuring the optical density (OD) at 540/630 nm with a Multiscan EX ELISA reader (Thermo Labsystems, Cheshire, WA, USA). The percentage of inhibition of cell growth was determined according to Equation (1), and expressed as IC_{50} values, defined as the concentration that induces 50% growth inhibition. IC_{50} values and the

standard deviation (SD) of triplicate experiments were calculated using GraphPad Prism 5 software for Windows. Doxorubicin (2 mg/mL, Teva Pharmaceuticals, Budapest, Hungary) was used as a positive control and the vehicle DMSO as the negative control (Table 3).

$$IC_{50} = \left[\frac{OD_{sample} - OD_{medium\ control}}{OD_{cell\ control} - OD_{medium\ control}} \right] \times 100 \quad (1)$$

Assay for Cytotoxic Effect: The effects of increasing concentrations of the compounds on cell growth were tested in 96-well flat-bottomed microtiter plates, as described for the antiproliferative assay, using 1×10^4 cells/well. The culture plates were incubated at 37 °C for 24 h; at the end of the incubation period, 20 µL of MTT solution (from a 5 mg/mL stock solution) was added to each well. After incubation at 37 °C for 4 h, 100 µL of sodium dodecyl sulfate (SDS) solution (10% SDS in 0.01 M HCl) was added to each well, and the plates were further incubated at 37 °C overnight. Cell growth was determined by measuring the optical density (OD) at 540 nm (ref 630 nm) with a Multiscan EX ELISA reader (Thermo Labsystems, Cheshire, WA, USA). Inhibition of cell growth was expressed as IC_{50} (Table 4).

Sample preparation: The compounds were dissolved in DMSO to achieve the final concentration of 5 mM. The starting concentration of the compounds was 100 µM and 2-fold serial dilutions were prepared for the antiproliferative and cytotoxic assays. The following concentrations were used: 100-50-25-12.5-6.25-3.125-1.56-0.78-0.39-0.195 µM.

Supplementary Materials: The following supporting information can be downloaded at: https://www.mdpi.com/article/10.3390/ph16010104/s1, Figures S1–S56: NMR and MS spectra.

Author Contributions: Conceptualization, A.V. and J.H.; methodology, M.Y., A.B., A.H. and R.B.; validation, G.S. and J.H.; formal analysis, J.H.; investigation, M.Y., A.B., A.H., G.S. and R.B.; resources, J.H.; writing—original draft preparation, J.H.; writing—review and editing, G.S., A.V. and J.H.; All authors have read and agreed to the published version of the manuscript.

Funding: This work was supported by the National Research, Development and Innovation Office, Hungary (TKP2021-EGA-32 by the Ministry of Innovation and Technology of Hungary).

Institutional Review Board Statement: Not applicable.

Informed Consent Statement: Not applicable.

Data Availability Statement: Data are contained within the article and Supplementary Materials.

Conflicts of Interest: The authors declare no conflict of interest.

References

1. Ayeka, P.A. Potential of mushroom compounds as immunomodulators in cancer immunotherapy: A review. *Evid. Based Complement. Altern. Med.* **2018**, *2018*, 7271509. [CrossRef]
2. Park, H.J. Current uses of mushrooms in cancer treatment and their anticancer mechanisms. *Int. J. Mol. Sci.* **2022**, *23*, 10502. [CrossRef]
3. Ikekawa, T. Beneficial effects of edible and medicinal mushrooms on health care. *Int. J. Med. Mushrooms* **2001**, *3*, 1–8. [CrossRef]
4. Zhou, J.; Gong, J.; Chai, Y.; Li, D.; Zhou, C.; Sun, C.; Regenstein, J.M. Structural analysis and in vitro antitumor effect of polysaccharides from Pholiota adiposa. *Glycoconj. J.* **2022**, *39*, 513–523. [CrossRef] [PubMed]
5. Zhang, Y.; Zhang, Y.; Gao, W.; Zhou, R.; Liu, F.; Ng, T.B. A novel antitumor protein from the mushroom Pholiota nameko induces apoptosis of human breast adenocarcinoma MCF-7 cells in vivo and modulates cytokine secretion in mice bearing MCF-7 xenografts. *Int. J. Biol. Macromol.* **2020**, *164*, 3171–3178. [CrossRef] [PubMed]
6. Daba, A.S.; Ezeronye, O.U. Anti-cancer effect of polysaccharides isolated from higher basidiomycetes mushrooms. *Afr. J. Biotechnol.* **2003**, *2*, 672–678.
7. Min, B.-S.; Gao, J.-J.; Nakamura, N.; Hattori, M. Triterpenes from the spores of Ganoderma lucidum and their cytotoxicity against Meth-A and LLC tumor cells. *Chem. Pharm. Bull.* **2000**, *48*, 1026–1033. [CrossRef] [PubMed]
8. Hsu, S.-C.; Ou, C.-C.; Li, J.-W.; Chuang, T.-C.; Kuo, H.-P.; Liu, J.-Y.; Chen, C.-S.; Lin, S.-C.; Su, C.-H.; Kao, M.-C. Ganoderma tsugae extracts inhibit colorectal cancer cell growth via G2/M cell cycle arrest. *J. Ethnopharmacol.* **2008**, *120*, 394–401. [CrossRef] [PubMed]

9. Takaku, T.; Kimura, Y.; Okuda, H. Isolation of an antitumor compound from Agaricus blazei Murill and its mechanism of action. *J. Nutr.* **2001**, *131*, 1409–1413. [CrossRef] [PubMed]
10. Yaoita, Y.; Kikuchi, M.; Machida, K. Terpenoids and sterols from some Japanese mushrooms. *Nat. Prod. Commun.* **2014**, *9*, 419–426. [CrossRef] [PubMed]
11. Yazdani, M.; Béni, Z.; Dékány, M.; Szemerédi, N.; Spengler, G.; Hohmann, J.; Ványolós, A. Triterpenes from Pholiota populnea as cytotoxic agents and chemosensitizers to overcome multidrug resistance of cancer cells. *J. Nat. Prod.* **2022**, *85*, 910–916. [CrossRef] [PubMed]
12. Yazdani, M.; Barta, A.; Berkecz, R.; Agbadua, O.G.; Ványolós, A.; Hohmann, J. Pholiols E–K, lanostane-type triterpenes from Pholiota populnea with anti-inflammatory properties. *Phytochemistry* **2023**, *205*, 113480. [CrossRef] [PubMed]
13. Zhao, Z.Z.; Chen, H.P.; Huang, Y.; Li, Z.H.; Zhang, L.; Feng, T.; Liu, J.K. Lanostane triterpenoids from fruiting bodies of Ganoderma leucocontextum. *Nat. Prod. Bioprospect.* **2016**, *6*, 103–109. [CrossRef] [PubMed]
14. Acton, E.M.; Narayanan, V.L.; Risbood, P.A.; Shoemaker, R.H.; Vistica, D.T.; Boyd, M.R. Anticancer specificity of some ellipticinium salts against human brain tumors in vitro. *J. Med. Chem.* **1994**, *37*, 2185–2189. [CrossRef] [PubMed]
15. Hall, M.D.; Handley, M.D.; Gottesman, M.M. Is resistance useless? Multidrug resistance and collateral sensitivity. *Trends Pharmacol. Sci.* **2009**, *30*, 546–556. [CrossRef] [PubMed]

IV.

Journal of Research in Pharmacy

Research Article

www.jrespharm.com

Isolation and characterization of chemical constituents from the mushroom *Clitocybe nebularis*

Morteza YAZDANI [1], Zoltán BÉNI [2], Miklós DÉKÁNY [2], Viktor PAPP [3], Andrea LÁZÁR [5], Katalin BURIÁN [5], Judit HOHMANN [1,4]*, Attila VÁNYOLÓS [1,6]

1 Department of Pharmacognosy, Interdisciplinary Excellence Centre, University of Szeged, H-6720 Szeged, Hungary.
2 Spectroscopic Research Department, Gedeon Richter Plc., Gyömrői út 19-21, H-1103 Budapest, Hungary.
3 Department of Botany, Szent István University, H-1118 Budapest, Villányi út 29-43, Hungary.
4 Interdisciplinary Centre of Natural Products, University of Szeged, H-6720 Szeged, Hungary.
5 Department of Clinical Microbiology, University of Szeged, H-6720 Szeged, Hungary.
6 Department of Pharmacognosy, Semmelweis University, H-1085 Budapest, Hungary.
* Corresponding Author. E-mail: hohmann@pharm.u-szeged.hu (J.H.); Tel. +36-62-545 558.

Received: 26 July 2020 / Revised: 31 August 2020 / Accepted: 11 September 2020

ABSTRACT: In the course of our mycochemical studies the extract of *Clitocybe nebularis* was investigated with the aim to identify its bioactive secondary metabolites. Multistep chromatographic purification of the MeOH extract of *C. nebularis* resulted in the isolation of two steroids and an organic acid from the $CHCl_3$ and ethyl acetate soluble fractions. The structures of the compounds were determined by NMR and MS spectroscopy as 5α-ergosta-7,22-diene-3β,5,6β-triol (cerevisterol) (**1**), (22*E*,24*S*)-5α-ergosta-7,22-diene-3β,5,6β,9α-tetraol (**2**), and indole-3-carboxylic acid (**3**). The antimicrobial activity of the compounds was analyzed by agar disc diffusion method against human pathogen strains of *Streptococcus agalactiae, Staphylococcus epidermidis*, *Moraxella catarrhalis*, *Haemophilus influenzae*, and *Proteus mirabilis*. The susceptibility assay revealed that compounds **2** and **3** have weak antimicrobial activity against *M. catarrhalis*. The current study represents the first isolation of compounds **1–3** from *C. nebularis*.

KEYWORDS: *Clitocybe nebularis*; steroids; antimicrobial activity; Tricholomataceae.

1. INTRODUCTION

Edible and even toxic mushrooms are a valuable source of therapeutically important or nutritive compounds. Many mushroom species were reported to produce a large variety of secondary metabolites with unique chemical structures and interesting biological activities. *Clitocybe nebularis* (Batsch) P. Kumm. [syn.: *Lepista nebularis* (Fr.) Harmaja] known as clouded agaric or cloud funnel, member of the family Tricholomataceae is a common species of both conifer and broad-leaved forests in temperate and hemiboreal zones across Europe and North America [1]. *C. nebularis* is generally considered edible, but the strong, aromatic odor dissuades some people and can cause upset after consuming [2,3]. Pharmacological investigations revealed the neuroprotective, antioxidant, antimicrobial and cytotoxic properties of the acetone extract of *C. nebularis* [4] and demonstrated its significant antiproliferative and cytotoxic activities [5,6].

Previously various types of bioactive compounds have been reported from sporocarps of *C. nebularis*. Nebularine a purine riboside with bacteriostatic activity was the first biologically active compound isolated and identified from this mushroom [7]. Besides its antimicrobial activity nebularine displayed a noncompetitive inhibitory effect on xanthine oxidase [8], and possessed plant cytotoxic [9], antifungal and antibacterial properties [10,11]. In addition to nebularine, phenylacetic acid, purine, uridine, adenine, uracil, benzoic acid, and mannitol were also isolated [10]. Clitocypin, the inhibitor of cysteine proteinases has been identified in fruit bodies of *C. nebularis*, and its structure has been determined to have single protein sequence of 150 amino acids [12]. Small and stable proteins named *Clitocybe nebularis* lectin (CNL) were identified in the fruiting bodies along with several similar isolectins. CNL is a β-trefoil type lectin forming homodimers, which displays a remarkable immunostimulation of human dendritic cells, producing a strong T helper cell type 1 response. CNL therefore can be regarded as a promising candidate for different applications in medicine [13].

How to cite this article: Yazdani M, Béni Z, Dékány M, Papp V, Lázár A, Burián K, Hohmann J, Ványolós A. Isolation and characterization of chemical constituents from the mushroom *Clitocybe nebularis*. J Res Pharm. 2020; 24(6): 908-913.

ISSN: 2630-6344

https://doi.org/10.35333/jrp.2020.250

The recently identified β-trefoil protein cnispin with protease inhibitory potency proved to be highly specific for trypsin [14]. The examination of free amino acids, fatty acids and sterols of *C. nebularis* revealed that the most abundant free amino acids are alanine, proline, serine and valine, while among fatty acids linoleic and palmitic acids predominated. The presence of ergosterol as the main sterol was also demonstrated [15]. Volatile compounds of *C. nebularis* were analyzed by GC-MS and 1-octen-3-ol and linalool were identified as key components [16].

The major objective of the present study was to identify the characteristic lipophilic secondary metabolites of *C. nebularis* and determine their antimicrobial activity.

2. RESULTS AND DISCUSSION

Mycochemical investigation of the chloroform ($CHCl_3$) and ethyl acetate (EtOAc) phases of the methanolic (MeOH) extract of *C. nebularis* resulted in the identification of three compounds (**1–3**) (Figure 1). Identification of the isolated compounds was carried out by 1D and 2D NMR studies. Structure elucidation revealed compounds **1–3** to be 5α-ergosta-7,22-diene-3β,5,6β-triol (=cerevisterol) (**1**), (22*E*,24*S*)-5α-ergosta-7,22-diene-3β,5,6β,9α-tetraol (**2**), and indole-3-carboxylic acid (**3**) [17–19]. Several attempts have been made to identify the major bioactive compounds of different *Clitocybe* species [20, 21], nevertheless, it is important to note that compounds **1**, **2** and **3** were isolated for the first time from *C. nebularis*.

Mushrooms are characterized by accumulation of steroids, and a high number of studies have been reported the isolation of steroids from edible mushrooms, e.g., *Wolfiporia cocos* [22], *Lentinus tigrinus* [23], *Lentinula edodes* and *Tricholoma matsutake* [24]. Steroids of *C. nebularis* have been analyzed by Morelli et al., and cyclolaudenol, 31-norcyclolaudenol, portensterol, ergosterol, and campesterol were found [25]. Interestingly in our experiment these steroids were not identified, but cerevisterol (**1**) and (22*E*,24*S*)-5α-ergosta-7,22-diene-3β,5,6β,9α-tetraol (**2**) could be isolated. Cyclolaudenol, 31-norcyclolaudenol are based on 19-cyclolanostane skeleton, while portensterol, ergosterol, and campesterol have ergostane scaffold, as well as our isolated compounds **1** and **2**. In the study of Senatore steroids of *C. nebularis* were analyzed by GC-MS measurements [15]. It was stated that C_{28} sterols are the principal sterols with lower amounts of C_{27} and C_{29} sterols. Ergosterol was found to be the most abundant sterol comprising 62-68% of the total sterol content. Among the minor compounds ergosterol derivatives ($C_{28}\Delta^{5,7}$, $C_{28}\Delta^{7,22}$ and $C_{28}\Delta^{7}$), $C_{28}\Delta^{5}$, $C_{28}\Delta^{5,22}$, $C_{28}\Delta^{5,24(28)}$ sterols, cholesterol, desmosterol, β-sitosterol, stigmasterol and fucosterol were detected in low or trace amount. Comparing the five studied *Clitocybe* species (*C. aurantiaca*, *C. candida*, *C. cinerascens*, *C. geotropa*, *C. nebularis*), no substantial differences were found by this method among mushrooms belonging to the same genus [15].

This is the first report on the presence of indole 3-carboxylic acid (**3**) in the genus *Clitocybe*, previously only structurally close indole derivatives (indole 3-carbaldehyde) were isolated from a *Clitocybe* species [26]. Indol derivatives were reported as the dominant odorous constituents responsible for the complex odor of the taxonomically related *Tricholom*a species [27].

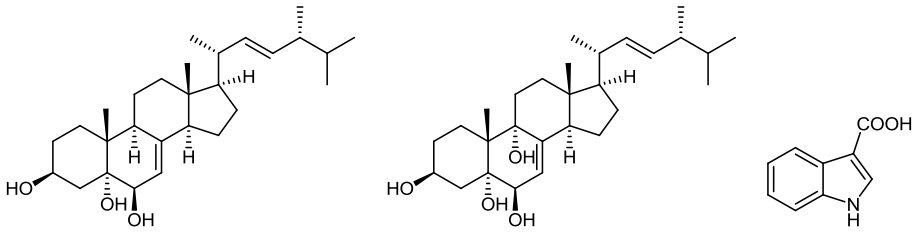

1 **2** **3**

Figure 1. Compounds isolated from *C. nebularis*.

The isolated compounds were subjected to antimicrobial evaluation with regards to the previous proved activities of *Clitocybe* species against various microorganisms [10,28]. The antibacterial activity of compounds **1–3** was investigated by agar disc diffusion method (Table 1). The antibacterial susceptibility test was measured against *Streptococcus agalactiae* (ATCC 13813), *Staphylococcus epidermidis* (ATCC 12228), *Moraxella catarrhalis* (ATCC 25238), *Haemophilus influenzae* (ATCC 49766), and *Proteus mirabilis* (HNCMB 60076) strains. Compound **2** and **3** inhibited marginally the growth of *M. catarrhalis* strain, whereas this strain shown resistance against compound **1**.

Earlier studies demonstrated that cerevisterol (**1**) inhibited the growth of bacteria other than tested here (MIC value 25 µg/mL against *S. typhi*, *S. aureus* and *A. niger*, and MIC 50 µg/mL against *E. faecalis*) [29], while it was inactive against *Bacillus subtilis*, *B. pumilus*, *S. aureus*, *M. luteus*, *C. albicans* and *A. niger* at 20 µg/mL tested by disk diffusion method [30]. Similarly indol 3-carboxylic acid (**3**) was tested previously against a series of pathogenic fungi (*Fusarium avenaceum, F. graminearum, F. culmorum and Pyricularia oryzae)* and bacteria (*S. aureus*, *E. coli* and *B. subtilis*) but no antifungal or antibacterial activity was observed [31]. For (22*E*,24*S*)-5α-ergosta-7,22-diene-3β,5,6β,9α-tetraol (**2**) no antibacterial data are available in the literature.

Table 1. Antimicrobial activity of compounds **1-3** isolated from *C. nebularis***.** (5 mg/mL concentration).

	Diameter of inhibition zone (mm)				
Compound	*S. agalactiae*	*S. epidermidis*	*M. catarrhalis*	*H. influenzae*	*P. mirabilis*
1	-	-	-	-	-
2	-	-	7	-	-
3[a]	-	-	7	-	-

S. agalactiae (*Streptococcus agalactiae* ATCC 13813), *S. epidermidis* (*Staphylococcus epidermidis* ATCC 12228), *M. catarrhalis* (*Moraxella catarrhalis* ATCC 25238), *H. influenzae* (*Haemophilus influenzae* ATCC 49766), *P. mirabilis* (*Proteus mirabilis* HNCMB 60076); [a] For compound **3** 4 mg/mL concentration was used.

3. CONCLUSION

The present study provides a detailed chemical analysis of the mushroom *C. nebularis* aiming at the isolation of apolar metabolites of the MeOH extract. Further studies are required to determine how the isolated compounds contribute to other bioactivities of this species. Our data together with earlier published ones demonstrate the high diversity of compounds in *C. nebularis* and points to the potential of the mushroom as a natural source of chemical compound for pharmacological applications.

4. MATERIALS AND METHODS

4.1. General

The chemicals used in this research were provided by Molar Chemicals and Sigma-Aldrich Hungary. Flash chromatography was carried out on a CombiFlash® Rf+ Lumen Instrument with integrated UV, UV VIS, and ELS detection using reversed and normal phase flash columns filled with RediSep C18 Bulk 950 (Teledyne Isco, Lincoln, NE, USA USA) and Silica 60 (0.045-0.063 mm) (Molar Chemicals, Halásztelek, Hungary), respectively. Preparative thin layer chromatography (TLC) was performed using silica plates (20x20 cm Silica gel 60 F_{254}, Merck 105554).

HRMS and MS analyses were performed on a Thermo Velos Pro Orbitrap Elite and Thermo LTQ XL (Thermo Fisher Scientific) system. The ionization method was ESI operated in positive (or negative) ion mode. The (de)protonated molecular ion peaks were fragmented by CID at a normalized collision energy of 35%. For the CID experiment helium was used as the collision gas. The samples were dissolved in methanol. Data acquisition and analysis were accomplished with Xcalibur software version 4.0 (Thermo Fisher Scientific). NMR data were collected in methanol-d_4 at 25 °C on a Bruker 500 MHz Avance III HD spectrometer equipped with a liquid helium cooled TCI cryoprobe. Chemical shifts were referenced to residual solvent signals (3.31 (^{1}H) and 49.15 ppm (^{13}C) MeOD-d_4). Standard ^{1}H, ^{13}C, 2D-HSQC, 2D-HMBC, and ROESY data were collected in all cases using the pulse sequences available in the Topspin 3.5 pulse sequence library. The NMR assignments of all isolated compounds were in agreement with those reported earlier in the literature [17–19].

4.2. Mushroom material

Samples of *C. nebularis* (Batsch) P. Kumm. were collected in 2017 from the environs of Sándorfalva and Csákányospuszta, Hungary and identified by A. Sándor (Hungarian Mycological Society) and V. Papp. Voucher specimens have been deposited in the mycological collection of the Hungarian Natural History Museum (VPapp-1110171).

4.3. Extraction and isolation

The fresh mushroom material (5.6 kg) was extracted with MeOH (20 L) at room temperature. After concentration, the MeOH extract (54 g) was dissolved in 50% aqueous MeOH and subjected to solvent-solvent partition using *n*-hexane (5 × 500 mL), $CHCl_3$ (5 × 500 mL), and then EtOAc (5 × 500 mL). The $CHCl_3$ soluble phase (2.12 g) was separated by flash chromatography (NP-FC) on silica gel (40 g) using a gradient system of *n*-hexane–acetone (linear from 100:0 to 0:100, t = 60 min). According to TLC monitoring, fractions with similar compositions were combined (C1-C15). Fractions C7 (142 mg), C8 (108 mg) and C9 (69 mg) were further chromatographed by RP_{18}-FC (12 g) using a mixture of H_2O and MeOH (linear gradient from 40 to 90% MeOH, t = 45 min), then further purified by FC on RP_{18} column (4 g) using H_2O–MeOH solvent system (linear gradient from 50% to 95% MeOH, t = 45 min), which resulted in the isolation of compounds **1** (31 mg) and **2** (2.7 mg). The EtOAc phase (4.15 g) was separated by NP-FC (80 g) using *n*-hexane–acetone with increasing polarity (from 100:0 to 65:35, t = 60 min), to obtain 20 major combined fractions (E1–20). Fractions E13 (33 mg), E14 (18 mg) and E15 (20 mg) were further separated by a combination of NP-FC (4 g sorbent, *n*-hexane–acetone (linear gradient from 75:25 to 30:70, t = 50 min) and preparative TLC using a $CHCl_3$–MeOH (97:3) solvent system to isolate compound **3** (2 mg).

4.4. Bacterial strains and culture conditions

The test microorganisms used in this study were 4 standard and 1 clinical isolate with different antibiotic resistance profile. The standard Gram-positive strains were *Streptococcus agalactiae* (ATCC 13813), and *Staphylococcus epidermidis* (ATCC 12228). The standard Gram-negative strains were *Moraxella catarrhalis* (ATCC 25238), and *Haemophilus influenzae* (ATCC 49766). *Proteus mirabilis* (HNCMB 60076) was applied as clinical strain. Bacterial cultures were grown on standard Mueller-Hinton agar (MH) and horse blood (MHF) plates at 37 °C under aerobic environment.

4.5. Determination of antibacterial activity

Screening of antibacterial activity of compounds against standard bacterial strains for their inhibition zones was carried out by standard disc diffusion method [32]. Concisely, the compounds were dissolved in DMSO at concentration 5 (**1** and **2**) and 4 (**3**) mg/mL. The bacterial suspension (inoculums 0.5 McFarland, 1–2×10^8 CFU ml^{-1}) was spread on plate and the sterile filter paper discs (6 mm in diameter) impregnated with 10 µL of the compound solution was placed. DMSO served as negative control, and ampicillin, erythromycin, imipenem, cefuroxime and vancomycin were used as positive control. The plates were incubated (35 +/-2 °C for 24 h) under aerobic conditions. The diameters of inhibition zones created by the compounds (including the disc) were measured and recorded.

Acknowledgements: Financial support for this research was provided by the Economic Development and Innovation Operative Program GINOP-2.3.2-15-2016-00012, the 20391-3/2018/FEKUSTRAT. A. Ványolós is thankful for the support of the Hungarian National Research, Development, and Innovation Fund (PD 124476). The authors thank A. Sándor for his help in the collection and identification of mushroom material.

Author contributions: Concept – A.V., J.H.; Design – A.V.; Supervision – A.V., J.H.; Resource – J.H..; Materials – K.B., Z.B., A.V.; Data Collection &/or Processing – M.Y., M.D., V.P., A.L.; Analysis &/or Interpretation - M.Y., Z.B., M.D., V.P., A.L.; Literature Search – A.V., Z.B., J.H., M.Y.; Writing – M.Y., J.H.; Critical Reviews – A.V, Z.B., K.B.

Conflict of interest statement: The authors declared no conflict of interest.

REFERENCES

[1] Knudsen H, Vesterholt J. Funga Nordica. (Vol 2). Agaricoid, Boletoid, Clavarioid, Cyphelloid and Gastroid Genera. Nordsvamp, Copenhagen: 2012. p. 1083.

[2] Desjardin DE, Wood MG, Stevens FA. *California Mushrooms: The Comprehensive Identification Guide*: Timber Press, New York, 2015. pp. 152-153.

[3] Kummer P. Dur Führer in die Pilzkunde. In: Luppe's Buchhandlung, Zerbst, 1871. pp. 1-146.

[4] Kosanić M, Petrović N, Stanojković T. Bioactive properties of *Clitocybe geotropa* and *Clitocybe nebularis*. J Food Meas Charact. 2020; 14: 1046-1053. [CrossRef]

[5] Bézivin C, Lohézic F, Sauleau P, Amoros M, Boustie J. Cytotoxic activity of Tricholomatales determined with murine

and human cancer cell lines. Pharm Biol. 2002; 40: 196-199. [CrossRef]

[6] Pohleven J, Obermajer N, Sabotič J, Anžlovar S, Sepčić K, Kos J, Brzin J. Purification, characterization and cloning of a ricin B-like lectin from mushroom *Clitocybe nebularis* with antiproliferative activity against human leukemic T cells. Biochim Biophys Acta. 2009; 1790: 173-181. [CrossRef]

[7] Lofgren N, Luning B. On the structure of nebularine. Acta Chem Scandinav. 1953; 7: 225.

[8] Konuk M, Akyol O, Yilmaz K, Yildirimkaya M, Nazaroglu NK, Kisa U. Blocking of the inhibitory effect of nebularine on xanthine oxidase. Biyokim Derg 1996; 21: 9-15.

[9] Brown EG, Konuk M. Plant cytotoxicity of nebularine (purine riboside). Phytochemistry. 1994; 37: 1589-1592. [CrossRef]

[10] Kim Y-S, Lee I-K, Seok S-J, Yun B-S. Chemical constituents of the fruiting bodies of *Clitocybe nebularis* and their antifungal activity. Mycobiology 2008; 36: 110-113.

[11] Venturini M, Rivera C, Gonzalez C, Blanco D. Antimicrobial activity of extracts of edible wild and cultivated mushrooms against foodborne bacterial strains. J Food Protect. 2008; 71: 1701-1706. [CrossRef]

[12] Brzin JE, Rogelj B, Popovič T, Štrukelj B, Ritonja A. Clitocypin, a new type of cysteine proteinase inhibitor from fruit bodies of mushroom *Clitocybe nebularis*. J Biol Chem. 2000; 275: 20104-20109. [CrossRef]

[13] Sabotič J, Kos J. CNL – *Clitocybe nebularis* lectin—the fungal GalNAcβ1-4GlcNAc-binding lectin. Molecules. 2019; 24: 4204. [CrossRef]

[14] Caglič PA, Renko M, Turk D, Kos J, Sabotič J. Fungal β-trefoil trypsin inhibitors cnispin and cospin demonstrate the plasticity of the β-trefoil fold. Biochim Biophys Acta Proteins Proteom. 2014; 844: 1749-1756. [CrossRef]

[15] Senatore F. Chemical constituents of some mushrooms. J Sci Food Agric. 1992; 58: 499-503. [CrossRef]

[16] Audouin P, Vidal J, Richard H. Volatile compounds from aroma of some edible mushrooms: morel (*Morchella conica*) wood blewitt (*Lepista nuda*), clouded agaric (*Clitocybe nebularis*), and false chanterelle (*Hygrophoropsis aurantiaca*). Sci Alim. 1989; 185-193.

[17] Jinming G, Lin H, Jikai L. A novel sterol from Chinese truffles *Tuber indicum*. Steroids. 2001; 66: 771-775. [CrossRef]

[18] Valisolalao J, Luu B, Ourisson G. Chemical and biochemical study of Chinese drugs. Part VIII. Cytotoxic steroids from *Polyporus versicolor*. Tetrahedron. 1983; 39: 2779-85. [CrossRef]

[19] Burton G, Ghini AA, Gros EG. ^{13}C NMR spectra of substituted indoles. Magn Reson Chem. 1986; 24: 829-831. [CrossRef]

[20] Wang H, Ng T. Isolation of a new ribonuclease from fruiting bodies of the silver plate mushroom *Clitocybe maxima*. Peptides. 2004; 25: 935-939. [CrossRef]

[21] Zhang G-Q, Wang Y-F, Zhang X-Q, Ng TB, Wang H-X. Purification and characterization of a novel laccase from the edible mushroom *Clitocybe maxima*. Procs Biochem. 2010; 45: 627-633. [CrossRef]

[22] Baosong C, Sixian W, Gaoqiang L, Li B, Ying H, Ruilin Z, Hongwei L. Anti-inflammatory diterpenes and steroids from peels of the cultivated edible mushroom *Wolfiporia cocos*. Phytochem Lett. 2020; 36: 11-16. [CrossRef]

[23] Ragasa CY, Tan MCS, De Castro ME, Mariquit M, Oyong GG, Shen CC. Sterols from *Lentinus tigrinus*. Pharmacog J. 2018; 10: 1079-1081.

[24] Ohnuma N, Amemiy, K, Kakuda R, Yaoita Y, Machida K, Kikuchi M. Sterol constituents from two edible mushrooms, *Lentinula edodes* and *Tricholoma matsutake*. Chem Pharm Bul. 2000; 48: 749-751. [CrossRef]

[25] Morelli I, Pistelli L, Catalano S. Some constituents of *Clitocybe nebularis* and of *Hydnum repandum*. Fitoterapia. 1981; 52: 45-47.

[26] Chen JT, Su HJ, Huang JW. Isolation and identification of secondary metabolites of *Clitocybe nuda* responsible for inhibition of zoospore germination of *Phytophthora capsici*. J Agric Food Chem. 2012; 60: 7341–7344. [CrossRef]doi.org/

[27] Fons F, Rapior S, Fruchier A, Saviuc P, Bessière JM. Volatile composition of *Clitocybe amoenolens*, *Tricholoma caligatum* and *Hebeloma radicosum*. Cryptogamie Mycol. 2006; 27: 45-55.

[28] Dimitrijevic M, Jovanovic VS, Cvetkovic J, Mihajilov-Krstev T, Stojanovic G, Mitic V. Screening of antioxidant, antimicrobial and antiradical activities of twelve selected Serbian wild mushrooms. Anal Methods. 2015; 7: 4181-4191. [CrossRef]

[29] Appiah T, Agyare C, Luo Y, Boamah VE, Boakye YD. Antimicrobial and resistance modifying activities of cerevisterol

isolated from *Trametes* species. Curr Bioact Compd. 2020; 16: 115-123. [CrossRef]

[30] Guoa K, Fanga H, Guia F, Wang Y, Xua Q, Deng X. Two new ring A-ceaved lanostane-type triterpenoids and four known steroids isolated from endophytic fungus *Glomerella* sp. Helv Chim Acta 2016; 99: 601–607. [CrossRef]

[31] Tian S, Yang Y, Liu K, Xiong Z, Xu L, Zhao L. Antimicrobial metabolites from a novel halophilic actinomycete *Nocardiopsis terrae* YIM 90022. Nat Prod Res. 2014; 28: 344–346. [CrossRef]

[32] Bauer A, Kirby W, Sherris J, Turck M. Antimicrobial investigations. Am J Clin Pathol. 1966; 45: 493-496.